

**UNIVERSIDADE FEDERAL DO RIO GRANDE DO SUL
INSTITUTO DE GEOCIÊNCIAS
PROGRAMA DE PÓS-GRADUAÇÃO EM GEOCIÊNCIAS**

**ESTRATIGRAFIA DE SEQUÊNCIAS E ARQUITETURA
FACIOLÓGICA DA FORMAÇÃO MORRO DO CHAPÉU,
CHAPADA DIAMANTINA-BA**

EZEQUIEL GALVÃO DE SOUZA

ORIENTADOR – Prof. Dr. Claiton M.S. Scherer

Volume I

Porto Alegre, 2018

**UNIVERSIDADE FEDERAL DO RIO GRANDE DO SUL
INSTITUTO DE GEOCIÊNCIAS
PROGRAMA DE PÓS-GRADUAÇÃO EM GEOCIÊNCIAS**

**ESTRATIGRAFIA DE SEQUÊNCIAS E ARQUITETURA
FACIOLÓGICA DA FORMAÇÃO MORRO DO CHAPÉU,
CHAPADA DIAMANTINA-BA**

EZEQUIEL GALVÃO DE SOUZA

ORIENTADOR – Prof. Dr. Claiton M.S. Scherer

BANCA EXAMINADORA

Prof. Dr. Juliano Kuchle – Instituto de Geociências, Universidade Federal do Rio Grande do Sul (UFRGS);

Dra. Renata Alvarenga – Instituto de Geociências, Universidade Federal do Rio Grande do Sul (UFRGS);

Prof. Dra. Joice Cagliari – Programa de Pós-Graduação em Geociências, Universidade do Vale do Rio dos Sinos (UNISINOS).

Tese de doutorado apresentada como requisito parcial para a obtenção do Título de Doutor em Ciências.

Porto Alegre, 2018

UNIVERSIDADE FEDERAL DO RIO GRANDE DO SUL**Reitor:** Rui Vicente Oppermann**Vice-Reitor:** Jane Fraga Tutikian**INSTITUTO DE GEOCIÊNCIAS****Diretor:** André Sampaio Mexias**Vice-Diretor:** Nelson Luiz Sambaqui Gruber

Souza, Ezequiel Galvão de

Estratigrafia de sequências e arquitetura faciológica da Formação
Morro do Chapéu, Chapada Diamantina - BA . / Ezequiel Galvão de
Souza. - Porto Alegre: IGEO/UFRGS, 2018.
[111 f.] il.Tese (Doutorado).- Universidade Federal do Rio Grande do Sul.
Programa de Pós-Graduação em Geociências. Instituto de
Geociências. Porto Alegre, RS - BR, 2018.

Orientador: Clayton Marlon dos Santos Scherer

1. Estratigrafia. 2. Proterozóico. 3. Morro do Chapéu. 4. Sistemas
costeiros. I. Título.

CDU 551.7

Catalogação na Publicação

Biblioteca Instituto de Geociências - UFRGS

Miriam Alves

CRB 10/1947

Universidade Federal do Rio Grande do Sul - Campus do Vale Av. Bento Gonçalves, 9500 - Porto
Alegre - RS - Brasil

CEP: 91501-970 / Caixa Postal: 15001.

Fone: +55 51 3308-6329 Fax: +55 51 3308-6337

E-mail: bibgeo@ufrgs.br

AGRADECIMENTOS

Agradeço primeiramente ao Deus da coincidência, do acaso, do agora. Seja lá qual forma ou nome ele tenha, creio que o que importa é a fé, a fé de que este é o melhor momento para se viver e que é através deste momento que construiremos os próximos dias da melhor maneira possível.

Agradeço ao Soni e a Negrinha por terem se empenhado tanto no papel de pais, por terem criado seus 4 filhos superando todas as dificuldades e nunca deixando faltar nada para nenhum deles. Por terem dado toda a liberdade durante as nossas escolhas, nos permitindo cair, levantar, bater de frente, perder e vencer, ensinando assim o valor das escolhas e da persistência. Por serem verdadeiros exemplos de dedicação e caráter, mostrando os verdadeiros valores da vida.

Agradeço aos meus irmãos Mara, Galvão e Kris, por todos os momentos vividos até hoje. Sem vocês não seria a pessoa que sou hoje e com certeza não teria tanta graça nesse mundo.

Agradeço à Marlise, minha companheira que há dois anos se puxa para compreender minhas insanidades e a loucura que é conviver com “alguém de peixes”. Tua companhia nesses últimos anos foi essencial, tua determinação e esforço são inigualáveis e nada nesse mundo pode te parar. Teu caminho está sendo trilhado e teu lugar está guardado. Te amo e te admiro cada dia mais, muito obrigado pelo carinho recíproco, pela compreensão e amor.

Agradeço a meu amigo/orientador por todos os bate-papos, geológicos ou não, que nos tornaram próximos e fizeram essa parceria durar quase 9 anos. Com certeza tive um privilégio que poucos alunos têm, o privilégio de tornar o orientador parte da minha família. Seja qual for meu caminho daqui por diante, nossas conversas e tuas orientações serão sempre levadas adiante, tanto na vida profissional quanto na pessoal. Obrigado, Claiton.

Agradeço ao Carlinhos, pelas conversas cedo da manhã, pelos alertas, pela organização, pela amizade e pela parceria. Tu és o cara, Charlinho, e nada disso estaria acontecendo sem teu apoio. Agradeço ao alemão Rodrigo, pela parceria constante e pelo esforço e competência pra solucionar os problemas dessas máquinas malucas do século XXI.

Agradeço ao mestre Francisco e todos os amigos que fiz em Morro do Chapéu/BA. Chico, qualquer coisa que eu diga aqui é pouco comparada ao que tu fizeste por mim. Tua experiência e conhecimento da natureza foram a essência para

este trabalho. Ver a paixão e admiração que tu tens pela natureza, bem como a facilidade para compreender as coisas, me deram muita energia nesta caminhada. Tua parceria, além de segurança no trabalho, nos gerou uma linda amizade e muitas histórias para serem contadas. Muito obrigado, Chico.

Agradeço aos grandes amigos e colegas de sala: João Pedro, Adriano, Lucas Bofill, Carrel Kifumbi e Erik Dario. Nossa parceria com certeza vai ficar marcada para sempre, como uma orogênese no registro geológico. Cada um do seu jeito, à sua maneira e ao seu tempo, como os sistemas deposicionais interagindo em uma bacia sedimentar, contribuiu para o meu crescimento profissional e pessoal. Vocês vão ter sempre um lugar especial na minha vida e a minha casa vai estar sempre aberta pra vocês. Agradeço também aos demais colegas de departamento de estratigrafia, com quem dividia meu dia a dia, tomava aquele cafezinho depois do almoço e conversávamos sobre os mais diferentes temas. Muito Obrigado.

"O analfabeto do século XXI não será aquele que não sabe ler e escrever, mas aquele que não consegue aprender, desaprender e aprender novamente"

Alvin Tofler

RESUMO

Situada na porção central do Cráton São Francisco, a Formação Morro do Chapéu abrange uma grande área no domínio Chapada Diamantina do Supergrupo Espinhaço. Sobreposta a Fm. Caboclo, com a qual compõem a Sequência superior deste Supergrupo, apresenta contato basal discordante e em paraconformidade com a mesma. Diversos trabalhos sob o âmbito de mapeamento geológico foram feitos nesta área, porém, sob o ponto de vista de sistemas deposicionais e estratigráfico, esta Sequência começou a ser estudada recentemente. Sob esse contexto de mitigar parte das incertezas vigentes e compreender de forma acurada os aspectos sedimentológicos e estratigráficos do intervalo superior da Bacia Espinhaço que se justifica a necessidade do presente estudo.

A partir do levantamento de seções estratigráficas ao longo dos principais rios e estradas nos arredores do município de Morro do Chapéu/BA, em um total de 30 afloramentos, obtiveram-se cerca de 1000 metros de seções colunares e 797 medidas de paleocorrentes. Destes dados foram propostos três artigos científicos os quais abordam: 1) sedimentologia dos conglomerados basais da Formação Morro do Chapéu; 2) a análise estratigráfica a partir do empilhamento de associações faciológicas; e 3) análise dos depósitos de shoreface e suas estruturas sedimentares geradas por fluxos combinados.

Os depósitos basais da Formação Morro do Chapéu apresentam características sedimentares peculiares em sua faciologia. Localizados em somente três afloramentos e com uma exposição lateral restrita, conglomerados com blocos e seixos, mal selecionados e com ampla variação composicional e textural permitem a indagação a respeito de sua origem. Aliados as características sedimentares, feições estruturais limitadas a estes conglomerados e a porção imediatamente abaixo dos

mesmos, permite a interpretação de uma deformação local desassociada aos eventos tectônicos da região. Tais fatores aliados à posição paleogeográfica do Cráton São Francisco-Congo durante o intervalo de deposição da Formação Morro do Chapéu, sugerem glaciações de alta latitude, contrárias aos modelos do Neoproterozóico de grandes glaciações às baixas latitudes.

No âmbito da estratigrafia de sequências, duas sequências incompletas foram definidas na Formação Morro do Chapéu. A sequência inferior é limitada entre duas discordâncias subaéreas, enquanto a superior por uma discordância subaérea na base e o contato tectônico no topo. Ambas são compostas pelos tratos de sistema de nível baixo, transgressor e nível alto (TSNB, TST e TSNA, respectivamente). A principal diferença entre estas duas sequências é a ocorrência dos depósitos de maré na sequência superior, indicando uma mudança na morfologia da costa que permitiu que efeito da maré fosse mais efetivo e consequentemente preservado.

O efeito da maré também é preservado nos depósitos de *shoreface*, onde formas de leito híbridas indicam a ação de fluxo oscilatório e unidirecional associados. Estas formas de leito são caracterizadas por anisotropia nas laminationes e variação na sua geometria. A partir da tríade rio/onda/maré registrada nos depósitos da Formação Morro do Chapéu, podemos inferir que durante a maré alta, as formas de leito tendem a migrar lateralmente devido a menor amplitude das oscilações que chegam ao fundo. Já durante a maré baixa, as formas de leito tendem a agradar devido a maior amplitude das oscilações que chegam ao fundo e diminuem a efetividade das correntes unidireccionais.

ABSTRACT

Located in the central area of the São Francisco Craton, the Morro do Chapéu Formation covers a large area in the Chapada Diamantina domain, on the Espinhaço Supergroup. The Upper Sequence of this Supergroup includes Morro do Chapéu and Caboclo formations with a paraconformity discordance. Several works under the scope of geological mapping were done in this area, however, from the depositional systems and stratigraphics point of view this Sequence started to be studied only recently. The need of the present study is to mitigate part of the current uncertainties and understand the sedimentological and stratigraphic aspects of the upper range of the Espinhaço Basin.

From stratigraphic sections along the main rivers and roads on the outskirts of Morro do Chapéu town, a total of 30 outcrops, 1000 meters of columnar sections and 797 measures of paleocurrents were obtained. Three scientific papers were proposed from these data, which address: 1) sedimentology of the basal conglomerates of the Morro do Chapéu Formation; 2) the stratigraphic analysis from the stacking of facies associations; and 3) analysis of shoreface deposits and their sedimentary structures generated by combined flows.

The basal deposits of the Morro do Chapéu Formation have unique sedimentary characteristics in their faciology. Founded in only three outcrops and with a restricted lateral exposure, conglomerates with blocks and pebbles, poorly selected and with wide compositional and textural variation allow the inquiry about their origin. Allied sedimentary characteristics, structural features limited to these conglomerates and them immediately below portion, allows the interpretation of a local deformation disassociated to the tectonic events of the region. These factors allied to the paleogeographic position of the São Francisco-Congo Craton during the

deposition interval of Morro do Chapéu Formation, suggest high latitude glaciations, contrary to the Neoproterozoic classic models of large glaciations at low latitudes.

In scope of sequence stratigraphy, two incomplete sequences were defined in the Morro do Chapéu Formation. The lower sequence is limited between two subaerial unconformities, while the upper one at the base is a subaerial unconformity and the tectonic contact at the top. Both are composed of lowstand, transgressive and highstand system tracts (TSNB, TST and TSNA, respectively). The main difference between these two sequences is the occurrence of tidal deposits in the upper sequence, indicating a change in the morphology of the coast that allowed tide effect to be more effective and consequently preserved.

The effect of the tide is also preserved in the shoreface deposits, where hybrid bedforms indicate the action of oscillatory and unidirectional flow associated. These bedforms are characterized by anisotropic laminations and geometry variation. From the river/wave/tide triad recorded in the Morro do Chapéu Formation deposits, we can infer that during high tide, the bedforms tend to migrate laterally due to the smaller amplitude of the oscillations that reach the bottomset. Even during low tide, the bedforms are aggradational because of the greater amplitude of the oscillations that reach the bottom and decrease the effectiveness of the unidirectional currents.

SUMÁRIO

CAPÍTULO I	2
1. Introdução	2
2. Estado da arte	5
3. Referências bibliográficas	12
CAPÍTULO II	15
Artigo 1	15
CAPÍTULO III	47
Artigo 2	47
CAPÍTULO IV	79
Artigo 3	79
APÊNDICE	98

Estruturação desta Tese

A presente tese de doutorado está estruturada em torno de artigos submetidos a periódicos e segmentada em quatro capítulos. Consequentemente sua organização compreende as seguintes partes principais:

Capítulo I – Oferece uma revisão conceitual do Supergrupo Espinhaço na área de estudo e traz à tona a problemática envolvida em sua estratigrafia e sedimentologia, compreendendo os seguintes tópicos: 1) Introdução; 2) Revisão do Estado da Arte; e 3) Referência bibliográficas utilizadas nesta etapa;

Capítulo II – apresenta o artigo científico intitulado “*Mesoproterozoic glaciations: negligenced or unknown sedimentary structures?*” e submetido à revista *Sedimentary Geology*; A forma como se encontra o artigo nesta tese é diferente da submetida para o periódico. As figuras foram inseridas no texto para melhor visualização do leitor.

Capítulo III – apresenta por sua vez o artigo científico intitulado “*A wave-dominated mesoproterozoic sedimentary sequence, Espinhaço Supergroup – NE/Brazil*”, submetido à revista *Pre-Cambrian Research*;

Capítulo IV – apresenta o artigo científico intitulado “Fluxos combinados e as formas de leito híbridas no Proterozoico: o exemplo da Formação Morro do Chapéu, Supergrupo Espinhaço/BA”, submetido à revista *Pesquisas em Geociências*;

Apêndice A – Seções colunares levantadas disponibilizadas em formato “*.pdf” somente no CD.

CAPÍTULO I

1. Introdução

1.1 Caracterização do problema

A correta interpretação de antigos depósitos sedimentares requer o conhecimento de dois aspectos independentes, porém interligados, da sucessão sedimentar: (i) interpretação do ambiente deposicional original, usando técnicas de análise de fácies e, (ii) a subdivisão da sucessão estratigráfica em unidades geneticamente relacionadas usando os princípios da estratigrafia de sequências.

Em pacotes sedimentares proterozóicos, as dificuldades para o reconhecimento e a correta interpretação faciológica dos depósitos são aumentadas. Isto decorre do fato da maioria das sucessões proterozoicas estarem deformadas, metamorfizadas ou com um grau de diagênese avançada, dificultando o reconhecimento e a interpretação das estruturas sedimentares, definição das sucessões verticais de fácies e, por conseguinte, a definição de um arcabouço estratigráfico de alta resolução.

A região da Chapada Diamantina/BA possui uma grande diversidade geológica, a qual contribui para o cenário didático das geociências, principalmente no contexto de sistemas deposicionais siliciclásticos pré-cambrianos. Dentro dessa diversidade está inserida a Formação Morro do Chapéu (FMC – Proterozóico/BA) que aflora em grandes domínios nos arredores do município homônimo, considerados seções-tipo ou áreas-tipo da unidade. Nesta região a caracterização das sequências deposicionais do intervalo inferior da Bacia Espinhaço é relativamente avançada sob o ponto de vista de mapeamento geológico e entendimento dos sistemas deposicionais. No entanto, os modelos apresentados para o intervalo superior carecem de informações detalhadas sobre evolução estratigráfica e sedimentar. É nesse contexto de mitigar parte das incertezas vigentes e compreender de forma acurada os aspectos sedimentológicos e estratigráficos da Bacia Espinhaço que se justifica a necessidade do presente estudo.

Assim, o presente projeto tem como principal objetivo uma análise faciológica de detalhe e a proposição da estratigrafia de sequências de alta resolução da FMC. Tal objetivo visa estabelecer um modelo de predição da arquitetura deposicional da Formação que contribua para novos estudos relacionados a sistemas proterozóicos,

bem como para a caracterização e gerenciamento de aquíferos e reservatórios em contextos geológicos similares.

1.2 Objetivos

Dada a variabilidade na classificação dos ambientes costeiros em função da tríade rio/onda/maré, torna-se necessária a análise faciológica em detalhe dos depósitos para uma correta reconstituição e classificação dos sistemas. Para tanto, o escopo geral deste projeto é a análise estratigráfica e da arquitetura de fáries dos sistemas deposicionais costeiros que compõem a FMC, buscando-se o entendimento dos mecanismos controladores da sedimentação em sucessões proterozoicas.

Destacam-se como objetivos específicos os seguintes itens:

- Modelo estratigráfico: Elaboração de um arcabouço de estratigrafia de sequências do intervalo de interesse, incluindo a identificação, caracterização e correlação de discordâncias e superfícies estratigráficas significativas;
- Modelo da arquitetura faciológica: Fotomosaicos interpretados de afloramentos; tabela de fáries e associações de fáries; seções colunares sintéticas das associações de fáries; plates de fotografias ilustrativas das fáries e associações de fáries; diagramas de paleocorrentes das associações de fáries geral e por seção colunar.

1.3 Localização da área de estudo

A FMC aflora no domínio geomorfológico Chapada Diamantina, região central do Cráton São Francisco, Bahia/BR. A geomorfologia desta região compõe um relevo acidentado, de serras tabulares e vales longos e estreitos. Por ser uma formação com grande abrangência territorial, inicialmente estabeleceram-se três áreas para a pesquisa: uma na borda norte da Chapada Diamantina; uma na porção central, aos arredores do município Morro do Chapéu; e outra mais ao sul, entre os municípios de Lençóis e Utinga (Figura 1).

Essas áreas foram escolhidas com base na análise de mapas geológicos integrados a modelos digitais de terreno, buscando feições íngremes que abrangessem a FMC, bem como seu contato com as formações adjacentes. Além disso, fez-se um refinamento no banco de dados de afloramentos da CPRM, contribuindo para definição das áreas a partir da quantidade e qualidade de afloramentos. Entretanto, o elevado grau de intemperismo e a descontinuidade dos

afloramentos nas áreas I e III inviabilizaram a aquisição e correlação dos dados, ficando o projeto restrito à área II (Figura 1 e 2).

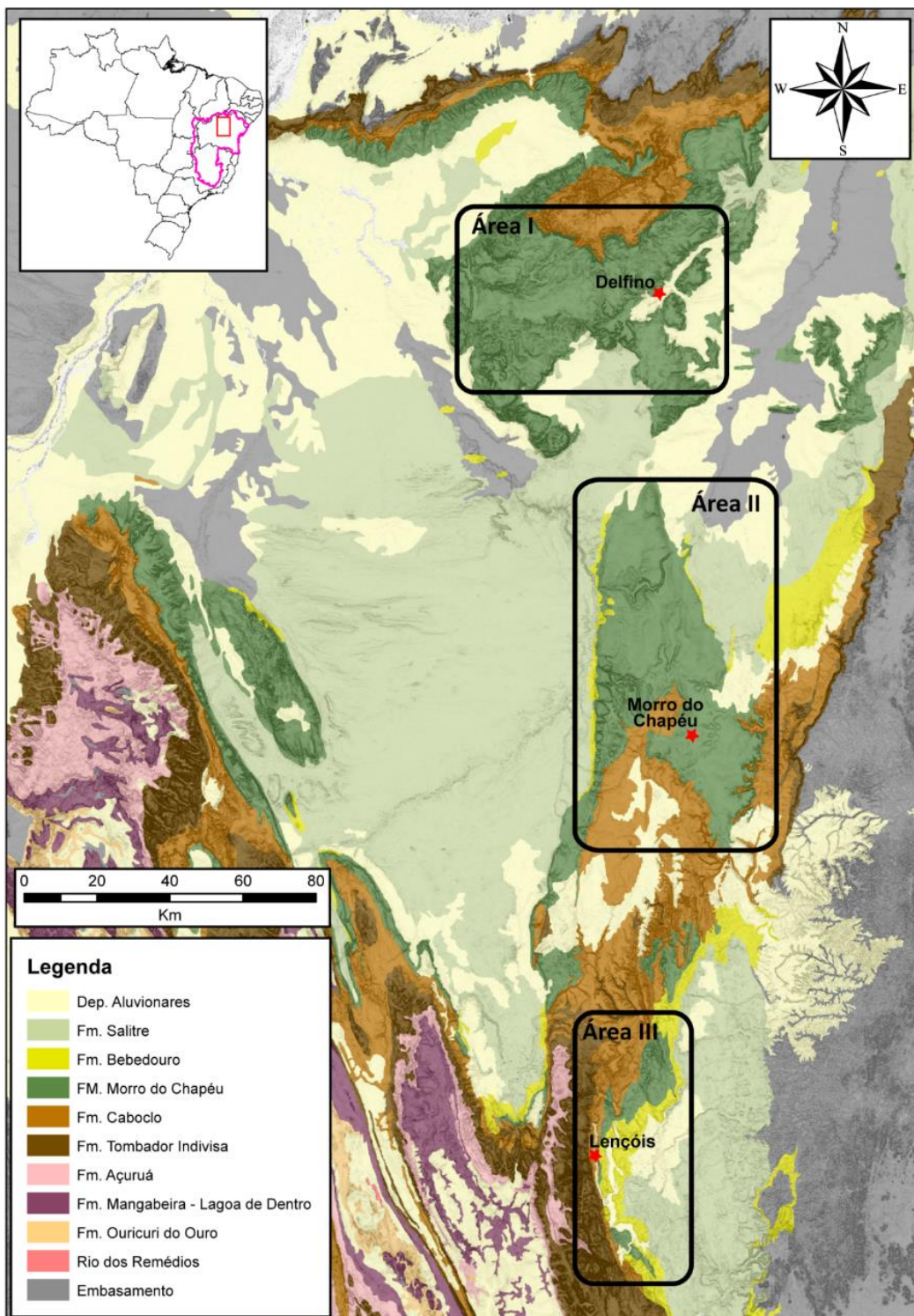


Figura 1: Mapa geológico da região de estudo, com a definição das áreas de foco e as cidades-base. A limitação do CSF está em rosa no mapa do Brasil. Fonte: CPRM/CBPM – 2003 (modificado).

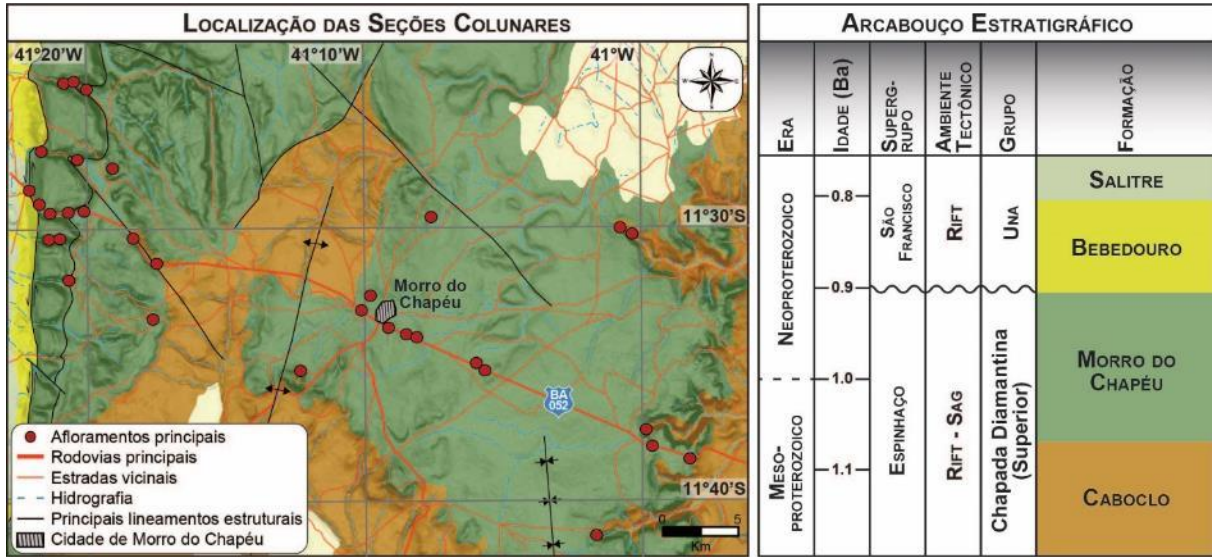


Figura 2: Mapa geológico básico da região de estudo com a distribuição das seções colunares levantadas. As cores para as Formações geológicas no mapa são as mesmas identificadas no quadro lateral do arcabouço estratigráfico.

2. Revisão do Estado da Arte

2.1 Contexto geológico

A unidade sedimentar no qual foi desenvolvido este trabalho pertence a uma das principais unidades geotectônicas do Brasil, o Cráton do São Francisco que, em conjunto com o Cráton do Congo, formava a paleoplaca Congo-São Francisco, reconhecida por muitos como membro do supercontinente Rodínia (Weil *et al.*, 1998; Campos Neto, 2000). A longa ligação da paleoplaca Congo-São Francisco, que se estende talvez até 3,0 Ga (Weil *et al.*, 1998) envolve um extenso período de construções de bacias sedimentares interiores aos cráticos.

O Cráton do São Francisco (Fig. 3), localizado no centro-leste do Brasil faz parte do Escudo Atlântico da Plataforma Sul-Americana, sendo individualizado como uma unidade geotectônica por Almeida (1977). É composto por um núcleo Arqueano e por dois segmentos de orógenos colisionais Paleoproterozóicos (Alkmim & Marshak, 1998; Alkmim & Martins-Neto, 2011), durante o evento geológico Transamazônico. Alkmim *et al.* (1993) redefiniu os limites do Cráton, anteriormente definidos por Almeida (1977). Circundado por faixas móveis de dobramentos é limitado a sul e oeste pela faixa Brasília, a noroeste limita-se com a faixa Rio Preto, a norte com as faixas Sergipana e Riacho do Pontal e a sudeste com a faixa Araçuaí. A leste o limite do Cráton é com as bacias sedimentares de Jequitinhonha, Almada, Camamu e Jacuípe.

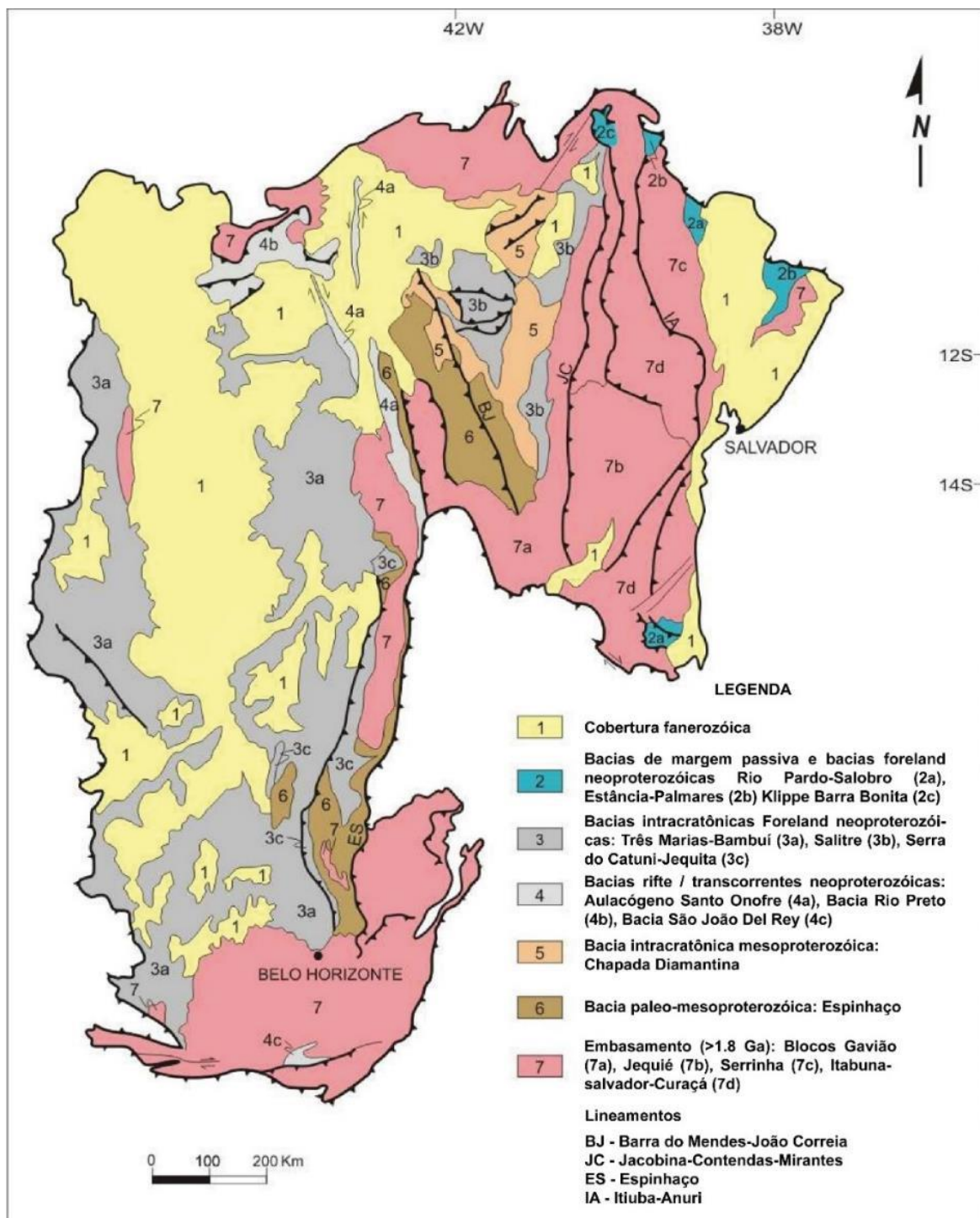


Figura 3: Mapa geológico simplificado do Cráton do São Francisco. Modificado de Delgado *et al.* (2003).

Dois grandes domínios morfotectônicos foram individualizados no Cráton do São Francisco: a Bacia do São Francisco e o Aulacógeno do Paramirim(Cruz & Alkmim, 2006). A Bacia do São Francisco ocupa todo o segmento alongado do cráton, enquanto que o Aulacógeno do Paramirim é a grande feição morfoestrutural localizada a norte. Estes domínios são separados pelo Corredor do Paramirim e registram sucessões sedimentares semelhantes, com coberturas metassedimentares pré-cambrianas e扇形的. O Aulacógeno do Paramirim

representa uma grande feição morfoestrutural da porção norte do Cráton do São Francisco e corresponde a duas bacias riftes intracratônicas superpostas e parcialmente invertidas, preenchidos principalmente por metassedimentos Proterozóicos (Schobbenhaus, 1996; Cruz & Alkmim, 2006).

O Supergrupo Espinhaço é dividido em três domínios: Serra do Espinhaço Meridional, Serra do Espinhaço Setentrional e Chapada Diamantina. O primeiro e o segundo domínio localizam-se a oeste do Corredor de Deformação do Paramirim, e o terceiro domínio localiza-se a leste. Para cada domínio foram adotadas nomenclaturas diferentes para as unidades deposicionais. No domínio Chapada Diamantina este Supergrupo é dividido em três grupos (Figs. 2 e 4): Grupo Rio dos Remédios, Grupo Paraguaçu e Grupo Chapada Diamantina (Pedreira, 1989; Dominguez, 1996).

Chemale et al. (2012) e autores posteriores (Santos et al., 2013; Guadagnin et al., 2015) dividem o Supergrupo em três megasequências (Inferior, Médio e Superior) que se acumularam em numerosas bacias desenvolvidas em resposta a pelo menos duas fases de rifteamento. O Grupo Rio dos Remédios compõe a Sequência Inferior (1.8 – 1.68 Ga) (Fig.4). Ocorre em um contexto rifte, sendo formada por depósitos fluviais e eólicos da Fm. Serra da Gameleira, vulcânicos ácidos alcalinos da Fm. Novo Horizonte, sistemas lacustres da Fm. Lagoa de Dentro e aluviais da Fm. Ouricuri do Ouro.

A Sequência Média (1.6 – 1.4 Ga) corresponde a um evento rifte no Domínio Espinhaço Norte e uma bacia sag no Chapada Diamantina. No Domínio Chapada Diamantina essa sequência compreende o Grupo Paraguaçu (Fm. Mangabeira e Açuruá) e a Fm. Tombador (Grupo Chapada Diamantina). É preenchida na base por sistemas aluviais/fluviais e eólicos da Fm. Mangabeira que são sobrepostos por depósitos transgressivos, marinhos rasos e deltaicos da Fm. Açuruá. Sobre o Grupo Paraguaçu, em discordância angular, deposita-se a Fm. Tombador como uma nova fase sag.

A Sequência Superior (1.19 – 0.9 Ga) se formou em um ambiente tectônico rifte-sag. Essa fase tectônica é representada pelos depósitos marinhos rasos da Fm. Caboclo e Morro do chapéu. Essa sequência marinha é interpretada como transgressiva e em paraconformidade com a Fm. Tombador.

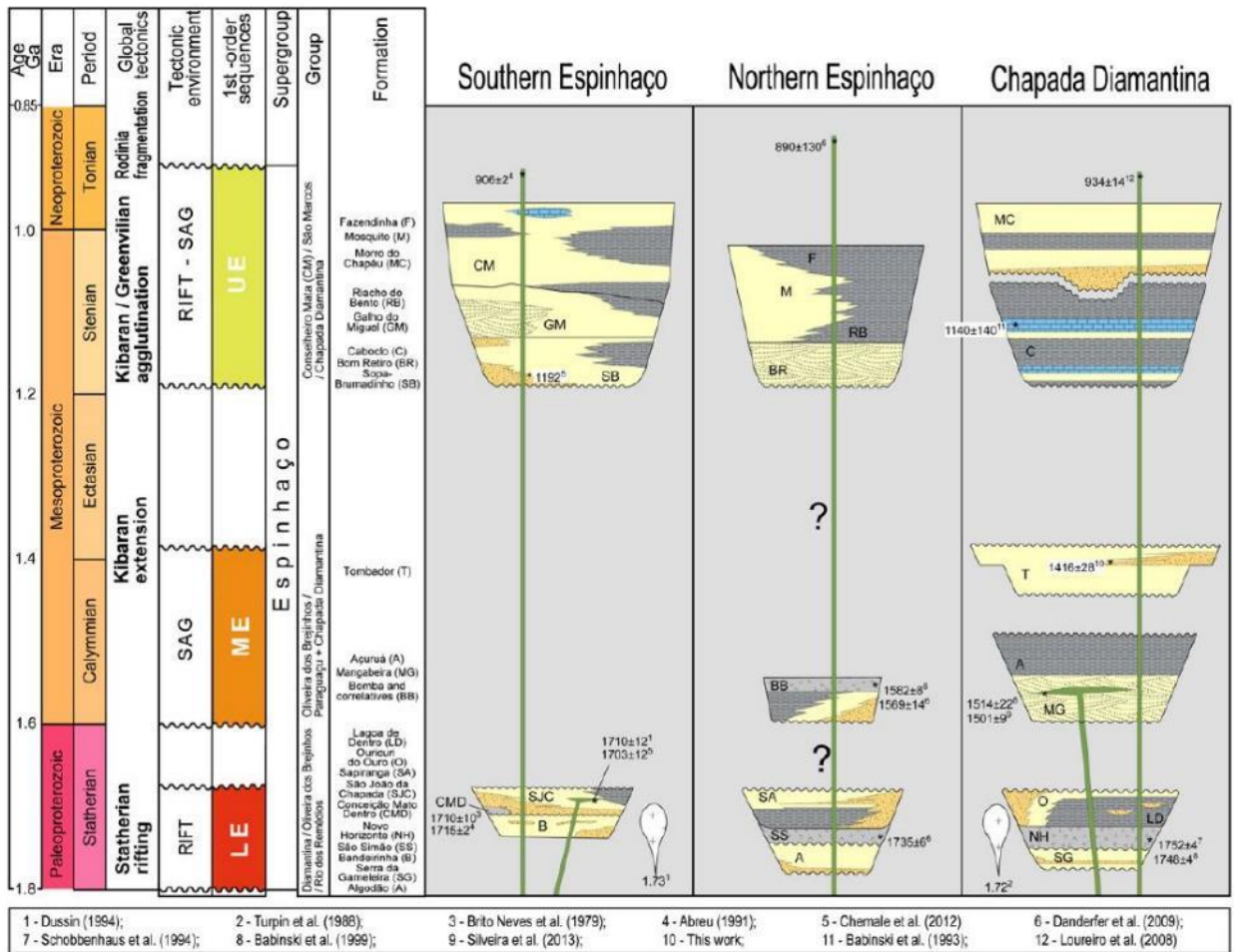


Figura 4: Correlação regional do Supergrupo Espinhaço mostrando os tipos de bacia, sistemas deposicionais, discordâncias, unidades litoestratigráficas, sequencias de primeira ordem e os principais eventos tectônicos globais. Retirado de Guadagnin *et al.* (2015).

2.2 Formação Morro do Chapéu

A FMC foi definida por Brito Neves (1967), com base em uma seção-tipo descrita na Serra das Lages, situada a noroeste de Morro do Chapéu (Figura 5). Esta unidade é composta, na base, por conglomerados e, no topo, por ortoquartzitos brancos e róseos, com estratificações plano-paralelas e cruzadas, com pelo menos duas intercalações de argilitos roxos micáceos. O contato superior na Serra das Lages é tectônico, caracterizado por uma falha de empurrão que a separa dos carbonatos do Grupo Una (Bambuí). Pedreira (1988) assume que o contato basal da FMC com a Fm. Caboclo ocorre de maneira transicional e interdigitada. Segundo o autor, é possível observar depósitos relacionados à planície de maré da Fm. Caboclo e fluvial deltaico da FMC intercalados em uma única seção a oeste do município homônimo. Entretanto, Espíndola (2013), mostra o contato discordante erosivo entre as Formações no povoado de Ventura, no qual os depósitos de plataforma híbrida rasa da Fm. Caboclo são erodidos pelos conglomerados basais da FMC.

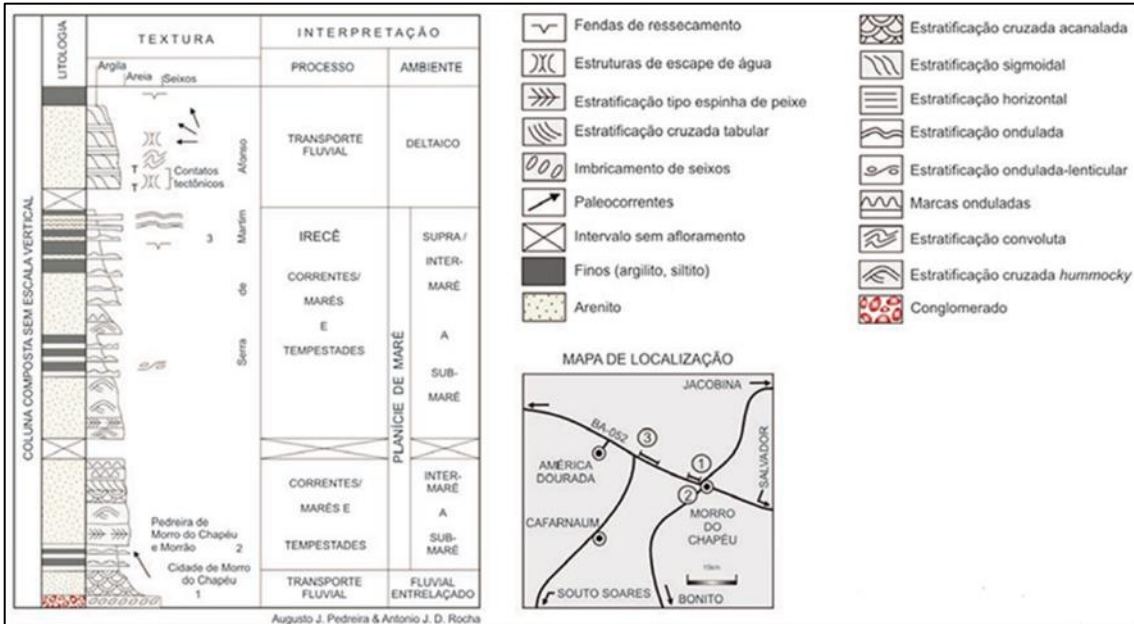


Figura 5: Seção composta da Fm. Morro do Chapéu. Retirado de Schobbenhaus (2012).

De acordo com Guimarães & Pedreira (1990), a formação consiste em diversos ciclos que começam por conglomerados polimíticos com estratificação cruzada acanalada e terminam com argilitos ou arenitos finos. Os arenitos são médios a finos, com estratificações plano-paralelas, cruzadas tabulares e acanaladas de porte médio a grande. De acordo com os autores, os pelitos ocorrem principalmente no topo da formação, associados a arenitos com marcas onduladas e ocasionalmente estratificações cruzadas do tipo espinha de peixe. Segundo Monteiro *et al.* (1984), a FMC é composta por sistemas fluviais entrelaçados e eólicos. Para Pedreira *et al.* (1989), seus depósitos correspondem a leques aluviais, lobos deltaicos e dunas eólicas.

A espessura da FMC varia conforme a área de estudo. Além da Serra das Lages onde foi definida com 250 m de espessura (Brito Neves, 1967), na região do município homônimo é da ordem de 390 m, segundo Pedreira *et al.* (1975); nos arredores de Utinga, Guimarães & Pedreira (1990) estabelecem 200 m; e na região de Lençóis, cerca de 40 m conforme Montes (1977).

No âmbito de correlações intercontinentais, Torquato e Fogaca (1981) com base em evidências estratigráficas, tectônicas e geocronológicas, correlacionaram o Supergrupo Espinhaço na Bahia e em Minas Gerais com o Grupo Chela (Angola) e as Formações Nosib e Khoabendus (Namíbia). A porção sem preenchimento entre os dois segmentos é resultado do arqueamento proto-Atlântico e posterior erosão.

2.3 Sistemas costeiros

Ao trabalhar com os depósitos da FMC, uma abordagem teórica sobre a classificação dos sistemas costeiros é fundamental, tendo em vista as interpretações prévias do seu registro sedimentar. Apesar de Dalrymple *et al.* (1992), Reading (1996) e Davis & Fitzgerald (2004) terem proposto modelos costeiros baseados em ambientes onde a sedimentação é controlada por um único processo deposicional dominante, as litofácies geradas em sistemas costeiros tendem a apresentar características mistas (Boyd *et al.*, 1992; Dalrymple *et al.*, 2006), onde grande parte é influenciada por mais de um processo sedimentar e pela combinação de fluxos. Boyd *et al.* (1992) propuseram um diagrama triangular, cujos vértices mostram os principais fatores atuantes no sistema costeiro (rios, ondas e marés). Este diagrama classifica os ambientes deposicionais costeiros baseado nos processos dominantes que controlam o transporte e a deposição sedimentar, além de incluir aspectos morfológicos destes sistemas. Yang *et al.* (2005) modificaram este diagrama diversificando a porção entre os vértices de maré e onda, inserindo os sistemas deposicionais de costas dominadas por onda, praias de maré (*tidal beach*), planícies de maré aberta (*open-coast tidal flat*) e planícies de maré aberta dominadas por maré (Figura).

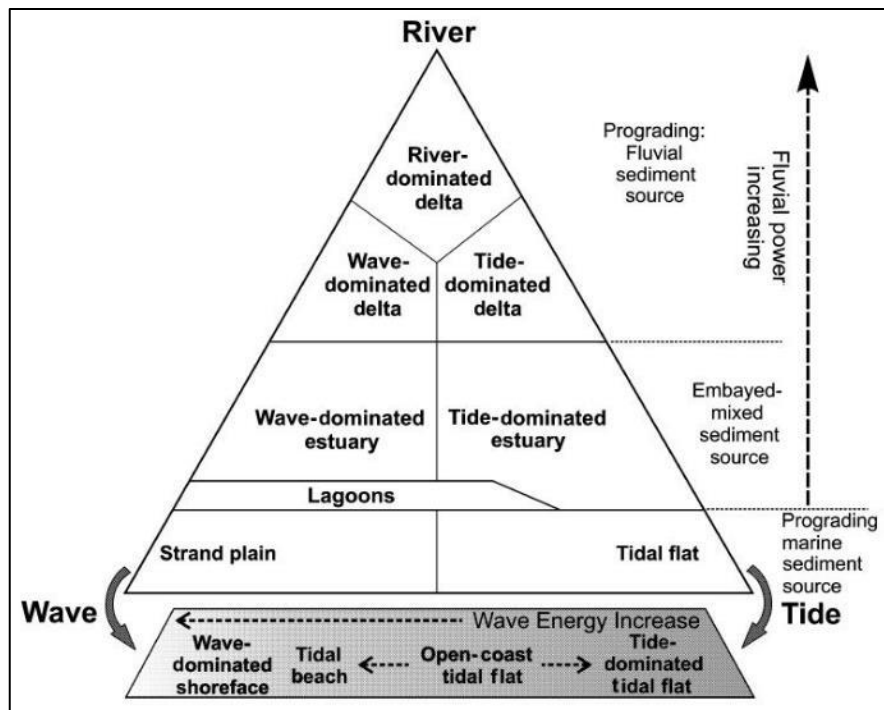


Figura 6: Classificação dos ambientes clásticos costeiros retirado de Yang *et al.* (2005), modificado de Boyd *et al.* (1992).

Curray (1964) apresentou uma classificação dos sistemas costeiros baseada no comportamento transgressor ou regressivo da linha de costa. O autor plotou os parâmetros de subida e queda relativa do nível do mar de encontro à erosão e

deposição para identificar tipos de regressão e transgressão (Figura 7). Boyd *et al.* (1992) utilizou desse estudo para distinguir entre dois grupos de sistemas deposicionais sedimentares (transgressivos e regressivos) e elaborou também uma representação gráfica para a distribuição destes sistemas nas linhas de costas transgressivas e regressivas, com a variação lateral da contribuição das marés e das ondas (Fig.8). O autor afirma que a classificação sedimentológica e estratigráfica dos ambientes costeiros pode ser embasada nos conceitos de transgressão e regressão, aliados ao grau de influência das ondas, marés e rios.

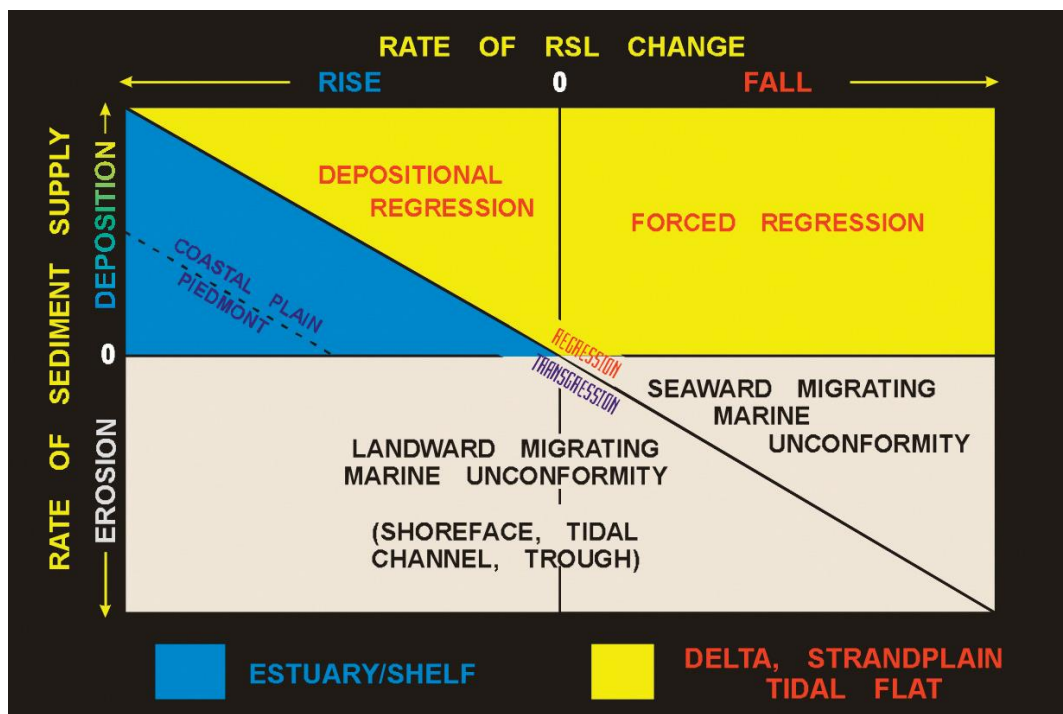


Figura 7: Diagrama relacionando as taxas de subida e queda do nível relativo do mar contra taxas de erosão e deposição, permitindo a discriminação de costas transgressivas das regressivas, e também das costas onde há deposição (metade superior) daquelas onde há erosão (metade inferior). Quanto maior a distância dos campos de equilíbrio dos ambientes em relação a diagonal transgressão/regressão, maior a taxa de transgressão ou regressão. Retirado de Boyd *et al.*(2010).

Quando a taxa de suprimento sedimentar excede a taxa de elevação do nível do mar, ou na acumulação de sedimentos durante a queda do nível do mar (área amarela da Figura), a morfologia da costa durante a regressão pode ser de costas alongadas/lobuladas (deltas) ou lineares (planícies costeiras ou de maré) (porção inferior da figura 8). A interação entre o aporte sedimentar fluvial e a influência dos processos marinhos na redistribuição dos sedimentos irá determinar se a costa será alongada/lobulada ou linear (Fisher *et al.*, 1969; Galloway, 1975). Quando a taxa de elevação do nível do mar relativo exceder o aporte sedimentar (área azul na figura 7), transgressão resulta na geração de estuários e lagoas nas costas com baías. A linha de costa move-se em direção ao continente, migrando de maneira linear em

toda a costa, formando planícies de maré e planícies costeiras (porção superior da figura 8).

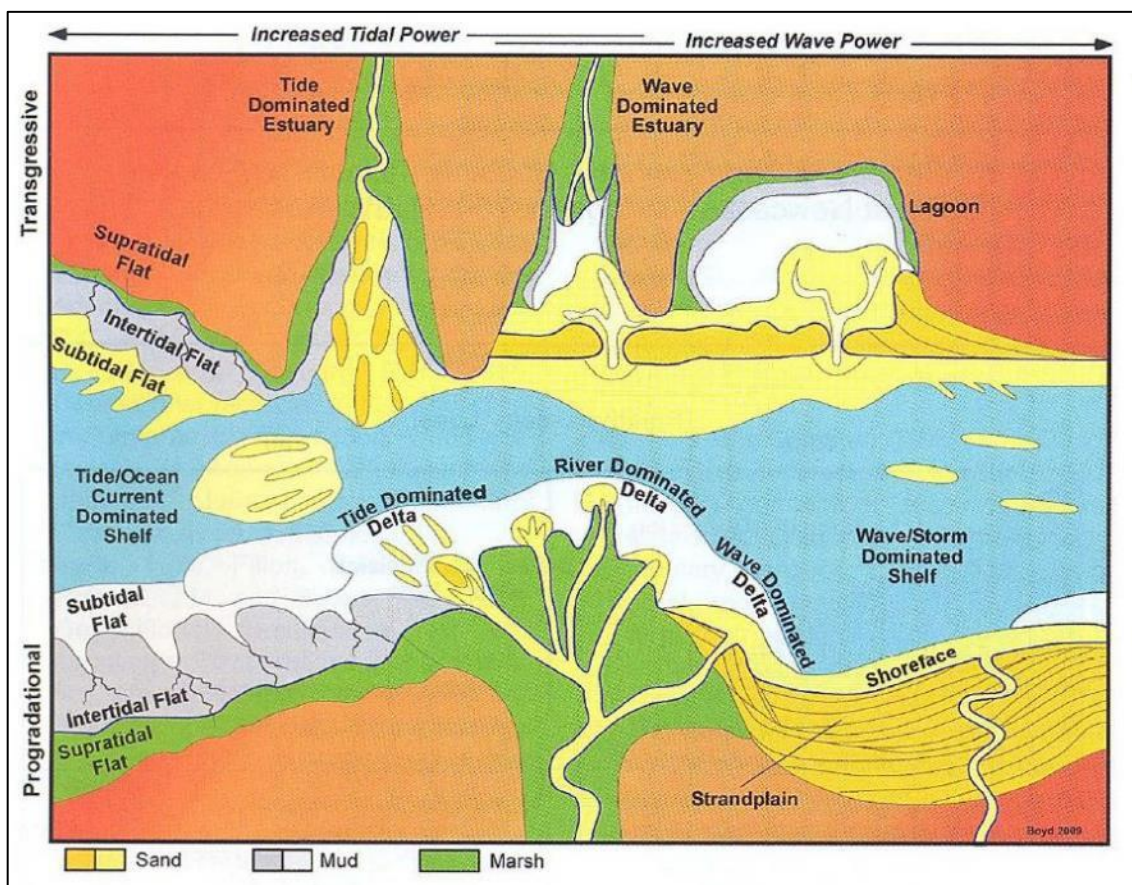


Figura 8: Caracterização dos ambientes costeiros baseada na movimentação da linha de costa (transgressão/regressão), atuação da ondas, das correntes de maré e dos sistemas fluviais. A porção superior representa uma linha de costa transgressiva, enquanto a inferior uma linha de costa regressiva. A influência das marés aumenta da direita para esquerda, enquanto que das ondas da esquerda para direita. Retirado de Boyd et al.(2010).

Há um consenso sobre as características dos depósitos nas regiões costeiras quando se trata individualmente os processos relacionados a rios, marés ou ondas. Os depósitos resultantes da ação de ondas e as correntes geradas por elas, bem como os processos cíclicos que as marés produzem, são ricos em estudos e modelos, bem como os relacionados a sistemas fluviais. Entretanto, apesar de vários estudos em sistemas costeiros atuais, não há modelos conceituais relacionados aos produtos gerados a partir da combinação destes processos, nem como é a distribuição e deposição dos sedimentos resultantes destes fluxos combinados.

3. Referências Bibliográficas

ALKMIM, F. F., BRITO NEVES, B. B., ALVES, J. A. C.; 1993. **Arcabouço tectônico do Cráton do São Francisco – uma revisão.** In: DOMINGUEZ, J. M. L., MISI, A. (Eds.), O Cráton do São Francisco, SBG, SGM, CNPq, Salvador, p. 45–62.

- ALKMIM, F. F., MARTINS-NETO, M. A.; 2011. **Proterozoic first-order sedimentary sequences of the São Francisco Craton, eastern Brazil.** Marine and Petroleum Geology, v. 33, p. 127-139.
- ALKMIN, F. F., MARSHAK, S.; 1998. **Transamazonian Orogeny in the Southern São Francisco Craton region, Minas Gerais, Brazil: evidence for Paleoproterozoic collision and collapse in the Quadrilátero Ferrífero.** Precambrian Research, v. 90, p. 29-58.
- ALMEIDA, F.F.M.; 1977. **O Cráton do São Francisco.** Revista Brasileira de Geociências, v.7, p. 349-364.
- BOYD R.; DALRYMPLE R.W.; ZAITLIN B.A.; 1992. **Classification of clastic coastal depositional environments.** Sedimentary Geology, v.80, p. 139-150.
- BRITO NEVES, B.B. de; 1967. **Geologia das Folhas de Upamirim e Morro do Chapéu.** Relatório Técnico. Recife: CONESP, v.17, 53p.
- CAMPOS NETO, M. C.; 2000. **Orogenic Systems from Southwestern Gondwana: an approach to Brasiliano-PanAfrican Cycle and Orogenic Collage in Southeastern.** In: CORDANI, U. G., MILANI, E. J., THOMAZ FILHO, A., CAMPOS, D. A. (Eds.) Tectonic Evolution of South America. Rio de Janeiro, 31º IGC, p. 335-365.
- CHEMALE Jr., F., DUSSIN, I. A., ALKIMIM, F. F., MARTINS, M. S., QUEIROGA, G., ARMSTRONG, R., SANTOS, M .N.; 2012.; **Unravelling a Proterozoic basin history through detrital zircon geochronology: The case of the Espinhaço Supergroup, Minas Gerais, Brazil.** Gondwana Research 22, 200-206.
- CRUZ, S. C. P., ALKMIM, F. F.; 2006. **The tectonic interaction between the Paramirim Aulacogen and the Araçuaí Belt, São Francisco Craton region, Easter Brazil.** Anais da Academia Brasileira de Ciências, v. 78, n. 1, p. 151-174.
- CURRAY, J.R.; 1964. **Transgressions and regressions.** In: MILLER, R.I. (ed.), Papers in Marine Geology, Shepard Commemorative Volume. Macmillan, New York, N.Y., p. 175-203.
- DALRYMPLE R.W.; YANG B.C.; CHUN S.S.; 2006. **Sedimentation on a wave-dominated, open coast tidal flat, south-western Korea: Summer tidal flat-winter shoreface.** Sedimentology, v.53, p. 693-696.
- DALRYMPLE R.W.; ZAITLIN B.A.; BOYD R.; 1992. **Estuarine facies models: conceptual basis and stratigraphic implications.** Journal of Sedimentary Petrology, v.62, p. 1130-1146.
- DAVIS JR. R.A. e FITZGERALD D.M.; 2004. **Beaches and Coasts.** Malden, Blackwell Publishing, 419 p.
- DOMINGUEZ, J.M.L.; 1996. **As coberturas plataformais do Proterozóico Médio e Superior.** In: BARBOSA, J.S.F.; DOMINGUEZ, J.M.L. (coords.) Geologia da Bahia: texto explicativo para o mapa geológico ao milionésimo. Salvador: Secretaria da Indústria, Comércio e Mineração/Superintendência de Geologia e Recursos Minerais, 400p.
- ESPÍNDOLA, E.; 2013. **Arquitetura de facies e evolução estratigráfica do sistema fluvi-estuarino da Formação Morro do Chapéu – Bahia.** Trabalho de conclusão de curso, 92p. Curso de Geologia, Instituto de Geociências - Universidade Federal do Rio Grande do Sul.
- FISHER, W.L.; BROWN, L.F.; SCOTT, A.J.; MCGOWEN, J.H.; 1969. **Delta Systems in the Exploration for Oil and Gas.** Bur. Econ. Geol., University of Texas, Austin, 78 p.

- GALLOWAY, W.E.; 1975. **Process framework for describing the morphologic and stratigraphic evolution of deltaic depositional systems.** In: BROUSSARD, M.L. (ed.), Deltas - Models for Exploration. Houston Geol. Soc., Houston, Texas, p. 87-98.
- GUADAGNIN, F., CHEMALE, F., MAGALHÃES, J., SANTANA, A., DUSSIN, I., TAKEHARA, L., 2015; **Age constraints on crystal-tuff from the Espinhaço Supergroup – Insight into the Paleoproterozoic to Mesoproterozoic intracratonic basin cycles of the Congo-São Francisco Craton.** Gondwana Research, v. 27, 363-376.
- GUIMARÃES, J.T.; PEDREIRA, A.J.; 1990. **Programa de Levantamentos Geológicos Básicos do Brasil – PLGB. Utinga - Folha SD.24-V-A-II, Estado da Bahia, Escala 1:100.000.** Texto Explicativo. Brasília: DNPM.
- MONTES, A.S.L.; 1977. **O Contexto Estratigráfico e Sedimentológico da Formação Bebedouro na Bahia: Um Possível Portador de Diamantes.** Brasília. Dissertação (Mestrado), 100p. Instituto Geociências - Universidade de Brasília.
- PEDREIRA, A. J.; DOSSIN, I. A.; UHLEIN, A.; DOSSIN, T. M.; GARCIA, A. J. V.; 1989. **Kibaran (Mid-Proterozoic) evolution and mineralizations in Eastern Brazil.** Newsletter, v. 2, p. 57-63.
- PEDREIRA, A.J.; 1988. **Sequências Depositionais no Precambriano: Exemplo da Chapada Diamantina Oriental.** In: Congresso Brasileiro de Geologia (35:1988), Goiânia. Anais do ... Belém, SBG, v.2, p. 648-659.
- PEDREIRA, A.J.; ARCANJO, J.B.A.; PEDROSA, C.J.; OLIVEIRA, J.E.; SILVA, B.C.E.; 1975. **Projeto Bahia: Geologia da Chapada Diamantina.** Texto e mapas. Relatório final. Salvador: CPRM.
- READING, H.G.; 1996. **Sedimentary Environments: Processes, Facies and Stratigraphy 3rd edition.** Blackwell Science, Oxford, 704p.
- SANTOS, M. N., CHEMALE Jr., F., DUSSIN, I. A., MARTINS, M., ASSIS, T. A. R., JELINEK, A. R., GUADAGNIN, F., ARMSTRONG, R.; 2013. **Sedimentological and paleoenvironmental constraints of the Statherian and Stenian Espinhaço rift system, Brazil.** Sedimentary Geology 290, 47-59.
- SCHOBENHAUS, C.; 1996. **As Tafrogêneses superpostas Espinhaço e Santo Onofre, Estado da Bahia: Revisão e notas propostas.** Revista Brasileira de Geociências, v. 4, p. 265-276.
- TORQUATO, J.R. e FOGAÇA, A.C.; 1981. **Correlação entre o Supergrupo Espinhaço no Brasil, Grupo Chela em Angola e as Formações Nosib e Khoabendus da Namíbia.** In: SIMPÓSIO SOBRE O CRÁTON DO SÃO FRANCISCO E SUAS FAIXAS MARGINAIS (1981), Salvador. Anais do... Salvador, SBG/SME/COM, p. 87-98.
- WEIL, A. B., VAN DER VOO, R., MAC NIOCAILL, C & MEERT, J. G.; 1998. **The Proterozoic supercontinent Rodinia: paleomagnetically derived reconstruction for 1100 to 800Ma.** Earth and Planetary Science Letters, v. 154, p. 13-24.
- YANG, B.C.; DALRYMPLE, R.W.; CHUN, S.S.; 2005. **Sedimentation on a wave-dominated, open coast tidal flat, south-western Korea: summer tidal-flat - winter shoreface.** Sedimentology, v.52, p. 235-252.

CAPÍTULO II

Acknowledgement of receipt of your submitted article ▶ Caixa de entrada x



Sedimentary Geology <eesserver@eesmail.elsevier.com>
para eu, ezequiel.zaza ▾

qua, 18 de jul 15:23 (Há 1 dia)



✉ inglês ▾ > português ▾ Traduzir mensagem

Desativar para: inglês x

Dear Mr. Galvão de Souza,

Your submission entitled "MESOPROTEROZOIC GLACIATIONS: NEGLIGENCED OR UNKNOWN SEDIMENTARY STRUCTURES?" has been received by Sedimentary Geology.

Your paper will be considered as belonging to the category Research Paper. Please contact us if this is not correct.

Please note that submission of an article is understood to imply that the article is original and is not being considered for publication elsewhere. Submission also implies that all authors have approved the paper for release and are in agreement with its content.

You will be able to check on the progress of your paper by logging on to <https://ees.elsevier.com/sedgeo/> as Author.

Your manuscript will be given a reference number in due course.

Thank you for submitting your work to this journal.

Kind regards,

Elsevier Editorial System

◀ Responder

◀ Responder a todos

▶ Encaminhar

1 **Title:** MESOPROTEROZOIC GLACIATIONS: NEGIGENCED OR UNKNOWN

2 SEDIMENTARY STRUCTURES?

3 **Authors name and filliations:**

4 Ezequiel Galvão de Souza^{1*}, Claiton Marlon Santos Scherer¹, João Pedro Formolo

5 Ferronatto¹, Adriano Domingos dos Reis¹, Carrel Kfumbi¹, Manoela Bettarel Bállico²

6 ¹ Instituto de Geociências – Universidade Federal do Rio Grande do Sul (UFRGS),

7 Campus do Vale. Av. Bento Gonçalves, 9500, Porto Alegre/RS, CEP 91509-900, Brazil.

8 ² Departamento de Geociências – Universidade Federal de Santa Catarina (UFSC),

9 Campus Universitário. Florianópolis/SC, CEP 88040-900, Brazil.

10 *** Corresponding author mailing address:** Instituto de Geociências – Universidade Federal
11 do Rio Grande do Sul (UFRGS), Campus do Vale. P.O. Box 15001, Porto Alegre, Rio
12 Grande do Sul, CEP 91509-900, Brazil.

13 E-mail: ezequiel.geol@gmail.com – Phone number: +55-51-33086372

14

15 **Abstract**

16 The Neoproterozoic glacial events are well known in the bibliography, while there are few
17 studies of Mesoproterozoic glacial events, a period characterize as a time of greenhouse
18 conditions and where glaciations with local occurrence could exist. However, the facies
19 analyze of Morro do Chapéu Formation focusing in basal conglomerates lead to a new
20 interpretation of these deposits. The wide range of debris-flow structures with superimposed
21 conglomerates and coarse-grained sandstones suggests a glacial induced jet-flux
22 depositional model. Despite the lack of direct radiometric constraints, the location of these
23 deposits at São Francisco Craton during a Mesoproterozoic interval (1.1 to 0.9 Ga) converge
24 with paleomagnetism studies for this same interval, which place this craton in high southern
25 palaeolatitudes. These deposits associated with others examples of Mesoproterozoic
26 suggests that the glaciations during this period was limited in high southern latitudes.

27 **1. Introduction**

28 Existing age constraints suggest that the Precambrian ice ages were episodic rather than
29 continuous, with a series of temporally discrete glaciation events occurring at the beginning
30 and end of the Proterozoic Eon (cf. Kaufman et al., 1997; Kennedy et al., 1998; Walter et al.,
31 2000; Kendall et al., 2004; 2006, Geboy et al., 2013). There is little to no evidence for
32 continental ice sheets of any kind during the intervening billion years, suggesting climatic
33 stability during this period (flippantly termed the “boring billion”, Planavsky et al., 2015).
34 Meanwhile, the late Proterozoic was characterized by extreme climatic volatility as registered
35 by the stratigraphic record of repeated low-latitude glaciations of unparalleled scale and
36 severity (Lyons et al., 2012; Knoll, 2014; Planavsky et al., 2015).

37 However, the lower part of the Morro do Chapéu Formation (late Mesoproterozoic) show
38 stronger evidences of glacial events, which led this study to describe a sedimentary facies
39 complex that forms part of a smaller glaciomarine coarse-grained sediment system. It is
40 inferred to have been deposited under the ice-proximal conditions of a jet-dominated
41 meltwater outflow at the east margin of the Morro do Chapéu Formation.

42 Two opposing well-known hypotheses in explanation of Proterozoic low-palaeolatitude
43 glaciation present contrasting scenarios for the climate system on the Proterozoic Earth - the
44 "snowball Earth" and "high obliquity" hypotheses. Although, paleomagnetic reconstructions
45 place the São Francisco craton at high southern latitudes (45 to over 60° S) in the late
46 Mesoproterozoic (Weil et al., 1998; Pesonen, et al., 2003; Tohver et al., 2006), allowing the
47 possibility that the glaciations of the Morro do Chapéu formation were local rather than global
48 in extent.

49 In the present contribution, we re-evaluate the interpretation of the basal conglomerates of
50 Morro do Chapéu formation, which was previously interpreted to be deposited by braided
51 rivers (Brito Neves, 1967; Pedreira, 1986; Battilani, 1996; Rocha, 1997; Espíndola, 2013).
52 The employ of late sedimentological parameters lead to interpret the deposits as proximal
53 grounding-line systems. These deposits lead to identify the position of a glacial terminus
54 through the time, due to their direct relationship with meltwater discharges emanating from
55 subaqueous subglacial tunnels, thus supporting paleogeographic and paleoclimatic
56 reconstructions studies in glaciated basins (e.g. Koch and Isbell, 2013).

57 **2. Geological setting**

58 The study area is located in the central zone of the São Francisco Craton (Almeida et al.,
59 1977; Fig.1A), in particular in the Chapada Diamantina Domain (Fig. 1B and C). This paper
60 focuses in the Morro do Chapéu Formation (Brito Neves, 1967), which is part of the Upper
61 Megasequence of the Espinhaço Supergroup (Fig. 1D). The Espinhaço Supergroup is
62 organized in three megasequences (termed the Lower, Middle and Upper sequences) that
63 accumulated in numerous basins developed in response to at least two phases of rifting
64 (Chemale et al., 2012; Santos et al., 2013; Guadagnin et al., 2015). The Espinhaço
65 Supergroup has an age c. 1.75 - 0.9 Ga based on radiometric age constraints
66 (Schobbenhaus et al., 1994; Babinski et al., 1999).

67 The Lower Megasequence (1.8 to 1.68 Ga), represented by Rio dos Remédios Group,
68 contains aeolian and alluvial sediments interbedded with alkaline acid lavas and tuffs of the
69 Novo Horizonte Fm. Siliciclastic rocks of the Ouricuri do Ouro and the Lagoa de Dentro

70 formations cover these deposits (Guimarães et al., 2005; Alkmim & Martins-Neto, 2012;
71 Guadagnin et al., 2015). The Middle Megasequence (1.6 to 1.38 Ga) comprise a rift-sag
72 basin initiated with aeolian and wadi deposits of the Mangabeira Formation that was follow
73 by transgressive shallow-marine to high-stand deltaic sediments of the Açuá Formation
74 (Guimarães et al., 2005). The fluvial and tide-dominated estuarine sediments of Tombador
75 Formation were accumulated unconformably over the Açuá Formation and represents the
76 sedimentation during the sag stage of the basin (Guadagnin et al., 2015; Fig. 1D).

77 The Caboclo and Morro do Chapéu formations form the Upper Megasequence (1.19 to
78 0.9 Ga) of the Espinhaço Supergroup at Chapada Diamantina Range. The coastal to
79 shallow-marine deposits of the Caboclo Formation were dated by Pb-Pb method as $1,140 \pm$
80 140 Ma in age (Babinski et al., 1993). Guadagnin et al., (2015) interpreted this marine
81 sequence as transgressive and displayed a paraconformable contact with the underlying
82 deposits of the Tombador Fm. According to this author, these deposits result from intraplate
83 sedimentation associated with the compressional tectonics at the margins of the Congo
84 Craton (Kokonyangi et al., 2006; De Waele et al., 2008; Fernandez-Alonso et al., 2012).

85 Three outcrops of Morro do Chapéu Formation have been described in detail and
86 organized in columnar sections (Fig. 1C). The outcrops are located across the three major
87 rivers of the city. The basal contact between the Morro do Chapéu and the Caboclo Fms. is
88 irregular while the upper contact with the Bebedouro Fm. is of tectonic origin, and
89 characterized by a thrust fault that separate the Morro do Chapéu Fm. and the São
90 Francisco Supergroup at the studied area (Schobbenhaus, 2012).

91 **3. Glacial features**

92 The facies of Morro do Chapéu Formation are described in Table 1, but some facies have
93 interesting features that need to be detailed here. In this context, it can be highlighted the
94 conglomerates located at the base of Morro do Chapéu Formation and their wide variety of
95 structures. The basal conglomerates occur restricted in sections 1 and 2 (Fig. 1C) and the
96 previous authors not described them in another areas too. They are disposed in two thin
97 layers (< 1.5 m) intercalated with sandstones and forming thick packages (< 6 m), which

superimpose each other compounding a ≈ 20 m thick section. Structures detailed here constitute a series of characteristics that are fundamental to corroborate the interpretation of facies association and depositional system, such as: 1) outsized-clasts; 2) faceted and polished clasts; 3) dropstone and load structures; 4) incipient turbate and dewatering structures; and 5) small limited fractures.

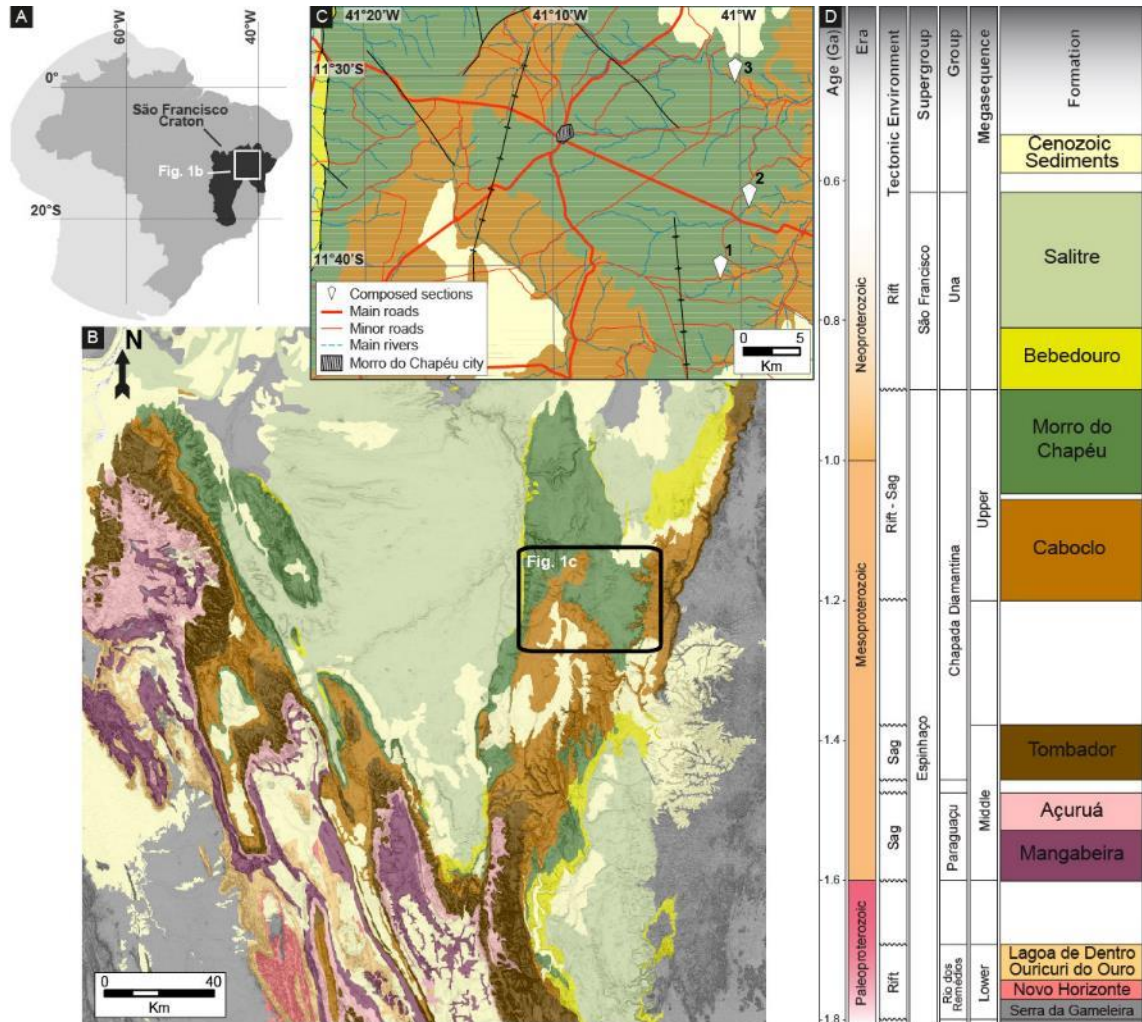


Fig. 1: A) Location of São Francisco Craton (in black) and position of Chapada Diamantina Domain indicated with a white square. B) Simplified geological map of the Chapada Diamantina Domain, based on data of Brazilian Geological Survey (CPRM). The dark green colour represents Morro do Chapéu Formation and the study area is indicated with a black square (Low-deformed part of Chapada Diamantina domain). C) Localities of the four studied composed cross-sections and the city. D) Schematic diagram of stratigraphic units and proterozoic megasequences of the Espinhaço Supergroup ate the Chapada Diamantina Range.

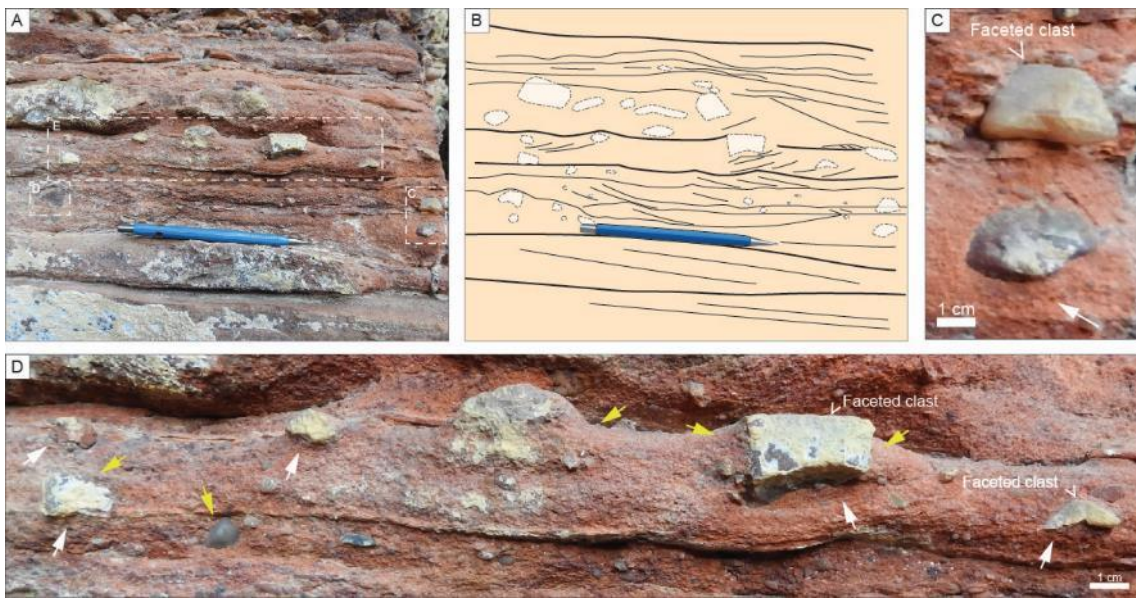
111 3.1. Outsized-clasts:
 112 Pebbles to boulders (< 35 cm) scattered and isolated at sandstones and conglomerates,
 113 frequently with flat horizontal surfaces (see details of figures 2, 3, 4 and 5). Sometimes these
 114 clasts occupy the top of layers and therefore becomes protruding in layers above, which
 115 drape the lamination over the clasts (Fig. 3G and 4D). These clasts could be interpreted as
 116 float clasts resulting from hyperconcentrated flows (Mulder & Alexander, 2001), common in
 117 subaqueous outwash systems in a proglacial context (Aquino et al., 2014; Rust, 1977; Cheel
 118 and Rust, 1986). Nevertheless, some of these clasts also could be presented as a
 119 dropstones, but due to the high energy of the flow, these clasts could be easily reworked by
 120 the meltwater flows after dumped on the substrate (Aquino et al., 2014; Lønne, 1995). The
 121 protruding clasts draped by layers above could be interpreted as water-laid cavity fill as a
 122 result of meltwater activity beneath the stagnant ice (Krüger & Kjaer, 1999).

123 **Table 1:** Facies of Morro do Chapéu Formation.

Facies	Code	Description	Interpretation
Matrix-supported massive conglomerate	Gsm	Matrix-supported, massive, poorly sorted granule to cobble (<20cm) gravel conglomerate, with chaotic organization and outsized clasts (boulders < 35 cm). Sometimes the clasts are imbricated or with vertical orientation. Scattered protuberant clasts occur at the upper part of strata. The clasts are subrounded to angular with variable sphericity and with a wide range of shapes including tabular/discoid, ball-shaped and elongated shapes. Facetted and polished surfaces occurs. Composition varies: volcanic rocks, white and pink quartzites, conglomerates, sandstones and quartz. The matrix is poorly sorted with sand to granule size and occasionally with granule lenses. The larger clasts have subangular shape and low sphericity.	Debris flows with outsized, vertical and protuberant clasts. The faceted and polished pebbles characteristics suggests intense abrasion. The vertical orientation and the deformed underlying lamination suggests dropstones accumulations.
Clast-supported conglomerate	Gcm	Clast-supported, massive to crudely stratified, poorly sorted pebble to boulder (< 40 cm) gravel, polymictic conglomerate. The clasts are well rounded to subangular, with low sphericity showing punctual to facetted contact between them. Outsized clasts occurs locally. The beds are continuous and with undulated bases, sometimes occurring in lenses.	Rapid sedimentation of coarse sediment from turbulent flows, heavily sediment-laden surges of floodwater with little or no traction, attributed to hyper-concentrated flows.
Crudely stratified pebbly sandstone	Sgs	Red to brown, medium- to coarse-grained, poorly sorted, massive to crudely stratified pebbly	Deposition from hyper-concentrated flows with traction

			sandstone. The pebbles are subrounded to angular with low sphericity. Sometimes they are faceted or fractured, locally showing vertical orientation of the long axe. Beds contain numerous clasts from granule to pebble-size deforming underlying lamination. Thin layers (2 cm) of symmetric ripple cross-laminated, fine-grained sandstones occurs. The lower limits of bedforms are irregular and frequently erosive.	processes. The faceted and polished pebbles characteristics suggests intense abrasion. The vertical orientation and the deformed underlying lamination suggests dropstones structures. The fine-grained sandstones represent low-energy stages where oscillatory flow occurred.
Massive sandstone	Sm		Light orange to light red, medium- to coarse-grained, poorly sorted, massive sandstone, with sparse granules and pebbles (< 3cm). Stratification thickness from 0.2 to 0.5 m thick.	Deposition from hyper-concentrated flows.
Low angle laminated sandstone	Sl		Light cream to light red, fine- to medium-grained, poorly sorted sandstone, with low angle lamination (<15°). Internally contain mudstone clasts, sparse granules and coarse sand, sometimes forming discrete levels (<1cm). Sets with 0.2 m thick.	Migration of bedforms with a high wavelength/amplitude ratio in transitional conditions between lower and upper flow regime.
Sigmoidal cross-stratified sandstone	Ss		Light brown, well-sorted, medium grained sandstone with small-scale (< 0.6 m thick) sigmoidal cross stratification. Locally granules on the foresets and sparse mudclasts.	Migration of sinuous-crested bedforms under unidirectional decelerating tractive flow, with high sediment rate in lower flow regime.
Trough cross-stratified sandstone	St		Light cream to light red, medium- to very coarse-grained, moderate sorted sandstone, with medium- to small-scale trough cross-stratification (0.1 to 1 m thick). Mudclasts, granules and pebbles in lenses, or along the bedforms foresets and bottomsets.	Migration of sinuous-crested subaqueous bedforms (3D), lower flow regime.
Tidal bundled trough cross-stratified sandstone	Stm		Light cream to light brown, medium to coarse-grained, moderate sorted sandstone with medium- to large-scale trough cross-stratification (0.3 to 1.5 m thick), frequently fluidized and with reactivation surfaces. Mudclasts and pebbles occur sparse or concentrated at the base of bedforms. Commonly exhibit foresets and sets bounded by mud drapes with thickness variations (0.5 to 3 cm) regularly spaced (3 to 40 cm).	Migration of tidal influenced sinuous-crested subaqueous bedforms (3D) under lower flow regime alternating ebb and flood-related sedimentation.
Planar cross-stratified sandstone	Sp		Light red, medium well-sorted sandstone with small-scale tabular cross stratification (<0.4 m).	Migration of straight-crested subaqueous bedforms (2D); lower flow regime.
Ripple cross-laminated sandstone	Sr		Light red to light cream, very fine- to medium-grained, well-sorted sandstone, with asymmetric ripple cross-lamination. Usually occurs as discrete layers on top of facies St or Sl. Well defined concave upward lee side and convex upward stoss side. Sinuous crestline bifurcated frequently. Wavelength = 4 to 6 cm.	Migration of subcritical to supercritical ripples under unidirectional lower flow regime.

Swaley cross-stratified sandstone	Scs	Light red, medium- to coarse-grained sandstone with cut and fill structures. Small-scale bedforms (< 60 cm) with undulated edges (wavelength < 1.2 m) and internally composed by low-angle and/or trough/sigmoidal cross-stratification and sparse mudclasts. Frequently with symmetric and asymmetric ripples at the base of foresets.	Migration of medium-scale bedforms with a high wavelength / amplitude ratio in conditions of combined flows regime. A continuous range of structures exists between symmetrically (low-angle) filled swales and associated trough cross-strata.
Wave ripple cross-laminated sandstone	Sw	Light cream, well-sorted, fine- to medium-grained sandstone with symmetrical and asymmetrical wavy ripple cross-lamination. The lee side is slightly concave-upward while stoss side has rounded convex-upward geometries. The internal truncated lamination varies the dip angle of the foresets. Sometimes the both stoss and lee side are concave-upward geometries, with straight crestline frequently showing two directions.	Wave-ripples migration under lower flow regime. The geometries vary because of combined flow conditions, where the behavior of vortex depends on the ratio between oscillatory and unidirectional components and determines the nature of the ripple external profile and internal lamination. The crestline with two directions represents interference wave-ripples.
Accretionary hummocky cross-stratified sandstone	Hcs	Light cream, well sorted, graded, medium- to coarse-grained sandstone. The individual beds are 1.3 m thick with common lateral thickness variations. The basal contact of the beds is sharp but non-erosive, and the top surfaces are undulated (wavelength = 0.8 to 4m). Internally the beds display milimetric laminae, generally with low angle in the lower portion of the bed, being progressively wave upwards. The thickness of each lamina increases laterally below the hummocks. The bedforms limits exhibit symmetrical and asymmetrical ripples, with a thin mudstone layer that covers the top of the beds. Locally granules and pebbles at the base of massive sandstone lenses.	Migration of large bedforms with a high wavelength / amplitude ratio in conditions of combined flows regime, without strong erosional currents.
Heterolithic mudstone and sandstone	Ht	This facies forms thick tabular beds (< 4 m) with broad lateral extent, which can commonly be traced over tens of meters. Interbedding of very-fine laminated sandstone and mudstone in millimetric to centimetric layers. Sandy laminae are massive or with ripple marks with deposition of mudstone in the ripple troughs. Mudstone exhibits sandy wavy lamination.	Alternation between deposition from traction and from suspension by wave action reworked.
Massive siltstone	Fm	Red to dark red, massive or crudely horizontally laminated siltstone, organized in 0.1 to 1.7 m lamina and strata.	Deposition from suspension and weak tractive flows.
Laminated mudstone	Fl	Reddish claystone to very fine sandstone, horizontal milimetric lamination. Sometimes in plain view sinusoidal or irregular reticulated cracks occur.	Deposition from suspension and weak bottom currents. The cracks result from synaeresis cracks.



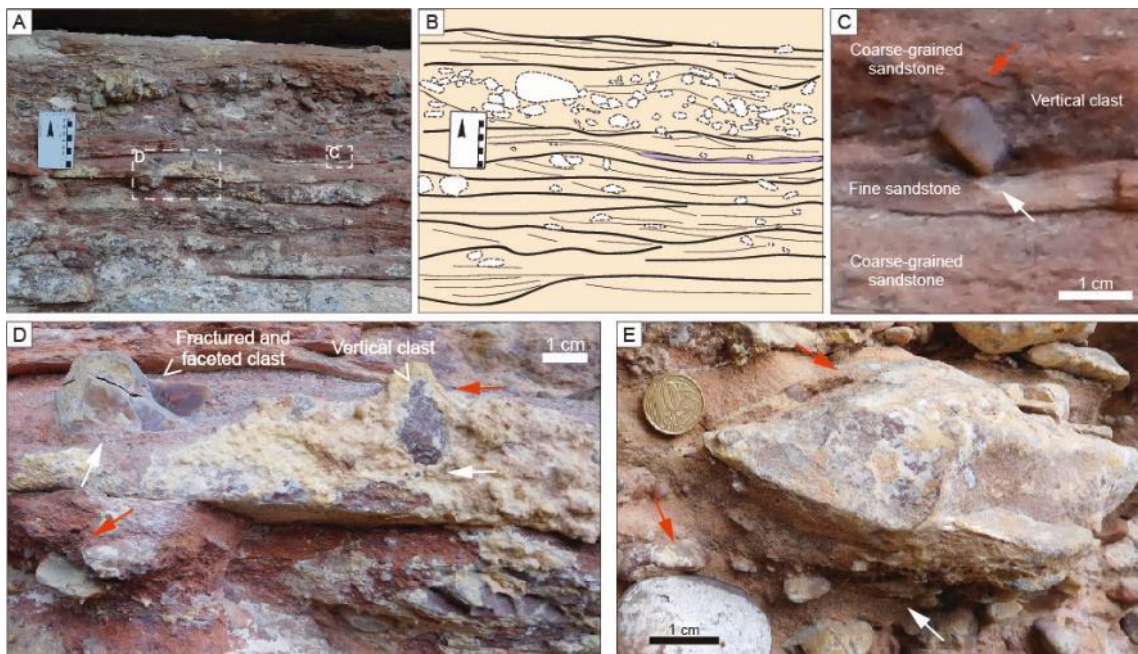
124 Fig. 2: A) Crudely stratified pebbly sandstone facies (Sgs) with other photos in dashed squares; B)
 125 Draw representing the main structures, note the alternate between tractive forms and scattered
 126 pebbles with bottom lamination deformed; C) Faceted clasts with bottom deformed lamination (white
 127 arrow); D) A level with outsized-clasts where the bottom lamination are deformed (white arrows) and
 128 some clasts overlaid by the top lamination (yellow arrows).

129 3.2. Faceted and polished clasts:

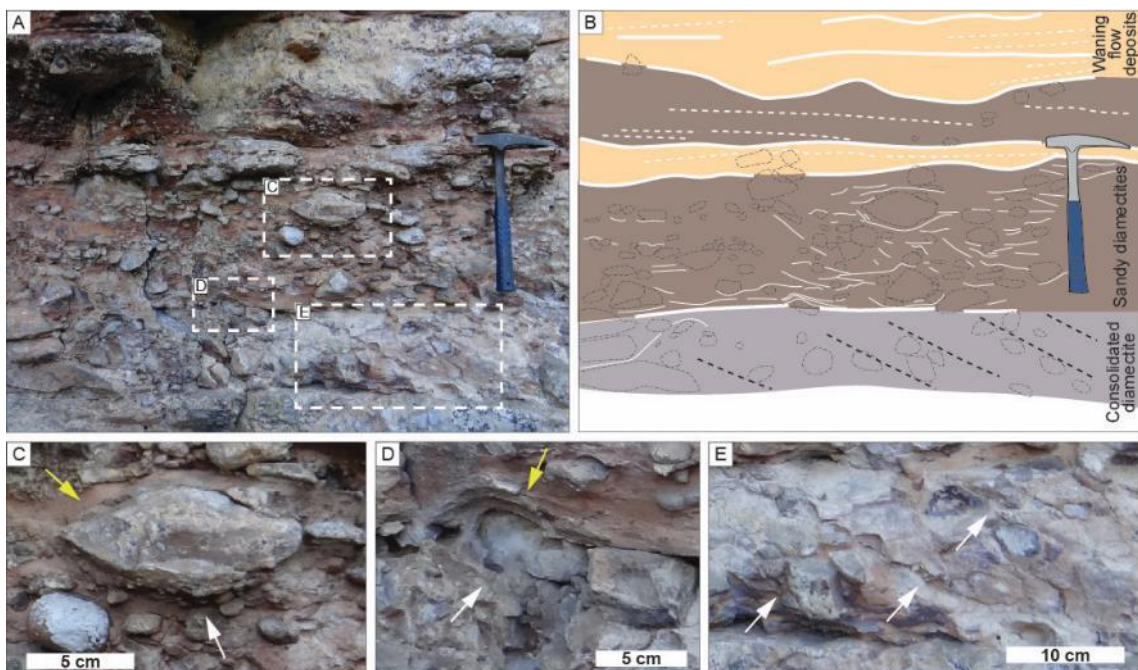
130 Associated to outsized-clasts, there are clasts within the gravel size range (< 26 cm),
 131 angular to sub-rounded with several well rounded ones (Fig. 5G). The bigger clasts are
 132 better rounded and very polished, which prevails quartzite composition (Fig. 4C and 6). The
 133 angular to sub-rounded clasts are faceted and polished too, sometimes with bottom and top
 134 flat surfaces (Fig. 5F and H). Of these, an aspect that stand out are some pebbles with
 135 bottom and top flat surfaces hosted in well-sorted sandstones. The sandstone overlays the
 136 pebble, which is isolated and aligned with the bed edge (Fig. 5H). This pebble shows a slight
 137 difference between the lateral faces, likely a bullet-shaped clast (Chakraborty & Ghosh,
 138 2008). The predominance of subangular and subrounded clasts, including, faceted, and
 139 bullet-shaped examples, are indicative of sediment that has been transported by wet-based
 140 glaciers in the zone of traction (cf. Boulton, 1978).

141 These characteristics associated with striated clasts are frequently described as product
 142 of glacial processes (Aquino et al., 2014; Brezinski et al., 2008; Ravier et al., 2014), although
 143 can occur in debris-flow too. Despite the lack of striated clasts in the deposits, faceting and
 144 polish are important features about the sedimentary processes intensity, besides being

145 typical primarily of glacial deposits (Schermerhorn, 1974; Brezinski et al., 2008). The high
 146 polish degree and the abundant occurrence of faceted clasts indicate a high level of abrasion



147 **Fig. 3:** All photos are of crudely stratified pebbly sandstone facies (Sgs), the white arrows show the
 148 bottom deformed lamination, while the red arrows show the overlaid by top lamination. Note the
 149 occurrence of fine-grained sediments (dark pink in B and described in C) and the occurrence of
 150 isolated vertical clasts.



151 **Fig. 4:** Stacking pattern of conglomerates and interpretative drawing (A and B) with glacial features
 152 denoted with white dashed squares. C) Outsized-clast deforming underlying lamination. D) Protunding
 153 clast (white arrow) draped by the upper lamination (yellow arrow); E) Small limited fractures in Gcm
 154 facies (white arrows).

155 suffer by the clasts, due to clast-to-clast or clast-floor contact. During movement of debris
156 flows, inter-particle abrasive forces are minimal because of laminar flow domain, clast
157 morphology is not modified during flowage and the clast shape is inherited from the parent
158 deposit (Brezinski et al., 2008; Benn & Evans, 1998). Consequently, glaciogenic processes
159 best explain the rounded, faceted, and polished clasts of the deposits.

160 3.3. Dropstone and load structures:

161 Some isolated pebble to boulder gravel size of these outsized-clasts show vertical or
162 oblique orientation of the long axes into the host sediment (see details in figures 2, 3, 4 and
163 5). Such clasts occur in the sandstones and conglomerates showing a contrast between the
164 depositional processes of the large clasts and the host sediments. In the sandstones this
165 contrast are marked by isolated or levels of pebbles and cobbles embedded in horizontal
166 laminated sandstones (Figures 2 and 3), whereas in conglomerates are observed chaotic
167 flow surfaces and occasional matrix deformation structures produced by embedded clasts
168 (Figure 4C). The main characteristics of these deformations are a gradual bending and a
169 weak disruption of underlying lamination, suggesting that the load structure or impact velocity
170 was low (Bennet et al., 1996) and local.

171 3.4. Incipient turbate and dewatering structures:

172 Turbate structures consist of a circular form of rearranged blocks delimited by a ring of
173 clasts around an axis that contains matrix or a core stone (Ravier et al., 2014). They can be
174 imbricated, with zero or limited contacts between the clasts, occurring in deforming
175 subglacial beds or in debris flows. The conglomerates of Morro do Chapéu Formation locally
176 show some similar structures, where smaller clasts surround larger clasts forming
177 semicircular shapes with limited contact between them (Figure 6). Sometimes these
178 structures are imbricated and clasts show planar clast-to-clast contacts with less matrix
179 between them. Occasionally, vertical oriented clasts show an alignment instead of circular
180 forms (Figure 6).

181



182 **Fig. 5:** Conglomeratic layer with glacial features. A) Overview of conglomeratic layer with others
 183 photos highlighted in dashed squares; B) Outsized-clasts with bottom deformed lamination (white
 184 arrows) and overlaid by the top lamination (black arrows); C) Outsized-clast with horizontal orientation
 185 and a slight difference between the lateral faces, likely a bullet-shaped clast (yellow arrows); D)
 186 Vertical clast in the middle part of layer, suggesting a turbulent flow; E) Faceted-clast with vertical
 187 orientation and overlapped by the top lamination (black arrow); F) Clast with horizontal orientation,

188 with bottom lamination deformed (black arrow) and slight difference between the lateral faces, likely a
189 bullet-shaped clast (red arrows); G) The wide range of clast forms and sizes in basal view; H) Another
190 clast with bullet-shape (red arrows) and bottom deformed lamination, overlaid by the top lamination
191 (black arrows). This photo occurs 20 m to east of photo A.

192 Turbulent flows within the matrix of debris flow can produce transitory rotational
193 deformations leading to similar type of structures (Phillips, 2006). However, overriding ice
194 flow will develop turbate structures in subglacial environments when induces to basal
195 shearing, high strain intensity and high porewater pressure (Ravier et al., 2014; Menzies,
196 2000). Furthermore, according to Menzies (2012) the lack of clast-to-clast contacts suggests
197 that the water-saturated sediments were deformed under high porewater pressure. This
198 characteristic empathizes the occurrence of vertical realigned clasts in conglomerates,
199 suggesting upwards dewatering of the conglomerate (Ravier et al., 2014). The imbricated
200 turbate structures with planar clast-to-clast contacts could be a second phase of deformation,
201 related to simple shear that could be related to stresses exerted by an overriding ice sheet or
202 debris flow (Ravier et al., 2014; Fleming et al., 2016).

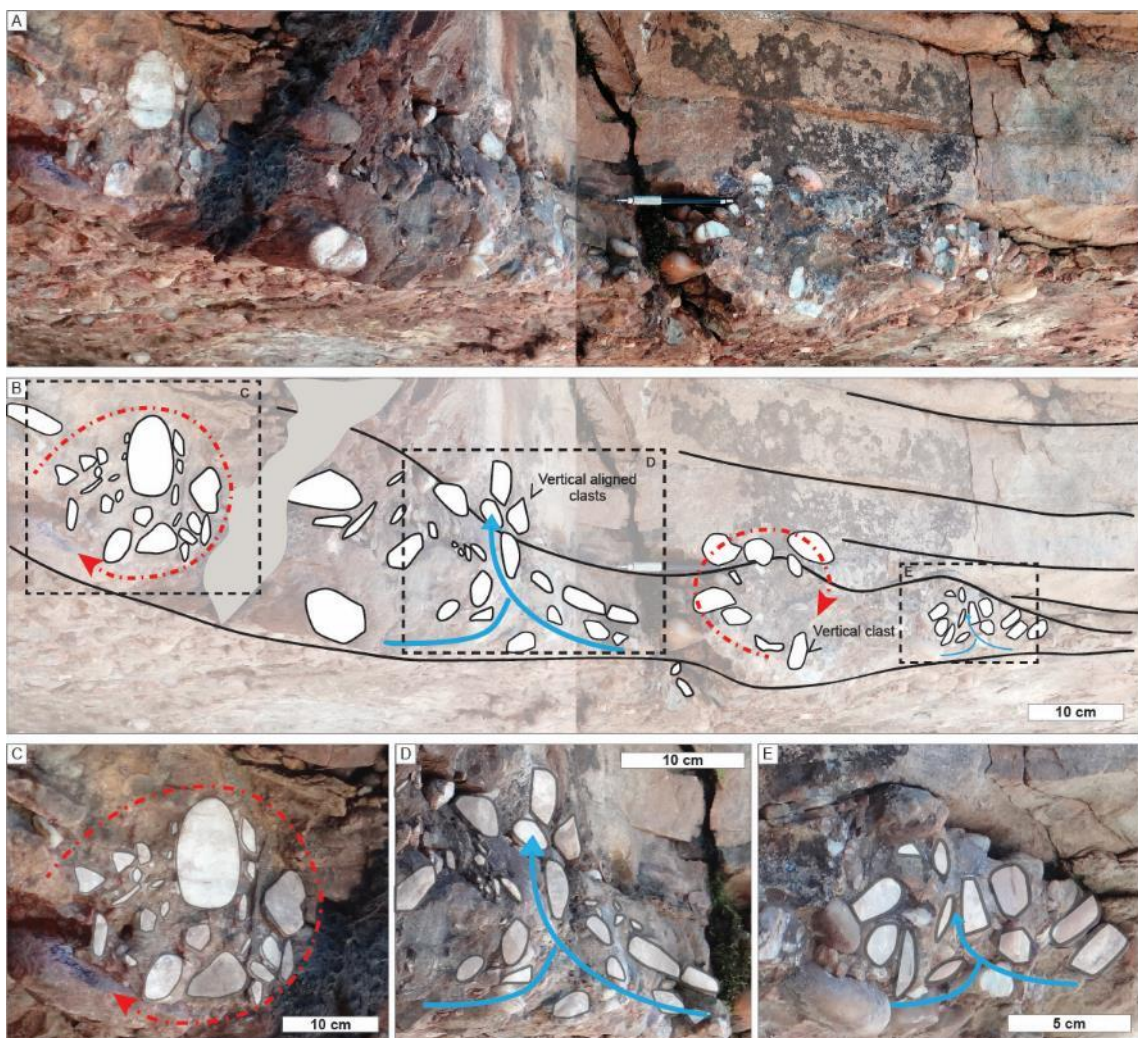
203 3.5. Small limited fractures:

204 A thin layer (< 30 cm) where diagonally aligned clasts are tagged by small fractures
205 regularly spaced and restricted at the layer (Fig. 4E). The marks are similar to trough-cross
206 stratification but show brittle deformation of some clasts, highlighting the simple shearing.
207 This feature indicate a localized stress field with strong normal and horizontal components,
208 attributed to the weight and lateral motions of subglacial shearing (Aquino, 2016; Hart &
209 Boulton, 1991). This hypothesis is reinforced due to occurrence of diamictite above the
210 fractures.

211 3.6. Deformed deposits of Caboclo Fm.:

212 A series of deformative structures occur immediately below discordant contact between
213 Caboclo and Morro do Chapéu formations. Although the rocks of the study area have been
214 folded by an E-W compression system forming a series of anti- and synclinal folds, the
215 deformation observed and described here is local and does not crosscut formations

216 boundaries (Figure 7). The mains deformational structures are: 1) boudinage and
 217 asymmetrical folds; and 2) extensional dihedral joints.



218 **Fig. 6:** A) The thin layer of basal conglomerate; B) Draw illustrating the turbate and dewatering
 219 structures, with other photos highlighted in dashed squares; C) Incipient turbate structure, with a larger
 220 clast vertical oriented while the small clasts are surrounding forming an incipient circular structure.
 221 Note other small clasts with vertical orientation as influenced by the larger clast; D and E) Dewatering
 222 structures where is possible note the change in the clasts orientations and vertical clasts aligned.

223 *Boudinage and asymmetrical folds:* Boudinage occurs on lenses of fine sandstones with
 224 low-angle cross stratification (Figure 7B). The lenses have until 1.5 m length and the around
 225 stratification is undulated and folded. A C-S zone occurs at the margins of the lenses
 226 resulting in an assemblage with W-E vergent. Folds observed within Caboclo Fm. indicate
 227 deformation under a simple shear stress component exerted by ice or debris flow and/or due
 228 to weight and movement of ice (Lønne, 1995; Ravier et al., 2014).

229 *Extensional dihedral joints:* Low pervasive conjugate dihedral joint networks with NW and
230 SE orientation (Figure 7C). The extensional dihedral joints correspond to brittle deformations,
231 probably localized along a zone where preglacial sediments are fractured. This zone
232 corresponds to deformed rocks around a fault surface and results from the initiation,
233 interaction and build-up of slip along faults (McGrath & Davison, 1995; Kim et al., 2004).

234 **4. Depositional model**

235 4.1. Glacial facies associations and stratigraphic architecture;

236 The detailed study of basal conglomerates allowed the identification of three facies
237 associations (Table 2) comprising conglomerates to medium-grained sandstones, which
238 represent two distinct moments of the glacier development (Figure 8). The first moment
239 comprises the consolidated diamictites with small limited fractures, while sandy diamictites
240 and waning-flows deposits compose the second moment. Both moments have high
241 sediment-load like grounding-line fans in ice proximal area (Figure 8C).

242 Sediment-laden meltwaters form subglacial tunnels at a glaciomarine grounding-line
243 resulting in hyperconcentrated and concentrated density flows (e.g. Mulder & Alexander,
244 2001; Russell & Arnott, 2003). This type of sedimentation could be well explained by the jet-
245 efflux model (Figure 8A), which the main features are the abrupt facies shift and the
246 presence of scours structures associated with these deposits (Gorrell & Shaw, 1991;
247 Brennand, 1994; Hornung et al., 2007).

248 The development of the efflux jet into the basin involve three stages or zones that
249 represent a proximal-to-distal continuum of flow evolution (Long et al., 1990; Powell, 1990;
250 Russell & Arnott, 2003; Hornung et al., 2007): *i*) zone of flow establishment; *ii*) zone of flow
251 transition; and *iii*) zone of established flow (Figure 8A). Distinct deposits record this evolution
252 along these three zones, including a wide range of facies deposited from high-energy,
253 sediment-laden to lower energy and bedload-dominated flows (Powell, 1990; Russell and
254 Arnott, 2003; Hornung et al., 2007).

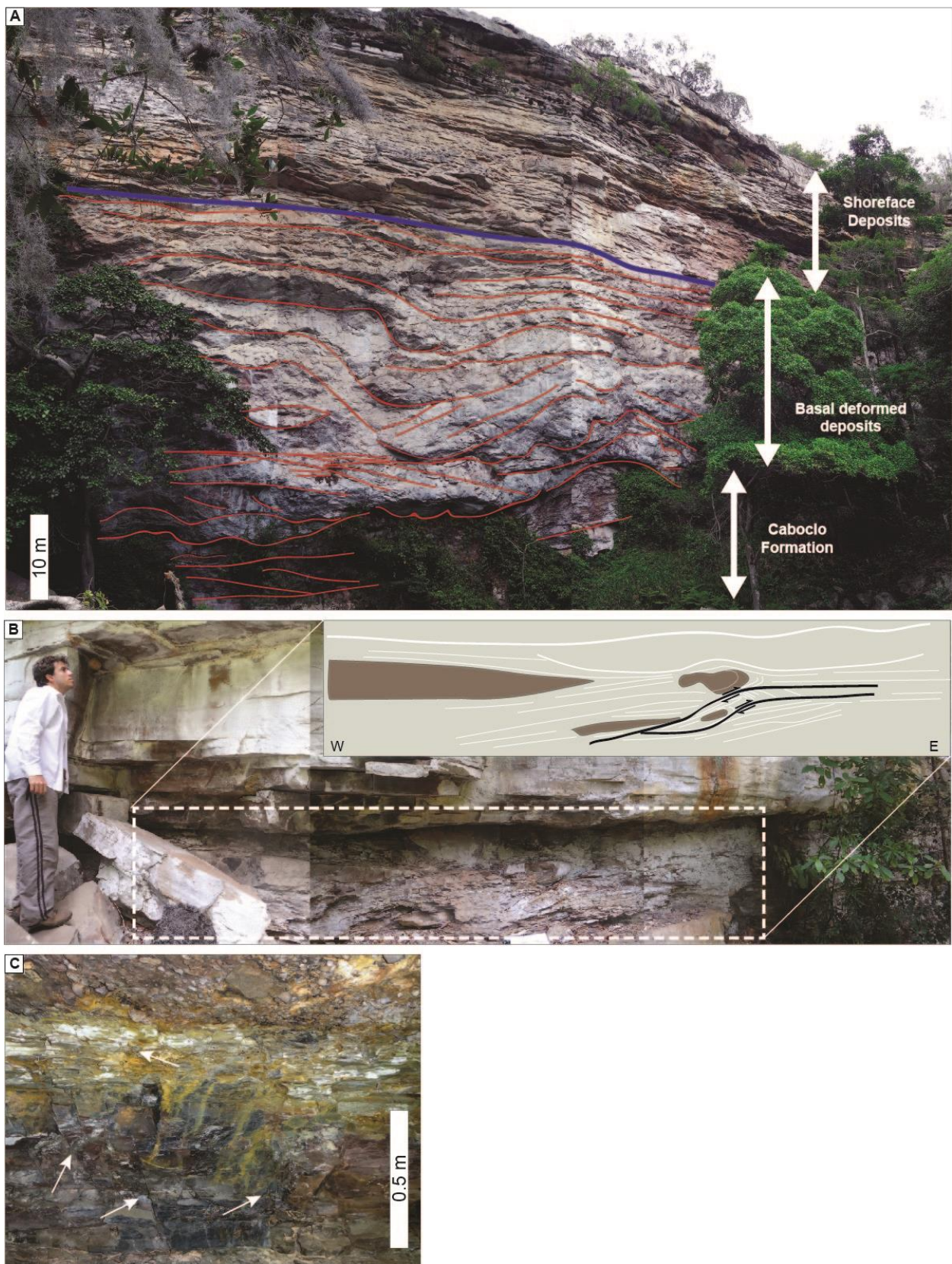
255 In the study area, the first moment of glacier development is comprised by consolidated
256 diamictites and represents the zone of flow establishment (Figure 8C - number 1). This zone

257 is the most near of the conduit outlet where the meltwater streams velocity is high and the jet
258 diameter expands very quickly, resulting in higher energy facies related to hyperconcentrated
259 and concentrated density flows (Long et al., 1990, 1991; Russell and Arnott, 2003; Hornung
260 et al., 2007). The origin of small limited fractures after this first moment characterizes an
261 advance of glacier (Figure 8C - number 2). These fractures appear just in the consolidated
262 diamictites, not exceeding the upper facies limit, and are interpreted as subglacial
263 glaciotectonic deformation associated with an ice advance in the area.

264 The surface between consolidated diamictites and sandy diamictites is marked by
265 protruding clasts draped by the upper lamination. This surface and the sandy diamictites
266 corresponds the zone of flow transition and the beginning of second moment of glacier
267 evolution. The second moment represent a glacier retreat characterized by the superposition
268 between deposits of the zone of flow transition above deposits of zone of flow establishment
269 (Figure 8C - number 3). The zone of flow transition marks a change from supercritical to
270 subcritical flow of the jet, because of the rapid flow deceleration and expansion with resulting
271 ambient fluid entrainment. In the study area, this change results in a rapidly shift from
272 conglomeratic to sandy facies associations with shallow cut-and-fill structures and levels of
273 dropstones.

274 The retreat glacier follows and results in deposition of zone of established flow above the
275 deposits of zone of flow transition. The waning-flows facies association represents the
276 downflow extend within the zone of flow established and comprises more diluted flows where
277 tractive bedforms domain (Figure 8C - number 4). Herein, this tractive bedforms are
278 represented by heavily sediment-laden surge of flood water and capped by massive or
279 laminated clay to silt, related to low-density waning turbidity flows.

280 The deposition proceeds with accumulation of shoreface deposits that although not
281 described in this work, can be observed in Figures 7 and 8. This characteristic suggest a
282 continuity of the glacier retreat and corroborate to the interpretation of the subaqueous
283 debris-flows in a glaciomarine context.

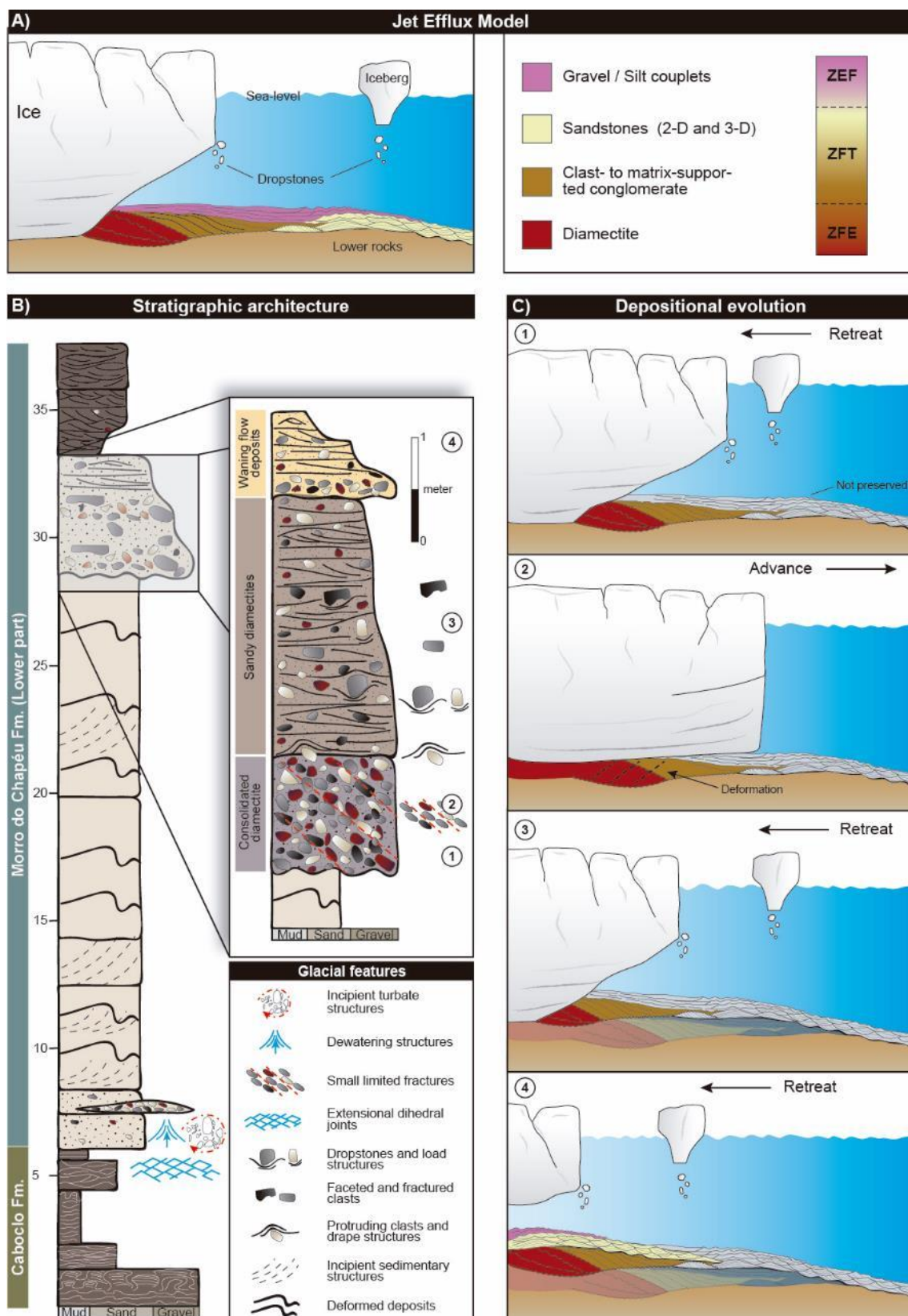


284 **Fig. 7:** A) Outcrop view with distinct facies associations limited, note the folding restrict to middle part
 285 of outcrop. B) Folding and boudinage of Caboclo deposits, W-E oriented. C) Dihedral joints in Caboclo
 286 Fm. with conglomerates above.

287

288 **Table 2:** Facies association descriptions and interpretations for the studied area.

Facies Association	Description	Facies code	Interpretation
Sandy Diamictites	A thick layer (< 2 m) of matrix-supported conglomerate (Gsm) with abrupt basal contact that grade, vertically and horizontally, to pebbly sandstones (Sgs) with crudely low-angle stratification (Sl) and thin layers (< 2 cm) of wave ripple cross-laminated sandstone (Sw). The range of grain size is wide and include locally outsized and vertical clasts, as well as dropstones with undelaying deformation.	Gsm Sgs Sw Sl	The subtle stratification, the close association with subaqueous tractive forms and the broad grain size variation suggest subaqueous deposition from sediment-laden efflux jets. This high discharge associated to faceted and polished pebbles and outsized clasts indicate that sedimentation took place within a proglacial ice-contact (Lønne, 1995). The vertical orientation and the deformed bottom suggest that they are dropstones that may indicate rain-out processes (Bennett et al., 2006). In subaqueous environments, structureless diamictites can form by release of sediment from a high concentration of debris-rich icebergs, close to a grounding line (Flemming et al., 2015). Sand-rich diamict facies commonly accumulate in areas subject to episodic traction currents and form part of a lithofacies continuum with pebbly sands and poorly sorted gravels (Eyles and Eyles, 2010). The subtle stratification suggests reworking by minor subaqueous currents and subsequent removal of fines during rain-out deposition of diamictite from floating ice (Flemming et al., 2015).
Consolidated Diamictites	A thin layer (< 1m) of matrix-supported, massive, poorly-sorted conglomerate (Gsm) with less matrix proportion than sandy diamictites. The clasts show an incipient stratification similar to pervasive fissility, and frequently are faceted and polished. The limits are abrupt and with a protuberant clasts in upper part.	Gsm	The wide range of grain-size distribution, the faceted clasts and the fissility observed in this deposits suggest shear-induced deformation or/and dewatering during or after deposition (Broster et al., 1979). Deformation induced by shear is typical of subglacial deposits, and triggered by the shear stress transmitted to the bed by overriding ice during ice-bed coupling periods. In addition, the diamictite is highly compacted resulting in a dense deposit due to dewatering during subglacial shearing (Ravier et al., 2015). Fissile diamictite containing faceted and striated clasts are generally interpreted as subglacial traction till, deformation till, or tectomict (Evans et al., 2006; Menzies et al., 2006; Menzies, 2012), implying deposition / deformation of diamictite at the glacier bed.
Waning-flows deposits	Thin layers (< 1 m) of clast-supported, massive conglomerate (Gcm) grading upward to low-angle (Sl), through cross-stratified (St) and ripple-cross laminated sandstones (Sr/Sw). The bedforms lower limits are irregular and frequently erosive, while the contact between conglomerates and sandstones are transitional.	Gcm Sl St Sr Sw	The association represents rapid sedimentation of coarse sediment from turbulent flows, heavily sediment-laden surges of flood water, attributed to waning-flows. The sandstones are interpreted as deposition as a subaqueous out-wash fan, within the distal zone shows normally graded sands with ripple scale cross-laminations capped by massive or laminated clay to silt are related to low-density waning turbidity flows (Ravier et al., 2014).



289 **Fig. 8:** Depositional model and stratigraphic architecture to basal conglomerates. A) The jet-efflux
 290 model of subaqueous ice-contact fan (modified of Hornung et al., 2007); B) Synthetic stratigraphic
 291 section illustrating the stacking pattern with interval of conglomerates highlighted and structures
 292 reported along the section. Note that the model constructed is based in the upper conglomerates only;
 293 C) Model illustrating the characteristics of glacier evolution. The numbers are explained in the text and
 294 indicated in the stratigraphic section.

295 4.2. Discussion with previous references;

296 The Morro do Chapéu Fm. was defined by Brito Neves (1967) as a unit with basal
297 conglomerates that are overlapped by uniform fine-grained sandstones and culminating in
298 quartzites intercalated with few mudstones. The subsequent authors (Pedreira, 1988;
299 Guimarães & Pedreira, 1990; Rocha, 1997; and Battilani et al., 1997) interpreted these
300 sediments as fluvial-estuarine system with inter- to sub-tidal deposits. All these works are
301 localized in the same area of this research and interpreted the basal conglomerates and
302 sandstones as a braided fluvial system (Brito Neves, 1967; Pedreira, 1986; Battilani, 1996;
303 Rocha, 1997; Espíndola, 2013). The development of this fluvial system starts after a huge fall
304 in mean sea-level, which exposed and eroded the sediments of Caboclo Fm. (Rocha, 1997),
305 generating incised valleys.

306 However, our interpretation differs from previous authors how is summarized in the facies
307 and facies association tables (Table 1 and 2, respectively). The focus in this study is re-
308 evaluate the basal conglomerates interpretation. The conglomerates have a restrict
309 occurrence and appears as layers two times in the first 30 meters of Morro do Chapéu Fm.
310 The first layer occurs directly above Caboclo Fm. and has the dewatering and turbate
311 structures, while the second layer occurs at ≈ 30 m of the cross section and shows the
312 majority of glacial features described. Between these two layers, the outcrop is not
313 assessable, but a structural feature is notable. The rocks are folded with a prevalent direction
314 (SE - NW), the same appointed as palaeocurrents by previous authors. This folding is
315 restricted to the section that previous authors characterized as incised-valley.

316 Associated to restricted occurrence of conglomerates and the folding structures, there is
317 the absence of fluvial characteristics in this interval (Figure 7A). There is a wide variety of
318 fluvial styles of braided rivers, characterized by the migration of large 3-D dunes and large
319 bar forms, including both upstream-, lateral- and downstream-accretion deposits (Miall,
320 2010). However, it does not exist in this interval of Morro do Chapéu deposits.

321 A question about this duality of interpretation is that proximal alluvial fans and fluvioglacial
322 outwash streams are commonly gravel-bed braided rivers. In both systems, there are a

323 widespread occurrence of subaqueous debris-flow deposits. Debris-flow processes therefore
324 depend on the properties of grains (size, density, and volume fraction), interstitial fluid
325 (density, viscosity, and volume fraction), and their mixtures (flow thickness, velocity or shear
326 strain rate, and permeability) (Sohn, 2000). These properties cans change almost
327 continuously as the slope gradient and channel width change along the flow path and as
328 sediment and water are incorporated into or removed from a debris flow (Fisher, 1983).

329 A mean characteristic in subaqueous debris-flow is the outsize clasts derived from the
330 fronts and tops of the debris-flow and deposited as debris-fall deposits. However, for this to
331 occur its necessary an effective segregation and transfer of the outsize clasts to the flow top
332 and front. Furthermore, the resulted depositional sequence that comprises debris-fall
333 deposits show a coarsening-upward pattern, that unseen in the Morro do Chapéu
334 conglomerates.

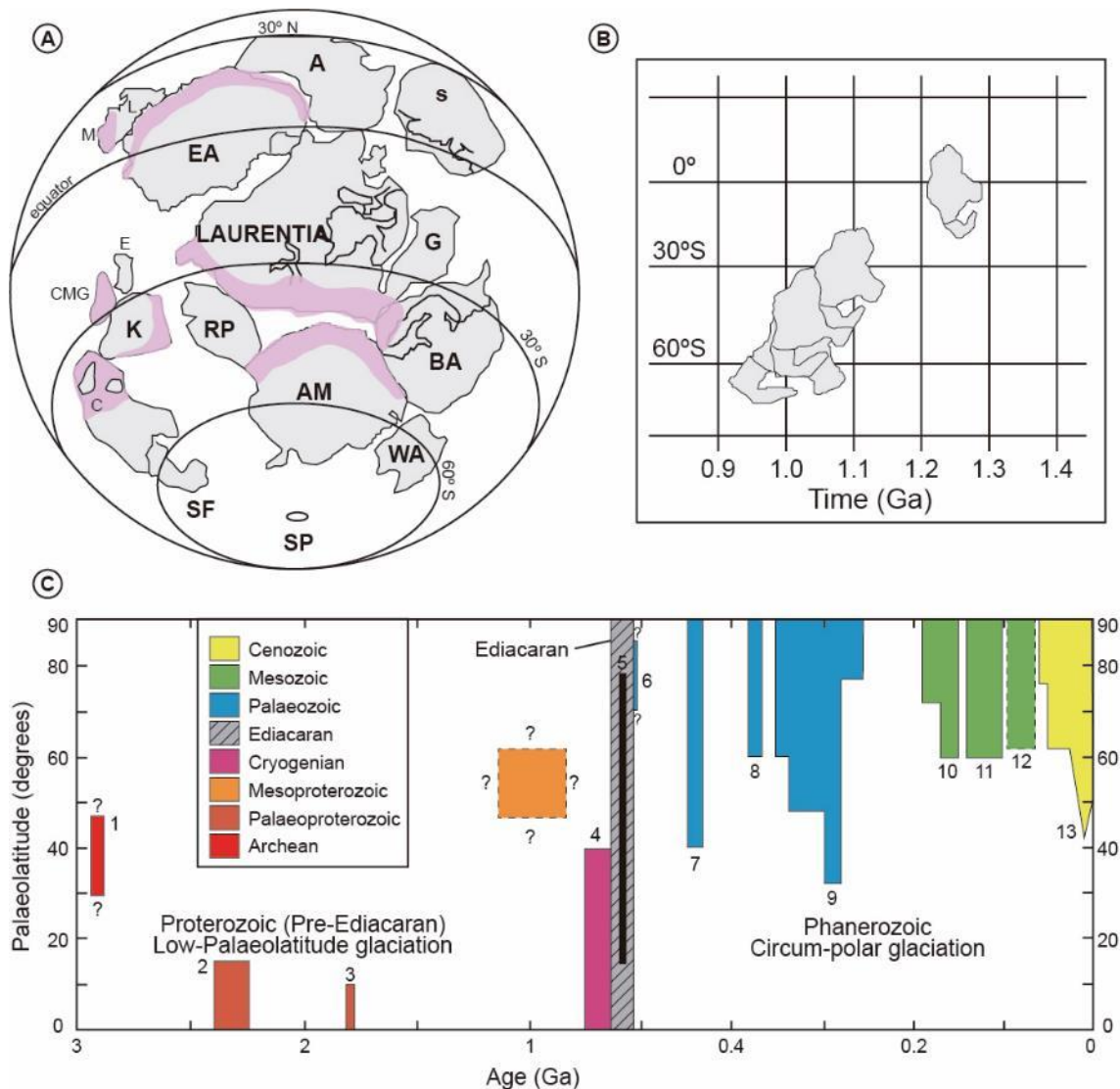
335 **5. Global evidences of glaciations for the age range**

336 The Morro do Chapéu Formation is between Caboclo and Bebedouro formations located
337 in the São Francisco Craton (Figure 1). The Morro do Chapéu lack direct radiometric
338 constraints but these formations were dated with 1140 ± 140 (Babinski et al., 1993) and 934 ± 14 Ga
339 (Loureiro et al., 2008), respectively. These ages limit the deposition of Morro do
340 Chapéu into this time interval, whithin paleomagnetic reconstructions place the São
341 Francisco craton at high southern latitudes (45 to over 60° S) (Figure 9A and B) (Weil et al.,
342 1998; Pesonen, et al., 2003; Tohver et al., 2006).

343 Others studies of late Mesoproterozoic deposits indicate that this was a period of a global
344 greenhouse conditions marked by eustatic highstand (Kah et al., 1999; 2012; Gilleaudeau
345 and Kah, 2013), and the proterozoic glaciations occurred under strongly seasonal climates
346 near sea level in low palaeolatitudes (Figure 9C) (Williams, 2016). Besides this, the features
347 showed in this study allow hypothesize that the glaciations of the Morro do Chapéu formation
348 were local rather than global in extent, so caution about its global significance is warranted.

349 However, to assistant this theory there is another example of glacial deposits with the
350 same age in adjacent area of São Francisco craton. Sub-glacial unconformities cut through

351 underlying carbonate platform deposits of the Serra do Poço Verde and Morro do Calcário
 352 formations (Geboy et al., 2013) in Vazante Group (Mesoproterozoic – Brasília Fold Belt). The
 353 Morro do Calcário formation accumulated during post-glacial transgression over sub-glacial
 354 valleys largely filled with carbonate breccia



355 **Fig. 9:** A) Proposed Rodinia reconstruction with all cratons rotated with respect to a 1010 Ma
 356 Laurentian paleopole according to the Weil et al., (1998). Grenvillian orogenic belts highlighted in
 357 purple areas. Uncertainties in the position of the cratons can be as large as 15°. AM - Amazonia
 358 craton; A - Australia craton; BA – Baltica (Fennoscandia); C – Congo craton; CMG - Coates Land–
 359 Maudheim–Grunehogna Province; E - Ellsworth–Whitmore Mountain Block; EA – East Antarctica; G -
 360 Greenland; I - India; K - Kalahari craton; M - Madagascar; RP - Rio de la Plata craton; S - Siberia
 361 craton; SF - São Francisco craton; WA - West Africa craton. Not included are the North and South
 362 China blocks, believed by some to border the western margin of Laurentia. B) Latitudinal drifts of
 363 Congo/São Francisco during 1.4 – 1.00 Ga according Pesonen et al., (2003). C) Palaeolatitudinal
 364 extent of glaciogenic deposits adapted after Eriksson et al. (2013), with mesoproterozoic occurrence of
 365 Morro do Chapéu and Vazante Group deposits. (1–2) Palaeoproterozoic, (3) Cryogenian, (4)
 366 Ediacaran, (5) Cambrian (see text for sources of data). (6) Ice-rafterd deposits for the Late Ordovician–

367 Early Silurian, (7) Late Devonian, (8) Early Carboniferous–Late Permian, (9–11) Early Jurassic–Late
368 Cretaceous, and (12) Cenozoic. Note change of time-scale at 500 Ma.

369 The upper part of Vazante Group stratigraphy show evidence of two discrete glacial
370 deposits, preserved as: i) discrete diamictite horizons bearing both angular and rounded,
371 faceted and striated clasts, sometimes preserved as dropstones in laminated shale; ii) the
372 presence of the cold-water carbonate mineral glendonite within one of the post-glacial shale
373 horizons; iii) Fe-oxide cementation and local accumulation of iron-formation; and iii) negative
374 $\delta^{13}\text{C}$ excursion in carbonate overlying the diamictites (Geboy et al., 2013).

375 **6. Conclusions**

376 The re-evaluation of Morro do Chapéu Formation basal deposits lead to new perspectives
377 about Mesoproterozoic glacial deposits. The wide range of structures related to ice action
378 compose a jet-efflux model within is possible note the glacier move variation. Besides the
379 lack of direct radiometric constraints and other analyses like in Vazante Group, the
380 sedimentological features of Morro do Chapéu conglomerates could be exceptional in the
381 late Mesoproterozoic that display evidence of glaciation. The glaciations may be regional
382 phenomena at high southern latitudes as showed by paleogeographic place of the São
383 Francisco craton during the late Mesoproterozoic Era - a period generally regarded as a time
384 of greenhouse conditions and globally high sea levels. However, more studies are necessary
385 to corroborate this hypothesis.

386 **7. References**

- 387 Alkmim, F.F., Martins-Neto, M.A., 2012. Proterozoic first-order sedimentary sequences of the São
388 Francisco craton, eastern Brazil. Marine and Petroleum Geology 33, 127-139.
- 389 Almeida, F.F.M., 1977. O craton de São Francisco. Brazilian Journal of Geology 7, 349-364.
- 390 Aquino, C.D., Buso, V.V., Faccini, U.F., Milana, J.P., Paim, P.S.G., 2016. Facies and depositional
391 architecture according to a jet efflux model of a late Paleozoic tidewater grounding-line system
392 from the Itararé Group (Paraná basin), southern Brazil. Journal of South American Earth Sciences
393 67, 180 – 200.

- 394 Aquino, C.D., Milana, J.P., Faccini, U.F., 2014. New glacial evidences at the Talacasto paleofjord
395 (Paganzo basin, W-Argentina) and its implications for the paleogeography of the Gondwana
396 margin. *Journal of South American Earth Sciences* 56, 278 – 300.
- 397 Babinski, M., Pedreira, A.J., Brito Neves, B.B., Van Schmus, W.R., 1999. Contribuição à
398 geocronologia da Chapada Diamantina. 7º Simpósio Nacional de Estudos Tectônicos. Brazilian
399 Geological Society, Lençóis, 118-120.
- 400 Babinski, M., Van Schmus, W.R., Chemale, F.Jr, Neves, B.B.B., Rocha, A.J.D., 1993. Idade
401 isocrônica Pb–Pb em rochas carbonáticas da Formação Caboclo em Morro do Chapéu, BA. II
402 Simpósio sobre o Cráton do São Francisco, Sociedade Brasileira de Geologia 2, Salvador (BA),
403 Anais, 160–163.
- 404 Battilani , G.A, Gomes, N.S, Guerra, W.J., 1997. Evolução diagenética dos arenitos da Formação
405 Morro do Chapéu, Grupo Chapada Diamantina, na região de Morro do Chapéu, Bahia. *Geonomos*
406 4, 81-89.
- 407 Battilani, G.A., 1996. Estudo do sistema deposicional da Formação Morro do Chapéu na Chapada
408 Diamantina, Região de Morro do Chapéu, Bahia. Monografia de graduação, 82p. Geologia,
409 Departamento de Geologia – Universidade Federal de Ouro Preto.
- 410 Benn, D.I., Evans, D.J.A., 1998. *Glaciers and Glaciation*. Oxford University Press, New York.
- 411 Bennet, M.R., Doyle, P., Mather, A.E., 1996. Palaeogeography, Palaeoclimatology, Palaeoecology
412 121, 331 – 339.
- 413 Bennett, M.R., Huddart, D., Waller, R.I., 2006. Diamict fans in subglacial water-filled cavities – a new
414 glacial environment. *Quaternary Science Reviews* 25, 3050 – 3069.
- 415 Boulton, G.D., 1978. Boulder shapes and grain-size distribution of debris as indicators of transport
416 paths through a glacier and till genesis. *Sedimentology* 25, 773 – 799.
- 417 Brennand, T.A., 1994. Macroforms, large bedforms and rhythmic sedimentary sequences in subglacial
418 eskers in south-central Ontario: implications for esker genesis and meltwater regime. *Sedimentary
419 Geology* 91, 9 – 55.
- 420 Brezinski, D.K., Cecil, C.B., Skema, V.W., Stamm, R., 2008. Late Devonian glacial deposits from the
421 eastern United States signal an end of the mid-Paleozoic warm period. *Palaeogeography,
422 Palaeoclimatology, Palaeoecology* 268, 143 – 151.

- 423 Brito Neves, B.B., 1967. Geologia das folhas de Upamirim e Morro do Chapéu Bahia. Relatório 17
424 Companhia Nordestina de Sondagens e Perfurações CONESP – SUDENE.
- 425 Broster, B.E., Dreimanis, A., White, J.C., 1979. A sequence of glacial deformation, erosion and
426 deposition at the ice-rock interface during the Last Glaciation: Cranbrook, British Columbia,
427 Canada. *Journal of Glaciology* 23, 283 – 295.
- 428 Chakraborty, C., Ghosh, S.K., 2008. Patterns of sedimentations during the Late Paleozoic,
429 Gondwanaland glaciations: An example from the Talchir Formation, Satpura Gondwana basin,
430 central India. *Journal of Earth System Science* 117, 499 – 519.
- 431 Cheel, R.J., Rust, B.R., 1986. A sequence of soft-sediment deformation (dewatering) structures in late
432 Quaternary subaqueous outwash near Ottawa, Canada. *Sedimentary Geology* 47, 77 – 93.
- 433 Chemale Jr., F., Dussin, I.A., Alkmim, F.F., Martins, M.S., Queiroga, G., Armstrong, R., Santos,
434 M.N., 2012. Unravelling a Proterozoic basin history through detrital zircon geochronology: The
435 case of the Espinhaço Supergroup, Minas Gerais, Brazil. *Gondwana Research* 22, 200-206.
- 436 Dalrymple, R.W., 2010. Tidal depositional systems. In: James, N.P., Dalrymple, R.W. (Eds.), *Facies*
437 *Models 4*, GEOText, vol. 6. Geological Association of Canada IV, pp. 201 – 231.
- 438 De Waele, B., Johnson, S.P., Pisarevsky, S.A., 2008. Paleoproterozoic to Neoproterozoic growth and
439 evolution of the Eastern Congo Craton: its role in the Rodinia puzzle. *Precambrian Research* 160,
440 127 – 141.
- 441 Dott, R.H.Jr., Bourgeois, J., 1982. Hummocky stratification: Significance of its variable bedding
442 sequences. *Geological Society of America Bulletin* 93, 663 – 680.
- 443 Espíndola, E., 2013. Arquitetura de fácies e evolução estratigráfica do sistema fluvio-estuarino da
444 Formação Morro do Chapéu – Bahia. Monografia de graduação, 92p. Geologia, Instituto de
445 Geociências – Universidade Federal do Rio Grande do Sul.
- 446 Evans, D.J.A., Phillips, E.R., Hiemstra, F., Auton, C.A., 2006. Subglacial till: formation, sedimentary
447 characteristics and classification. *Earth Science Reviews* 78, 115 – 176.
- 448 Fernandez-Alonso, M., Cutten, H., De Waele, B., Tack, L., Tahlon, A., Baudet, D., Barrit, S.D., 2012.
449 The Mesoproterozoic Karagwe-Ankole Belt (formerly the NE Kibara Belt): the result of
450 prolonged extensional intracratonic basin development punctuated by two short-lived far-field
451 compressional events. *Precambrian Research* 216 – 219, 63 – 86.

- 452 Fisher, R., 1983. Flow transformations in sediment gravity flows. *Geology* 11, 273 – 274.
- 453 Fleming, E.J., Benn, D.I., Stevenson, C.T.E., Petronis, M.S., Hambrey, M.J., Fairchild, I.J., 2016.
454 Glacitectonism, subglacial and glacilacustrine process during a Neoproterozoic panglaciation,
455 north-east Svalbard. *Sedimentology* 63, 411 – 442.
- 456 Geboy, N.J., Kaufman, A.J., Walker, R.J., Mini, A., Oliveira, T.F., Miller, K.E., Azmy, K., Kendall,
457 B., Poulton, S.W., 2013. Re-Os age constraints and new observations of Proterozoic glacial
458 deposits in the Vazante Group, Brazil. *Precambrian Research* 238, 199 – 213.
- 459 Gilleaudeau, G., Kah, L., 2013. Oceanic molybdenum drawdown by epeiric sea expansion in the
460 Mesoproterozoic. *Chemical Geology* 356, 21 – 37.
- 461 Gorrell, G., Shaw, J., 1991. Deposition in an Esker, bead and fan complex, Lanark, Ontario Canada.
462 Desimentary Geology 72, 285 – 314.
- 463 Guadagnin, F., Chemale, F., Magalhães, J., Santana, A., Dussin, I., Takehara, L., 2015a. Age
464 constraints on crystal-tuff from the Espinhaço Supergroup – insight into the Paleoproterozoic to
465 Mesoproterozoic intracratonic basin cycles of the Congo–São Francisco Craton.
466 *Gondwana Research*, 27, 363–376.
- 467 Guadagnin, F.; Chemale Jr., F.; Magalhães, A. J.C.; Alessandretti, L.; Bállico, M. B.; Jelinek, A. R.,
468 2015b. Sedimentary petrology and detrital zircon U-Pb and Lu-Hf constraints of Mesoproterozoic
469 intracratonic sequences in the Espinhaço Supergroup: Implications for the Archean and
470 Proterozoic evolution of the São Francisco Craton. *Precambrian Research*, v.266, p.227 – 245
- 471 Guimarães, J.T., Martins, A.A.M., Andrade Filho, E.L., Loureiro, H.S.C., Arcanjo, J.B.A., Neves, J.P.,
472 Abram, M.B., Silva, M.G., Melo, R.C., Bento, R.V., 2005. Projeto Ibitiara–Rio de Contas
473 Geological map. Brazilian Geological Survey and Bahia Mineral Research Company, scale
474 1:200.000.
- 475 Guimarães, J.T., Pedreira, A.J., 1990. Geologia da Chapada Diamantina Oriental, Bahia (Folha
476 Utinga). In: Guimarães, J.T. & Pedreira, A.J. (Orgs.) - Programa de Levantamentos Geológicos
477 Básicos do Brasil. Utinga (Folha SD.24-V-A-II) Estado da Bahia, Texto Explicativo. Brasília,
478 DNPM/CPRM, 19-92.
- 479 Hambrey, M.J., Harland, W.B., 1981. Earth's Pre-Pleistocene Glacial Record. Cambridge University
480 Press, Cambridge, 1021 pp.

- 481 Hart, J.K., Boulton, G.S., 1991. The interrelation of glaciotectonic and glaciodepositional processes
482 within the glacial environment. *Quaternary Science Review* 10, 335 – 350.
- 483 Hornung, J., Asprion, U., Winsemann, J., 2007. Jet efflux deposits of a subaqueous ice-contact fan,
484 glacial Lake Rinteln, northwestern Germany. *Sedimentary Geology* 193, 167 – 192.
- 485 Kah, L.C., Bartley, J.K., Teal, D.A., 2012. Chemostratigraphy of the Lat Mesoproterozoic Atar Group,
486 Taoudeni Basin, Mauritania: muted isotopic variability, facies correlation, and global isotopic
487 trends. *Precambrian Research* 200, 82 – 103.
- 488 Kah, L.C., Sherman, A.G., Narbonne, G.M., Knoll, A.H., Kaufman, A.J., 1999. Delta C-13
489 stratigraphy of the Proterozoic Bylot Supergroup, Baffin Island, Canadá: implications for regional
490 lithostratigraphic correlations. *Canadian Journal of Earth Sciences* 36, 313 – 332.
- 491 Kaufman, A.J., Knoll, A.H., Narbonne, G.M., 1997. Isotopes, ice ages, and terminal Proterozoic earth
492 history. *Proceedings of the National Academy of Sciences USA* 94, 6600 – 6605.
- 493 Kendall, B., Creaser, R.A., Ross, G.M., Selby, C., 2004. Constrains on the timing of Marinoan
494 Snowball Earth glaciations by Re-187 – Os-187 dating of a Neoproterozoic, post-glacial black
495 shales in Western Canada. *Earth and Planetary Science Letters* 222, 729 – 740.
- 496 Kendall, B., Creaser, R.A., Selby, D., 2006. Re-Os geochronology of post-glacial black shales in
497 Australia: constrains on the timing of Sturtian glaciations. *Geolofy* 34, 729 – 732.
- 498 Kennedy, M.J., Runnegar, B., Prave, A.R., Hoffmann, K.H., Arthur, M.A., 1998. Two or four
499 Neoproterozoic glaciations? *Geology* 26, 1059 – 1063.
- 500 Kim, Y.S., Peacock, D.C.P., Sanderson, D.J., 2004. Fault damage zones. *Journal of Structural Geology*
501 26, 503 – 517.
- 502 Knoll, A.H., 2014. Paleobiological perspectives on early eukaryotic evolution. *Cold Spring Harbor
503 Perspectives in Biology* 6, 1 – 14
- 504 Koch, Z.J., Isbell, J.L., 2013. Processes and products of groundling-line fans from the Permian Pagoda
505 Formation, Antarctica: Insight into glaciogenic conditions in polar Gondwana. *Gondwana
506 Research* 24, 161 – 172.
- 507 Kokonyangi, J.W., Kampunzu, A.B., Armstrong, R., Yoshida, M., Okuradia, T., Arima, M., Ngulube,
508 D.A., 2006. The Mesoproterozoic Kibaride belt (Katanga SE D. R. Congo). *Journal of African
509 Earth Sciences* 46, 1 – 35.

- 510 Krüger, J., Kjaer, K.H., 1999. A data chart for field description and genetic interpretation of glacial
511 diamicts and associated sediments-with examples from Greenland, Iceland and Denmark. *Boreas*
512 28, 386 – 402.
- 513 Leckie, D.A., Walker, R.G., 1982. Storm and tide-dominated shorelines in Cretaceous Moosbar-Lower
514 Gates Interval – Outcrop equivalents of Deep basin gas trap in western Canada. *AAPG Bulletin*
515 66, 138 – 157.
- 516 Long, D., Steffler, P.M. Rajaratnam, N., 1990. LDA study of flow structure in submerged hydraulic
517 jump. *Journal of Hydraulic Research* 28, 437 – 460.
- 518 Lønne, I., 1995. Sedimentary facies and depositional architecture of ice-contact glaciomarine systems.
519 *Sedimentary Geology* 98, 15 – 13.
- 520 Loureiro, H.S.C., Lima, E.S., Macedo, E.R., Silveira, F.V., Bahiense, I.C., Arcanjo, J.B.A., Moraes
521 Filho, J.C., Neves, J.P., Guimarães, J.T., Teixeira, L.R., Abram, M.B., Santos, R.A., Melo, R.C.,
522 2008. Projeto Barra–Oliveira dos Brejinhos Geological map. BrazilianGeologicalSurveyand
523 Bahia Mineral ResearchCompany, scale 1:200.000
- 524 Lyons, T.W., Reinhard. G.D., Xiao, S., 2012. Geobiology of the Proterozoic Eon, In: Knoll, A.H.,
525 Canfield, D.E., Konhauser, K.O. (Eds.), *Fundamentals og Geobiology*. Chichester, John Wiley
526 and Sons.
- 527 McGrath, A.G., Davison, I., 1995. Damage zone geometry around fault tips. *Journal of Structural*
528 *Geology* 17, 1011 – 1024.
- 529 Menzies, J., 2000. Micromorphological analyses of microfabrics and microstructures indicative of
530 deformation processes in glacial sediments. In: Maltman, A.J., Hubbard, B., Hambrey, M.J.
531 (Eds.), *Deformation of Glacial Material*. London, Geological Society, Special Publication, 176,
532 pp. 245 – 257.
- 533 Menzies, J., 2012. Strain pathways, till internal architecture and microstructure – perspectives on a
534 general kinematic model – a ‘blueprint’ for till development. *Quaternary Science Reviews* 50,
535 105 – 124.
- 536 Menzies. J., van der Meer, J.J.M., 2006. Till – as a glacial “tectomict”, its internal architechture, and
537 the development of a “typing” method for till differentiation. *Geomorfology* 75, 172 – 200.
- 538 Miall, A.D., 2010. *The geology of stratigraphic sequences 2*. Heidelberg, Springer, 522 p.

- 539 Middleton, G.V., Hampton, M.A., 1976. Subaqueous sediment transport and deposition by sediment
540 gravity flows. In: Stanley, D.J., Swift, D.J.P. (Eds.), *Marine sediment transport and environmental*
541 *management*. Wiley, pp. 197 – 218.
- 542 Mulder, T., Alexander, J., 2001. The physical character of sedimentary density currents and their
543 deposits. *Sedimentology* 48, 269 – 299.
- 544 Noe-Nygaard, N., Surlyk, F., 1988. Washover fan and backish bay sedimentation in the Berriasian-
545 Valanginian of Bornholm, Denmark. *Sedimentology* 35, 197-217.
- 546 Pedreira, A.J., 1986. Coberturas proterozoicas: Grupo Chapada Diamantina e Una. Rio de Janeiro,
547 CPRM.
- 548 Pedreira, A.J., 1988. Sequências deposicionais no Precambriano: Exemplo da Chapada Diamantina
549 Oriental. In: 35° Congresso Brasileiro de Geologia, Belém, 1988. Anais. Sociedade Brasileira de
550 Geologia, 648-659.
- 551 Pesonen, L.J., Elming, S.A., Mertanen, S., Pisarevsky, S., D'Agrella-Filho, M.S., Meert, J.G.,
552 Schmidt, P.W., Abrahamsen, N., Bylund, G., 2003. Palaeomagnetic configuration of continents
553 during the Proterozoic. *Tectonophysics* 375, 289– 324.
- 554 Phillips, E.R., 2006. Micromorphology of a debris flow deposit: evidence of a basal shearing,
555 hydrofracturing, liquefaction and rotational deformation during emplacement. *Quaternary Science*
556 *Review* 25, 720 – 738.
- 557 Planavsky, N.J., Tarhan, L.G., Bellefroid, E.J., Evans, D.A.D., Reinhard, C.T., Love, G.D., Lyons,
558 T.W., 2015. Late Proterozoic transitions in climate, oxygen, and tectonics, and the
559 rise of complex life. *The Paleontological Society Papers* 21, 47 – 82.
- 560 Plummer, P.S., Gostin, V.A., 1981. Shrinkage cracks: desiccation or synaeresis. *Journal of*
561 *Sedimentary Petrology* 51, 1147 – 1156.
- 562 Powell, R.D., 1990. Glacimarine processes at grounding-line fans and their growth to ice-contact
563 deltas. In: Dowdeswell, J.A., Scourse, J.D. (Eds.), *Glacimarine Environments: Process and*
564 *Sediments*. London, Geological Society, Special Publications, 53, pp. 53 – 73.
- 565 Pratt, B.R., 1998. Syneresis cracks: subaqueous shrinkage in argillaceous sediments caused by
566 earthquake-induced dewatering. *Sedimentary Geology* 117, 1 – 10.

- 567 Ravier, E., Buoncristiani, J., Clerc, S., Guiraud, M., Menzies, J., Portier, E., 2014a. Sedimentological
568 and deformational criteria for discriminating subglaciofluvias deposits from subaqueous ice-
569 contact fan deposits: A Pleistocene example (Ireland). *Sedimentology* 61, 1382 – 1410.
- 570 Ravier, E., Buoncristiani, J., Guiraud, M., Menzies, J., Clerc, S., Goupy, B., Portier, E., 2014b.
571 Porewater pressure control on subglacial soft sediment remobilization and tunnel valley
572 formation: A case study from the Alnif tunnel valley (Marocco). *Sedimentary Geology* 304, 71 –
573 95.
- 574 Ravier, E., Buoncristiani, J., Menzies, J., Guiraud, M., Portier, E., 2015. Clastic injection dynamics
575 during ice front oscillations: A case example from Sólheimajökull (Iceland). *Sedimentary
576 Geology* 323, 92 – 109.
- 577 Rocha, A.J.D., 1997. Programa de Levantamentos Geológicos Básicos do Brasil. Morro do Chapéu
578 (Folha SC.24-Y-C-V) Estado da Bahia. Brasília, CPRM, 157pp.
- 579 Roussell H.A.J., Arnott, R.W.C., 2003. Hydraulic-jump and hyperconcentrated flow deposits of a
580 glaciogenic subaqueous fan: Oak Ridge Moraine, southern Ontario, Canada. *Journal of
581 sedimentary Research* 73, 887 – 905.
- 582 Rust, B.R., 1977. Mass flow deposits in a Quaternary succession near Ottawa, Canada; diagnostic
583 criteria for subaqueous outwash. *Canadian Journal of Earth Sciences* 14, 175 – 184.
- 584 Santos, M.N., Chemale Jr., F., Dussin, I.A., Martins, M., Assis, T.A.R., Jelinek, A.R., Guadagnin, F.,
585 Armstrong, R., 2013. Sedimentological and paleoenvironmental constraints of the Statherian and
586 StenianEspinhaço rift system, Brazil. *Sedimentary Geology* 290, 47–59.
- 587 Schermerhorn, L.J.G., 1974. Late Precambrian mixites: glacial and/or nonglacial? *American Journal of
588 Science* 274, 673–824.
- 589 Schobbenhaus, C., Hoppe, A., Baummann, A., Lork, A., 1994. Idade U/Pb do vulcanismo Rio dos
590 Remédios Chapada Diamantina, Bahia. In: Scheibe, L.F. (Org.), 38º Congresso Brasileiro de
591 Geologia. Brazilian Geological Society, 397-398.
- 592 Schobbenhaus, C.; 2012. In: Carlos Schobbenhaus, C., Silva, C.R. (Orgs.), Geoparques do Brasil:
593 propostas. Rio de Janeiro, CPRM.

- 594 Sohn, Y.K., 2000. Depositional processes of submarine debris flows in the Miocene fan-deltas,
595 Pohang Basin, SE Korea with special reference to flow transformation. *Journal of Sedimentary
596 Reserach* 70, 491 – 503.
- 597 Tohver, E., D'Agrella-Filho, M.S., Trindade, R.I.F., 2006. Paleomagnetic record of Africa and South
598 America for the 1200–500 Ma interval, and evaluation of Rodinia and Gondwana assemblies.
599 *Precambrian Research* 147, 193–222
- 600 Walter, M.R., Veevers, J.J., Calverl C.R., Gorjan, P., Hill, A.C., 2000. Dating the 840-544 Ma
601 Neoproterozoic inhterval by isotopes of strontium, carbon, and sulfur in seawater, and some
602 interpretative models. *Precambiran Research* 100, 371 – 433.
- 603 Weil, A.B., Van der Voo, R., Niocaill, C.M., Meert, J.G., 1998. The Proterozoic supercontinent
604 Rodinia: paleomagnetically derived reconstructions for 1100 to 800 Ma. *Earth and Planetary
605 Science Letters* 154, 13–24.
- 606 Williams, G.E., Schmidt, P.W., Young, G.M., 2016. Strongly seasonal Proterozoic glacial climate in
607 low palaeolatitudes: Radicalli different climate system on the pre-Ediacaran Earth. *Geoscience
608 Frontiers* 7, 555 – 571.
- 609

CAPÍTULO III

Successfully received: submission A WAVE-DOMINATED MESOPROTEROZOIC SEDIMENTARY SEQUENCE, ESPINHAÇO SUPERGROUP, CHAPADA DIAMANTINA – NE/BRAZIL for Precambrian Research ➔ Caixa de entrada x

 **Precambrian Research** <EvideSupport@elsevier.com>
para eu ▾

qua, 18 de jul 17:09 (Há 1 dia)   

 inglês ▾ > português ▾ [Traduzir mensagem](#) [Desativar para: inglês x](#)

This message was sent automatically. Please do not reply.

Ref: PRECAM_2018_320
Title: A WAVE-DOMINATED MESOPROTEROZOIC SEDIMENTARY SEQUENCE, ESPINHAÇO SUPERGROUP, CHAPADA DIAMANTINA – NE/BRAZIL
Journal: Precambrian Research

Dear Mr. Galvão de Souza,

Thank you for submitting your manuscript for consideration for publication in Precambrian Research. Your submission was received in good order.

To track the status of your manuscript, please log into EVISE® at: http://www.evise.com/evise/faces/pages/navigation/NavController.jsp?JRNL_ACR=PRECAM and locate your submission under the header 'My Submissions with Journal' on your 'My Author Tasks' view.

Thank you for submitting your work to this journal.

Kind regards,

Precambrian Research

Have questions or need assistance?
For further assistance, please visit our [Customer Support](#) site. Here you can search for solutions on a range of topics, find answers to frequently asked questions, and learn more about EVISE® via interactive tutorials. You can also talk 24/5 to our customer support team by phone and 24/7 by live chat and email.

Copyright © 2018 Elsevier B.V. | [Privacy Policy](#)
Elsevier B.V., Radarweg 29, 1043 NX Amsterdam, The Netherlands, Reg. No. 33156677.
...

[Mensagem cortada] [Exibir toda a mensagem](#)

 [Responder](#)  [Encaminhar](#)

1 A WAVE-DOMINATED MESOPROTEROZOIC SEDIMENTARY SEQUENCE,
2 ESPINHAÇO SUPERGROUP, CHAPADA DIAMANTINA – NE/BRAZIL

3 Ezequiel Galvão de Souza¹, Claiton Marlon Santos Scherer¹, Adriano Domingos dos
4 Reis¹, Manoela Bettarel Bállico², João Pedro Formolo Ferronatto¹, Lucas Medeiros Bofill¹,
5 Carrel Kfumbi¹

6 ¹Instituto de Geociências – Universidade Federal do Rio Grande do Sul, Av. Bento Gonçalves, 9500; 91509-900
7 Porto Alegre/RS, Brazil.

8 ²Departamento de Geociências – Universidade Federal de Santa Catarina, Campus Universitário.
9 Florianópolis/SC, CEP 88040-900, Brazil

10

11 **1. Abstract**

12 The Mesoproterozoic Morro do Chapéu Formation is the uppermost record of the
13 Proterozoic intracontinental Espinhaço basin that developed on the Congo-São Francisco
14 Paleoplate. This record is composed of wave-influenced delta, unconfined sheetfloods,
15 subtidal deposits wavy-dominated and shallow marine sediments, which experienced a sag
16 phase on the Upper Espinhaço Megasequence. We used high resolution sedimentary facies
17 analysis combined to sedimentological-stratigraphic descriptions of 30 outcrops to
18 discriminate shallow marine from fluvial deposits and develop a regional evolution model to
19 the sag phase. The succession is composed by 17 lithofacies combined in seven distinct facies
20 associations, organized in ascending order: 1) alluvial deposits; 2) wave-influenced delta; 3)
21 shoreface deposits; 4) fluvial sheetfloods; 5) subtidal deposits; 6) resumption of upper
22 shoreface deposits; and 7) lower shoreface and offshore deposits. The stacking of facies
23 associations constitute two incomplete stratigraphic sequences with transgressive trends,
24 within the wave-generated structures are frequent. The tabular and widely lateral continuous
25 deposits suggest a coastal area connected to a wide and low gradient alluvial braidplain,
26 within distal deposits were reworked by tidal and wave currents, and the relative sea level
27 variation the main control of sedimentation. This study evidences the Proterozoic coastal
28 sedimentation, furthermore, increases the knowledge of patterns of sedimentation for
29 Precambrian basins formed in similar tectonic settings.

30 **2. Introduction**

31 The study of Precambrian basins, which are similar to the Phanerozoic basins, can provide
32 important information about the paleogeography and distribution of continents and the
33 evolution of supercontinents. The spatial and temporal evolution of depositional systems in
34 these basins depends on a complex relationship between sediment supply, eustatic variations,
35 climate and tectonic process at the time of deposition (Bosence, 1998). To understand how

36 actuate each of these factors is very important to describe the sedimentary deposits with a
37 detailed facies analysis.

38 The Espinhaço Supergroup has been interpreted as an intracontinental rift-sag basin that
39 developed on the Paleoproterozoic Congo-São Francisco Paleoplate (Brito Neves et al., 1979;
40 Chemale et al., 1993; Martins-Neto, 2000; Alkmim and Martins-Neto, 2012) and on the
41 Neoproterozoic to early Paleozoic deformed Araçuaí Belt along the margin of the São
42 Francisco Craton (Marshak and Alkmim, 1989; Chemale et al., 1993). According to Chemale
43 et al. (1992), the Espinhaço Supergroup was accumulated in response to at least two phases of
44 rifting, comprising three megasequences (Lower, Middle and Upper). The sag phase of the
45 Upper Sequence corresponds to Morro do Chapéu Formation, which is characterized by basal
46 conglomerates overlapped by uniform fine-grained sandstones, culminating in sandstones and
47 few mudstones intercalated (Brito Neves, 1967).

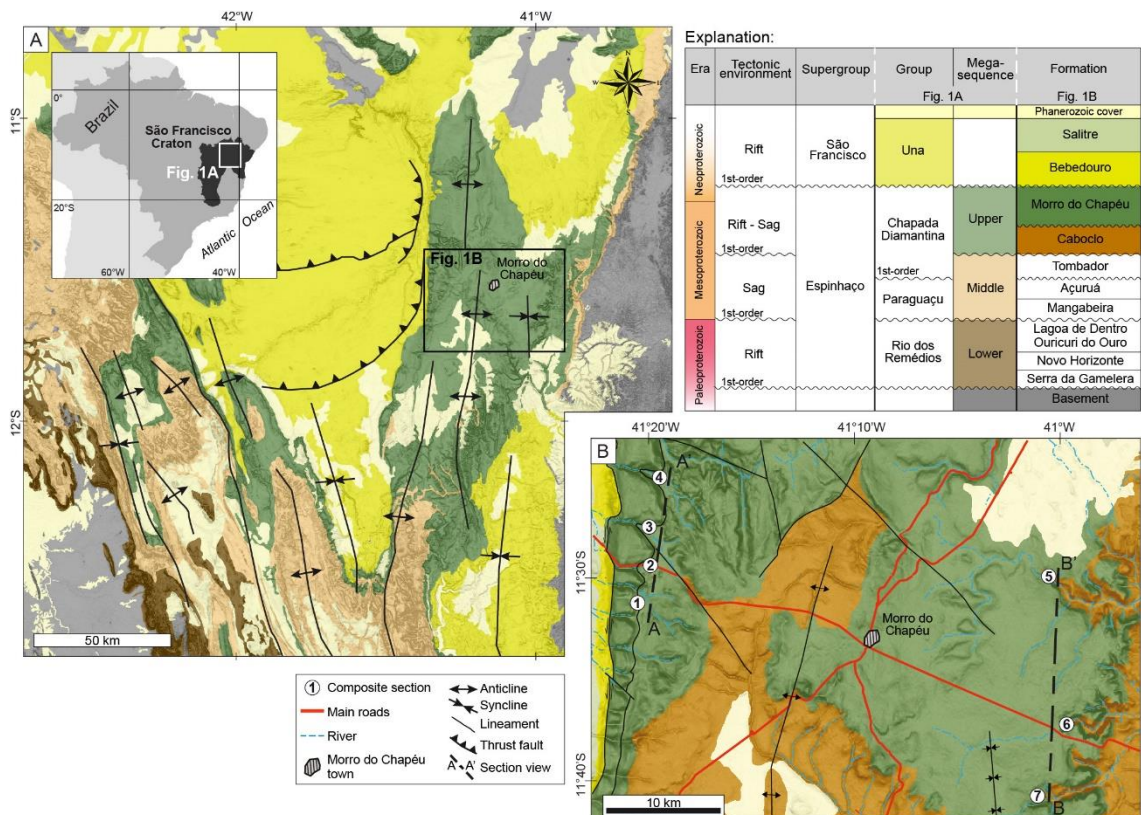
48 This Morro do Chapéu Formation comprises thick successions that contain few
49 information data about some fluvial and estuarine systems at the time of deposition. In spite
50 of the very old age, the exposure and the preservation of successions are exceptional,
51 localizing in a very low-grade metamorphism area, within the sedimentary rocks still exhibit
52 primary structures. In this paper we present the findings of a study based on facies analysis,
53 photomosaics interpretations and paleocurrents data of Morro do Chapéu Formation. The
54 paper aims to (1) identify facies associations and their occurrence as depositional systems; (2)
55 propose an example of stratigraphic framework to Pre-cambrian coastal succession; and (3)
56 identify the main active processes during the Morro do Chapéu accumulation.

57 **3. Geological setting**

58 Morro do Chapéu Formation (Brito Neves, 1967) is located in the central-northern area of
59 São Francisco Craton (Fig. 1A), part of the Espinhaço Supergroup (ES). The ES was
60 deposited between amalgamation of the Congo–São Francisco paleoplate at ca. 1.8 Ga and the
61 partial break-up at ca. 0.9 Ga (Brito Neves et al., 1979; Chemale et al., 1993; Martins-Neto,

62 2000; Alkmim and Martins-Neto, 2012). During Gondwana supercontinent assemblage (late
 63 Neoproterozoic to early Paleozoic Eras) the ES deposits were deformed by large-scale NS
 64 striking folds and thrust faults (Marshak and Alkmim, 1989; Chemale et al., 1993), which
 65 increase the deformation westward (Fig. 1A). The ES is exposed in three physiographic
 66 regions, namely the Southern and Northern Espinhaço mountain ranges and the Chapada
 67 Diamantina.

68 The ES is organized in three megasequences (termed the Lower, Middle and Upper
 69 sequences) that accumulated in numerous basins developed in response to at least two phases
 70 of rifting (Chemale et al., 2012; Santos et al., 2013; Guadagnin et al., 2015). The Caboclo and
 71 Morro do Chapéu formations form the Upper Megasequence (1.19 to 0.9 Ga) at Chapada
 72 Diamantina domain (Fig. 1 – Explanation) and the basal contact between them is irregular.
 73 The upper contact with the Bebedouro Formation is tectonic, characterized by thrust fault that
 74 separate the ES and the São Francisco Supergroup in the studied area.



75 **Fig. 1.** A) Simplified geological map of the Chapada Diamantina Domain, based on data of Brazilian
 76 Geological Survey (CPRM). The dark green colour represents Morro do Chapéu Fm. and the study
 77 area is indicated with a black square (Low-deformed part of Chapada Diamantina domain). The inset

78 shows the location of São Francisco Craton (in black) and position of Chapada Diamantina Domain
79 (white square). B) Seven studied compound cross-sections and town localities.

80 The Morro do Chapéu Formation is characterized by basal conglomerates overlapped by
81 uniform fine-grained sandstones, culminating in sandstones and few mudstones intercalated
82 (Brito Neves, 1967). Different authors (Pedreira, 1988; Guimarães & Pedreira, 1990; Rocha,
83 1997; Battilani et al., 1997) interpreted these sediments as fluvial-estuarine system with inter-
84 to sub-tidal deposits. The development of fluvial system starts after a significant fall in
85 relative sea level, which exposed and eroded the sediments of Caboclo Fm., generating
86 incised valleys (Brito Neves, 1967; Rocha, 1997; Battilani et al., 1997).

87 There are not direct radiometric constraints of Morro do Chapéu Fm., but surrounding
88 formations (Caboclo and Bebedouro) were dated with 1140 ± 140 (Babinski et al., 1993) and
89 934 ± 14 Ga (Loureiro et al., 2008), respectively (Fig. 1 – Explanation), assigning an age of
90 about 1 Ga to Morro do Chapéu Formation. Paleomagnetic reconstructions place the São
91 Francisco craton at high southern latitudes (45 to over 60° S) during deposition of Morro do
92 Chapéu Formation (Weil et al., 1998; Pesonen, et al., 2003; Tohver et al., 2006).

93 **4. Methods**

94 Thirty outcrops were measured in detail and organized in seven compound sections (Fig.
95 1B) located along of the main roads and major rivers in the study area. Sedimentological
96 sections were measured at 1:100 scale, with a total combined thickness of ~1000 m, which
97 record grain size, physical sedimentary structures and paleocurrent data. Dip azimuths of
98 foresets present in cross-bedded sandstones sets determined the paleocurrents. The azimuth
99 and dip angle of the foresets were later corrected to remove the effects of structural tilt.

100 **5. Results**

101 5.1. Facies and facies associations:

102 The lithofacies description and interpretation are summarized in Table 1 and figures 2 and
 103 3. The succession has been subdivided into seven facies associations, which are discussed
 104 below.

105 Table 1: Lithofacies description

Facies	Code	Description	Interpretation
Clast-supported conglomerate	Gcm	Clast-supported, massive to crudely stratified, poorly sorted pebble to boulder (< 40 cm) gravel, polymictic conglomerate. The clasts are well rounded to subangular, with low sphericity showing punctual to faceted contact between them. Outsized clasts occurs locally. The beds are continuous and with undulated bases, sometimes occurring in lenses.	Rapid sedimentation of coarse sediment from turbulent flows, heavily sediment-laden surges of flood water with little or no traction, attributed to hyper-concentrated flows.
Matrix-supported massive conglomerate	Gsm	Matrix-supported, massive, poorly sorted granule to cobble (< 20cm) gravel conglomerate, with chaotic organization and outsized clasts (boulders < 35 cm). Sometimes the clasts are imbricated or with vertical orientation. Scattered protuberant clasts occur at the upper part of strata. The clasts are surrounded to angular with variable sphericity and with a wide range of shapes including tabular/discoid and elongated shapes. Composition varies: volcanic rocks, white and pink quartzites, conglomerates, sandstones, mudstones and quartz. The matrix is poorly sorted with sand to granule size and occasionally with granule lenses. The larger clasts have subangular shape and low sphericity.	Low-cohesive debris flows, where bigger clasts are sustained by buoyancy and cohesion of the sandy framework. Outsized, vertical and protuberant clasts indicates different responses to dispersive forces and buoyancy, which bigger clasts tend to concentrate in the upper and front limits of flows, due to the density contrast between them and the surrounding particles.
Massive sandstone	Sm	Light orange to light red, medium- to coarse-grained, poorly sorted, massive sandstone, with sparse granules and pebbles (< 3cm). Bed thickness from 0.2 to 0.5 m thick.	Deposition from hyper-concentrated flows or result of post-depositional fluidization processes that obliterate the original stratification.
Low angle laminated sandstone	Sl	Light cream to light red, fine- to medium-grained, poorly sorted sandstone, with low angle lamination (<15°). Internally contain mudstone clasts, sparse granules and coarse sand, sometimes forming discrete levels (<1cm). Sets with 0.2 m thick.	Migration of bedforms with a high wavelength/amplitude ratio in transitional conditions between lower and upper flow regime.
Sigmoidal cross-stratified sandstone	Ss	Light brown, well-sorted, medium grained sandstone with small-scale (< 0.6 m thick) sigmoidal cross stratification. Locally granules on the foresets and sparse mudclasts.	Migration of sinuous-crested bedforms under unidirectional decelerating tractive flow, with high sediment rate in lower flow regime.

Trough cross-stratified sandstone	St	Light cream to light red, medium- to very coarse-grained, moderate sorted sandstone, with medium- to small-scale trough cross-stratification (0.1 to 1 m thick). Mudclasts, granules and pebbles are organized in lenses, or along the bedforms foresets and bottomsets.	Migration of sinuous-crested subaqueous bedforms (3D), under unidirectional lower flow regime.
Planar cross-stratified sandstone	Sp	Light red, medium well-sorted sandstone with small-scale tabular cross stratification (<0.4 m).	Migration of straight-crested subaqueous bedforms (2D); under lower flow regime.
Ripple cross-laminated sandstone	Sr	Light red to light cream, very fine- to medium-grained, well-sorted sandstone, with asymmetric ripple cross-lamination. Usually occurs as discrete layers on top of facies St or Sl. Well defined concave upward lee side and convex upward stoss side. Sinuous crestline bifurcated frequently. Wavelength = 4 to 6 cm.	Migration of subcritical to supercritical ripples under unidirectional lower flow regime.
Tidal bundled trough cross-stratified sandstone	Stm	Light cream to light brown, medium- to coarse-grained, moderate sorted sandstone with medium- to large-scale trough cross-stratification (0.3 to 1.5 m thick), frequently fluidized and with reactivation surfaces. Mudclasts and pebbles occur sparse or concentrated at the base of bedforms. Commonly exhibit foresets and sets bounded by mud drapes with thickness variations (0.5 to 3 cm) regularly spaced (3 to 40 cm).	Migration of tidal influenced sinuous-crested subaqueous bedforms (3D) under lower flow regime alternating ebb and flood-related sedimentation.
Wavy trough cross-stratified sandstone	Stw	Light cream, medium- to coarse-grained, poorly sorted sandstone with scattered pebbles and mudclasts. The bedforms are < 0.6 m with undulated limits, sometimes with scour and drape features. Internally low-angle and trough-cross stratification are lateral continuous. Sometimes symmetric ripples occurs at the base of foresets.	Migration of sinuous-crested subaqueous bedforms (3D), under combined flow regime. The oscillatory component determines the external geometry, which the trough cross-stratification result when the oscillatory component is non-existent.
Swaley cross-stratified sandstone	Scs	Light red, medium- to coarse-grained sandstone with cut and fill structures. Small-scale bedforms (< 60 cm) with undulated edges (wavelength < 1.2 m), internally composed by low-angle and/or trough/sigmoidal cross-stratification and sparse mudclasts. Frequently with symmetric and asymmetric ripples at the base of foresets.	Migration of medium-scale bedforms with a high wavelength / amplitude ratio in conditions of combined flows regime. A continuous range of structures exists between symmetrically (low-angle) filled swales and associated trough cross-strata.
Wave ripple cross-laminated sandstone	Sw	Light cream, well-sorted, fine- to medium-grained sandstone with symmetrical and asymmetrical wavy ripple cross-lamination. The lee side is slightly concave-upward while stoss side has rounded convex-upward geometries. The internal truncated lamination varies the dip angle of the foresets. Sometimes the both stoss and lee	Wave-ripples migration under lower flow regime. The geometries vary because of combined flow conditions, where the behavior of vortex depends on the ratio between oscillatory and unidirectional components and determines

			side are concave-upward geometries, with straight crestline frequently showing two directions.	the nature of the ripple external profile and internal lamination. The crestline with two directions represents interference wave-ripples.
Accretionary hummocky cross-stratified sandstone	Hcs		Light cream, well-sorted, graded, medium-to coarse-grained sandstone. The individual beds are 1.3 m thick with common lateral thickness variations. The basal contact of the beds is sharp but non-erosive, and the top surfaces are undulated (wavelength = 0.8 to 4m). Internally the beds display milimetric laminae, generally with low angle in the lower portion of the bed, being progressively wave upwards. The thickness of each lamina increases laterally below the hummocks. The bedforms limits exhibit symmetrical and asymmetrical ripples, with a thin mudstone layer that covers the top of the beds. Locally granules and pebbles occur at the base of massive sandstone lenses.	Migration of large attenuated bedforms with a high wavelength / amplitude ratio under oscillatory flow regime, intercalated with decantation or attenuation of the flow moments.
Anisotropic migrating hummocky cross-stratified sandstone	Hma		Light cream to pink, well-sorted, fine- to medium-grained sandstone. The individual beds are 0.5 m thick with lateral thickness variations, sharp basal contact and convex-upward top surface. Internally the beds display sigmoidal or trough cross-stratification with mud drapes on the foresets.	Migration of large attenuated bedforms with a high wavelength / amplitude ratio under combined flow regime with domain of unidirectional flow.
Heterolithic mudstone and sandstone	Ht		This facies forms thick tabular beds (< 4 m) with broad lateral extent, which can commonly be traced over tens of meters. Interbedding of very-fine laminated sandstone and mudstone in millimetric to centimetric layers. Sandy lamina are massive or with ripple marks with deposition of mudstone in the ripple troughs. Mudstone exhibits sandy wavy lamination.	Alternation between deposition from traction and from suspension by wave action reworked.
Massive siltstone	Fm		Red to dark red, massive or crudely horizontally laminated siltstone, organized in 0.1 to 1.7 m lamina and strata.	Deposition from suspension and weak tractive flows.
Laminated mudstone	Fl		Reddish claystone to very fine sandstone, horizontal milimetric lamination. Sometimes in plain view sinusoidal or irregular reticulated cracks occur.	Deposition from suspension and weak bottom currents. The cracks result from syneresis cracks.



106 **Fig. 2.** Photos of selected examples of lithofacies. A) Gcm – Clast-supported conglomerate; B) Gsm –

107 Matrix-supported massive conglomerate; C) Sm – Massive sandstones; D) Sl – Low angle cross-
108 laminated sandstone; E) Ss – Sigmoidal cross-bedded sandstone; F) St – Trough cross-stratified
109 sandstone; G) Sp – Planar cross-stratified sandstone; H) Sr – Ripple cross-laminated sandstone.



110 **Fig. 3.** Photos of selected examples of lithofacies. A) Stm – Tidal bundled trough cross-stratified
 111 sandstone; B) Stw – Wavy trough cross-stratified sandstone; C) Ht – Heterolithic mudstone and
 112 sandstone; D) Fl – Laminated mudstone; E) Swaley cross-stratified sandstone; F) Hma – Anisotropic
 113 migrating hummocky cross-stratified sandstone; G) Sw – Wave ripple cross-laminated sandstone; H)
 114 Hcs – Accretionary hummocky cross-stratified sandstone.

115 5.1.1 Alluvial deposits (FA1)

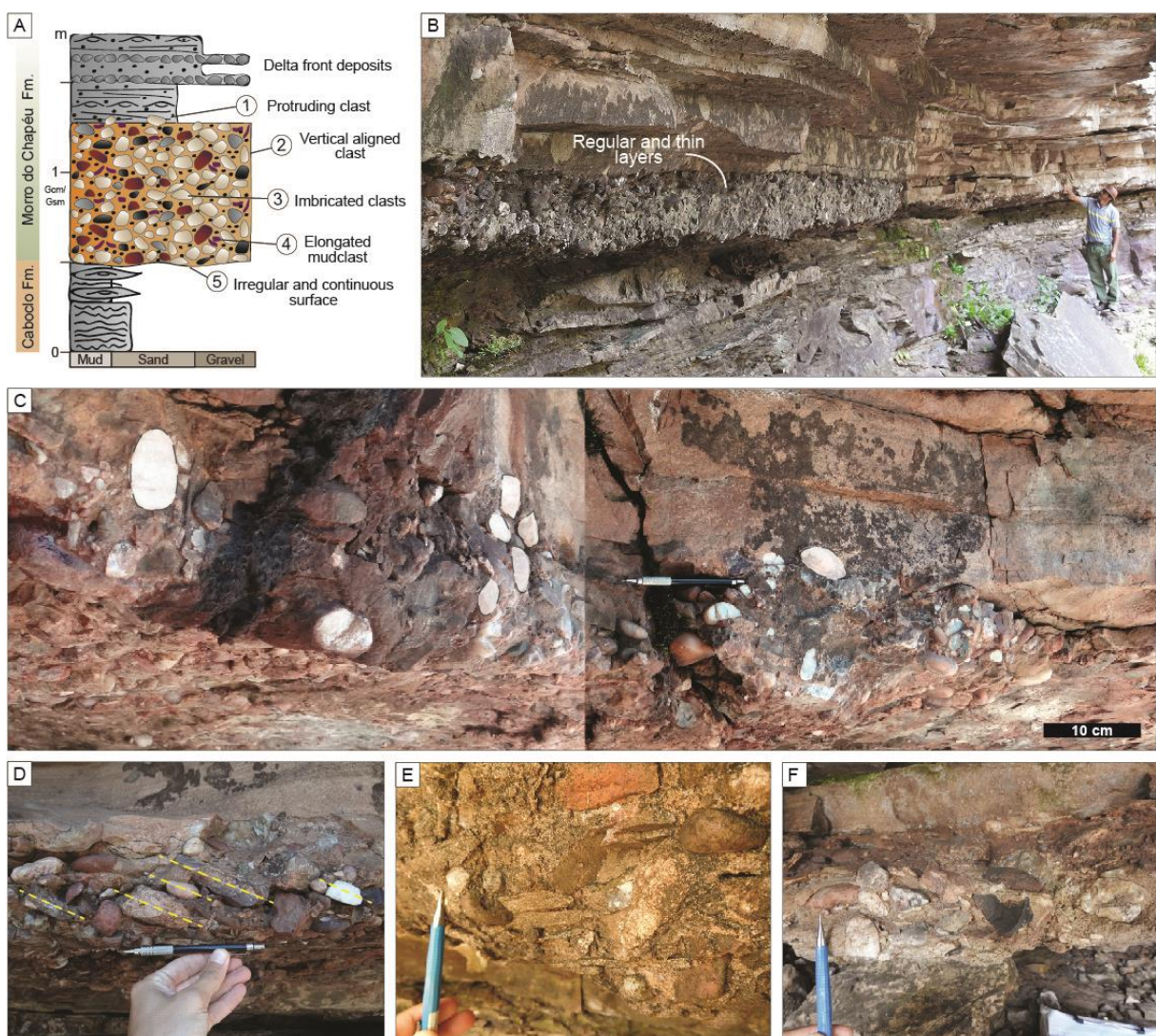
116 *Description:* Thin layer (< 0.4 m) with wide lateral extent of clast-supported
 117 conglomerates (Gcm facies) (Fig. 4D, E and F), limited by continuous and undulated surfaces
 118 above Caboclo Fm. deposits (Fig. 4B). Sometimes vertical aligned clasts occur. Isolated
 119 blocks and bigger clasts occupy the top of layers and therefore becomes protruding in layers
 120 above, which drape the lamination over the clasts (Fig.4C). Locally the clasts are parallel
 121 oriented with major axis to NW.

122 *Interpretation:* These deposits are interpreted as turbulent hyperconcentrated flows
 123 associated to gravelly ephemeral flash floods (Todd, 1989; Lowe 1979, 1982). They represent
 124 gravity flows in which the mixture of high load of sediments associated with small fluid
 125 percentages moves under the action of gravity (Blair e McPherson, 1994a). The vertical
 126 aligned clasts indicate water-scape structures. Isolated blocks and protruding clasts indicate
 127 different responses to dispersive forces and buoyancy, which bigger clasts tend to concentrate
 128 in the upper and front limits of flows, due to the density contrast between them and the
 129 surrounding particles. The imbricated clasts are common in debris flows, (Postma et al., 1988;
 130 Todd, 1989, 1996). Proximity of source area is indicated by textural maturity of sediments.

131 5.1.2 Wave-influenced delta-front (FA2)

132 *Description:* This facies association is organized in 4 to 8 m thick, coarsening-upward
 133 cycles, compounding clinoforms gently dipping with progressive increase in dip angle to the
 134 top (sigmoid geometry – Fig. 5D). The coarsening upward cycles change from lower fine-
 135 grained sandstones with thin sandstone beds, to coarse-grained thicker sandstone beds (Fig.
 136 5D). Poorly sorted sandstones to cobble conglomerates with scattered mudclasts characterize
 137 the topmost thicker beds. Internally these bodies are massive (Sm) or with trough cross-

138 bedded (St) and low angle (Sl) stratification associated to current ripples (Sr). Sedimentary
 139 structures also show an upward increase in scale when compared with the lower deposits. The
 140 lower bodies show wavy ripple lamination (Sw) and swaley cross stratification (Scs),
 141 alternated with some current ripples (Sr), silty heterolithic deposits (Ht) and centimeter-scale
 142 trough cross (St), low angle (Sl) and sigmoidal (Ss) stratified sandstones (Fig. 5 B and D).
 143 Scattered mud clasts and few soft-sediment deformation structures occur. In some cases,
 144 coarse-grained sandstones alternate and overlay thin layers of pebbles to cobbles, commonly
 145 floating in a sandy matrix. The mean dip direction of foresets from trough cross-stratification
 146 is to 287°, with a wide distribution from 200° to 350°.

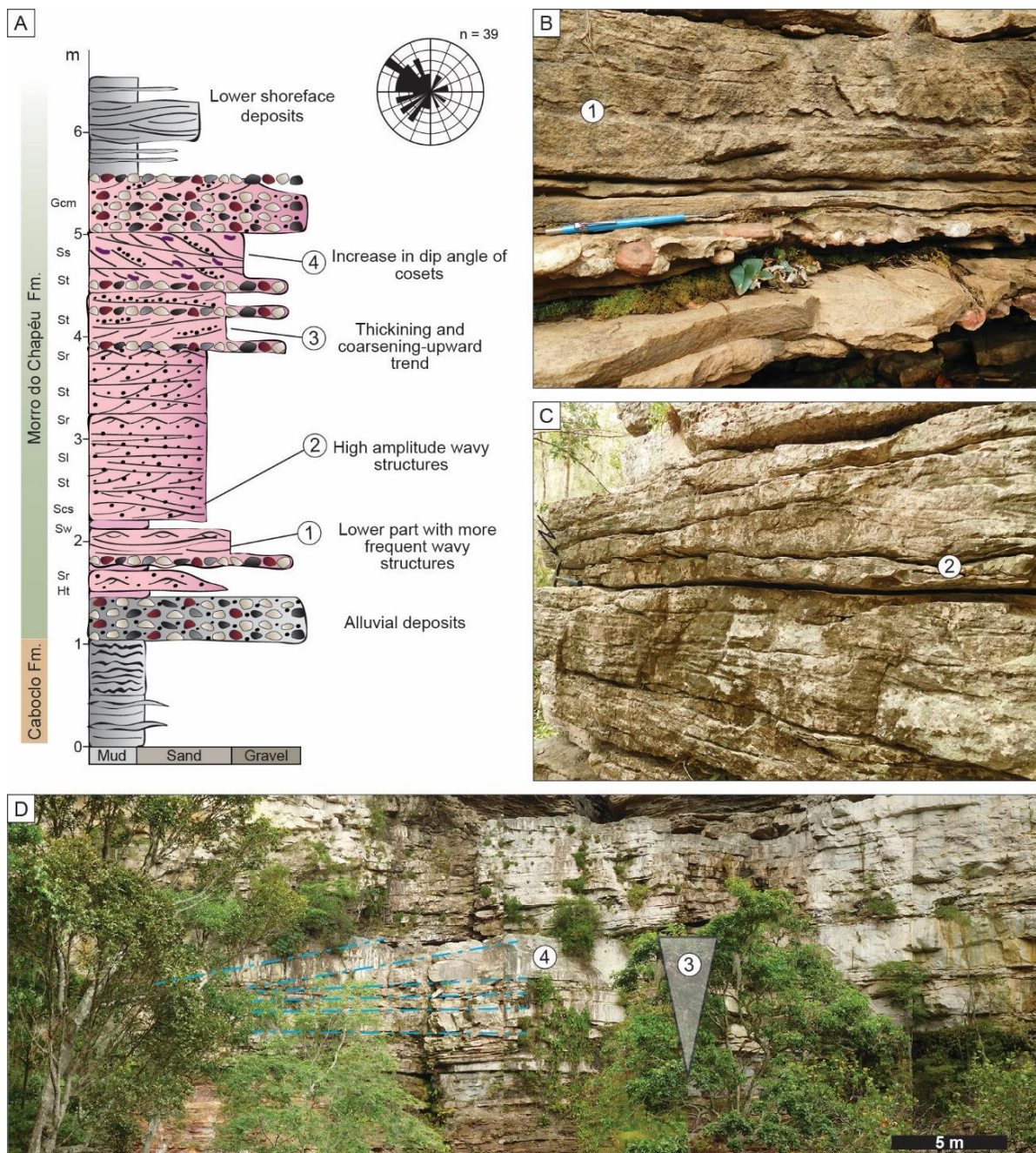


147 **Fig. 4.** A) Schematic stratigraphic columnar section of alluvial deposits with main characteristics
 148 enumerated; B) The single occurrence as a regular and thin layer with wide lateral extent; C) Layer
 149 details and representation of main larger clasts; D) Imbricated clasts; E and F) Variation of form and
 150 composition of clasts.

151 *Interpretation:* The occurrence of coarsening and thickening-upward of sandy bodies, a
152 few hundred meters long and up to 8 m thick suggest deltaic deposits. The clinoforms gently
153 dipping with progressive increase in dip angle are interpreted as mouth-bar deposits in the
154 delta-front, representing the unconfined deposits accumulated at the mouths of the distributary
155 channels as they enter the basin (Massari and Parea, 1990; Rossi et al., 2016). The coarser
156 grained sandstones with unidirectional flows (St, Ss, Sl and Sr facies) associated with thin
157 layers of pebbles to cobbles are interpreted as episodic floods that reach mouth-bar
158 (Bhattacharya et al., 2003). Massive (Sm) or low angle cross-stratified sandstones (Sl) are
159 likely to be emplaced during high discharge periods and are indicative of river floods (Rossi
160 et al., 2016). The lower bodies, which thinner grained sandstones and silty heterolithic domain
161 associated with decimeter thick Scs, Sw and low angle laminae points towards a lateral and/or
162 distal deepening trend, which can occur over only a few hundred meters. This variability can
163 represent a relative increase in wave energy in the more distal delta front system or that mouth
164 bars originally were more influenced by wave processes. The paleocurrent of thicker trough
165 cross-stratified sandstones allied to textural maturity suggest a proximity of source area
166 situated at E-SE of deposits. The 150° variation corroborate to deltaic origin.

167 5.1.3 Fluvial Deposits (FA3)

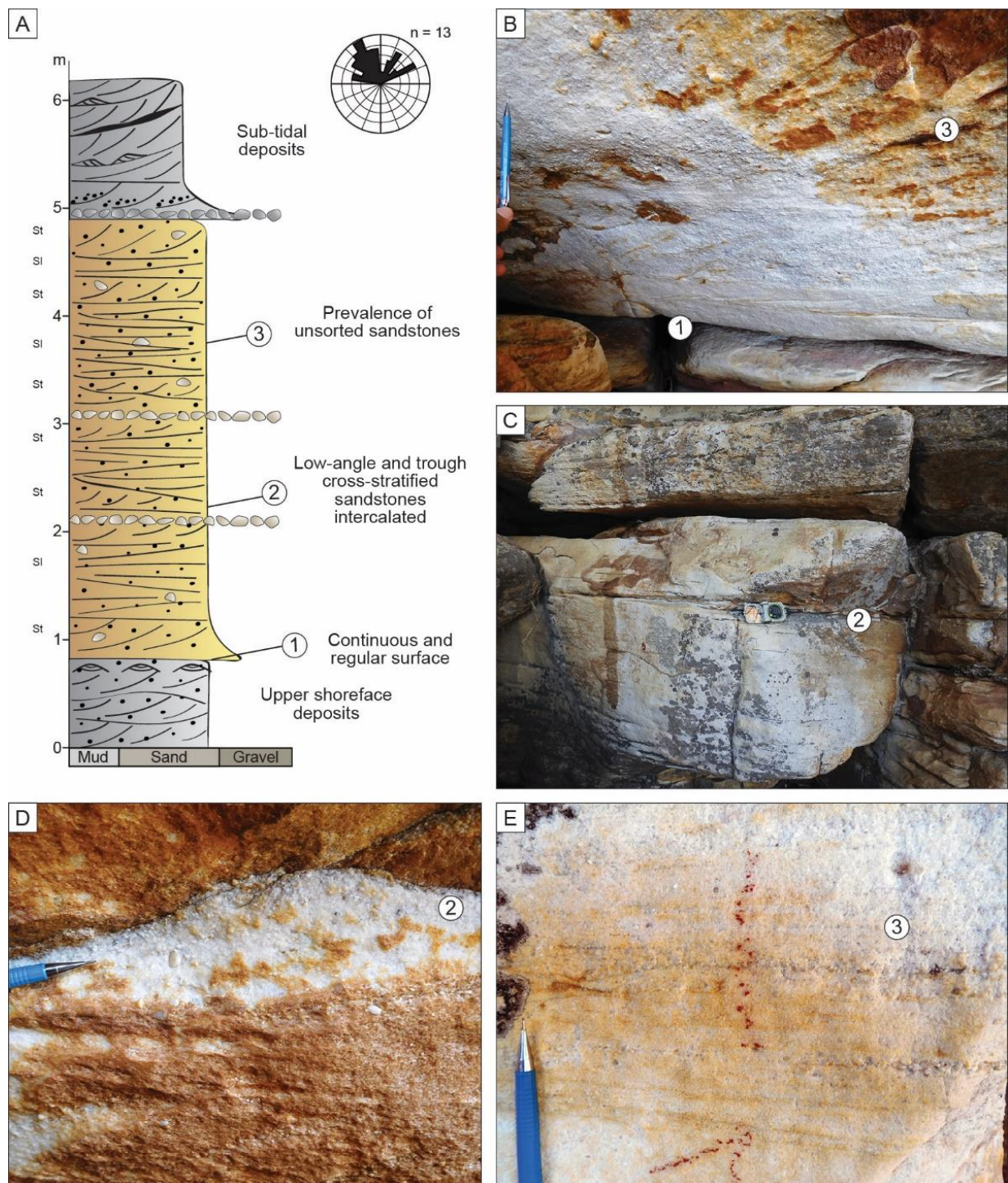
168 *Description:* Homogeneous tabular bodies of coarse-grained sandstones up to 8 m thick
169 limited by regular and lateral continuous surfaces characterized the FA3 (Fig. 6). This facies
170 association is mainly organized in finning and thinning upward cycles, 0,3 to 1 m thcij,
171 compound by large-scale trough and low angle cross-bedded sandstones (St and Sl facies)
172 (Fig. 6B and C). Internally these coarse-grained sandstones are poor sorted with scattered
173 granules and pebbles or concentrated in bottom strata (Fig. 6D and E). Paleocurrent
174 directions from cross-strata show mean dip direction to 320° with range of 65°.



175 **Fig. 5.** A) Schematic stratigraphic columnar section of wave-influenced delta with main characteristics
 176 enumerated; B) Lower part with conglomerate lag and symmetrical ripples marks (1); C) Thicker
 177 strata with swaley cross-stratified sandstones associated – white circle indicates the hammer for scale;
 178 D) Outcrop showing the thickening-upward and increase in dip angle of layers.

179 *Interpretation:* The occurrence of tabular bodies limited by regular and lateral
 180 continuous surfaces, internally composed by poor sorted, low angle cross-stratified coarse-
 181 grained sandstones, with granules and pebbles lying at base of sets, suggests deposition of
 182 unconfined sheets and poorly defined fluvial channels, resulted from high-energy flood
 183 deposition (Nemec and Postma, 1993; Blair, 2000). Tabular deposits composed of laminated

184 sandstones can be result of a series of ephemeral unconfined sheetfloods (Tunbridge, 1981;
 185 within the finning and thinning upward trend represents a
 186 decrease in flow energy (Nemec and Steel, 1984). The thick tabular geometry can results from
 187 amalgamation of board and shallow braided channel deposits (Miall, 1996).



188 **Fig. 6.** A) Stratigraphic columnar section of fluvial deposits with main characteristics enumerated;
 189 Regular surface with coarse-grained, trough cross-stratified sandstones above; C) Thick layers of low-

190 angle and trough cross-stratified sandstones; D) Detail of granules and pebbles concentration; E)
191 Detail of grain size sort.

192 5.1.4 Subtidal deposits (FA4)

193 *Description:* Well-sorted, fine- to medium-grained sandstones, limited by regular
194 surfaces, with up to 8 m thick and wide lateral continuous (Fig. 7). Low angle (Sl) and trough
195 cross-stratification (St) are associated to ripple marks (Sr), which sometimes show opposite
196 direction to stratification (Fig. 7 B, E and G). Sigmoidal surfaces regularly spaced with mud
197 drapes along the foresets (Stm) eroding the top of below foresets are common (Fig. 7E and F).
198 Cosets with up to 0.2 m thick are limited by flat surfaces dipping slightly to same direction of
199 the foresets (Fig. 7 C, D and F). Ripple marks aggradation occur at the top of bedforms.
200 Trough cross-stratifications show a dominant dip direction of foresets to 310°, varying
201 between 240° to 360°. Ripple marks show mean direction to 105°, varying from 45° to 135°.

202 *Interpretation:* The sandy bodies limited by flat and regular surfaces, which trough
203 cross-stratification domain with reactivation surfaces, mud drapes capping foresets and ripple
204 marks dipping to opposite direction, indicate that these deposits are related to subtidal
205 conditions (Allen, 1980; Visser, 1980; Clifton, 1983). Superposed sets limited by flat surfaces
206 dipping slightly to same direction of the foresets represent compound dunes migrating on the
207 main dune lee side (Dalrymple and Choi, 2007). Sigmoidal surfaces that erode below foresets
208 are interpreted as reactvation surfaces and indicate variations on the lee side due to change in
209 tidal currents direction (Shanley et al., 1992). The regular spaced mud drapes represent cyclic
210 deposition of tidal (Visser, 1980). Bidirectional paleocurrent indicate alternating ebb and
211 flood episodes, with domain of ebb regime.

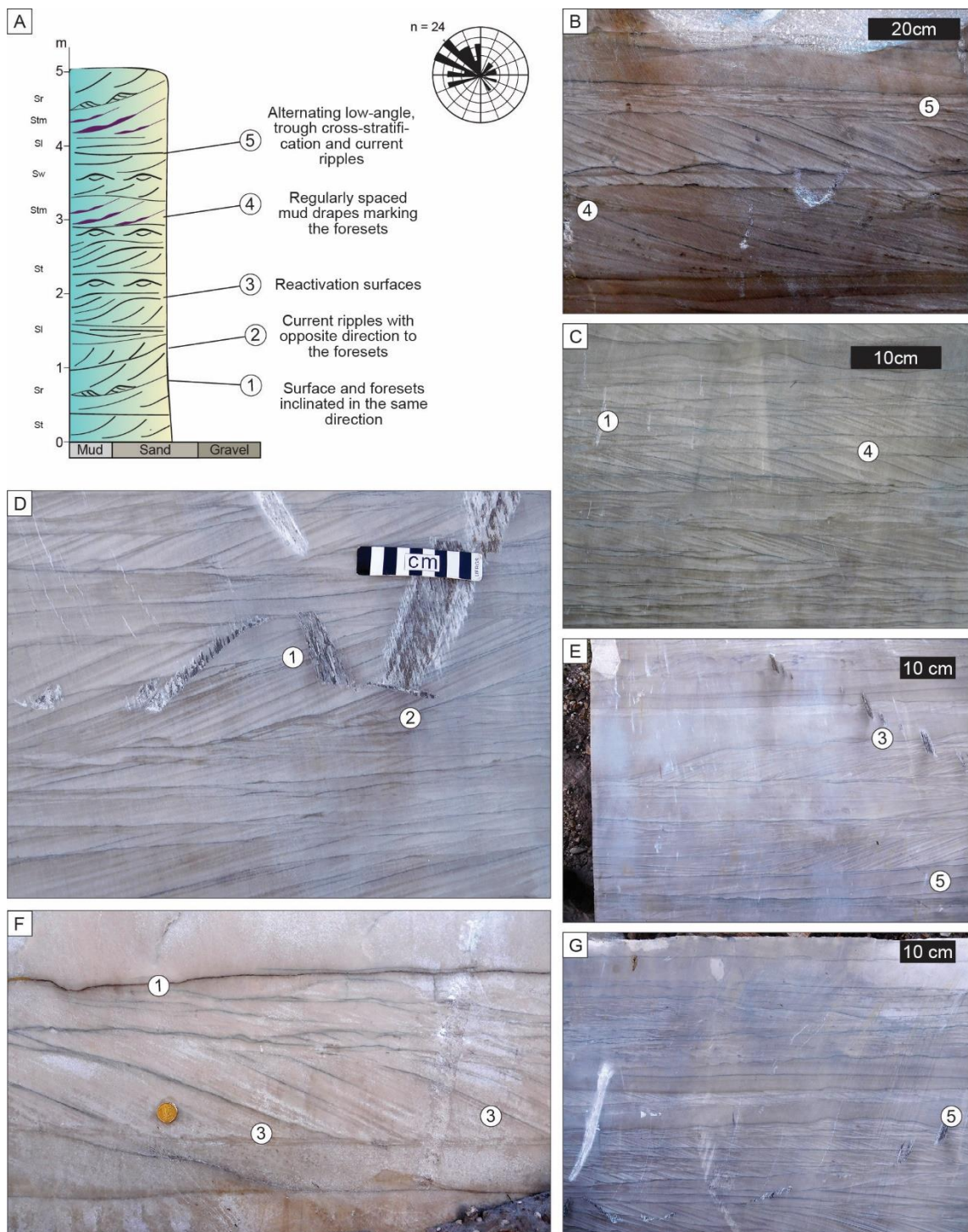
212 5.1.5 Upper shoreface deposits (FA5)

213 *Description:* Thick sandy amalgamated, superimposed packages, up to 20 m thick.
214 Internally the sandstones bodies show alternations between unidirectional, oscillatory and
215 combined flows structures (Fig. 8). Swaley cross-stratifications and wavy or current ripples

216 (Scs, Sw and Sr) are the most common sedimentary structures, while sigmoidal and planar-
217 tabular cross-stratification and massive sandstones (Ss, Sp and Sm) are minor components.
218 The sets are small (< 0.7 m) and can vary laterally to low angle (Sl) or wavy trough cross-
219 stratification (Stw). Some hummocky cross-bedding (Hcs and Hma) occur and locally are
220 separated by thin laminated mudstones. The increase in scale of sandstones combined with
221 disappearing of the mudstones results in upward-coarsening packages. A wide grain size
222 variation occurs in these deposits from well sorted fine-grained sandstone to poorly sorted
223 granule to pebble sandstone (Fig. 8A). The trough cross-stratifications show a dominant dip
224 direction to 325°, while the ripple marks show two mean directions (30° and 230°).

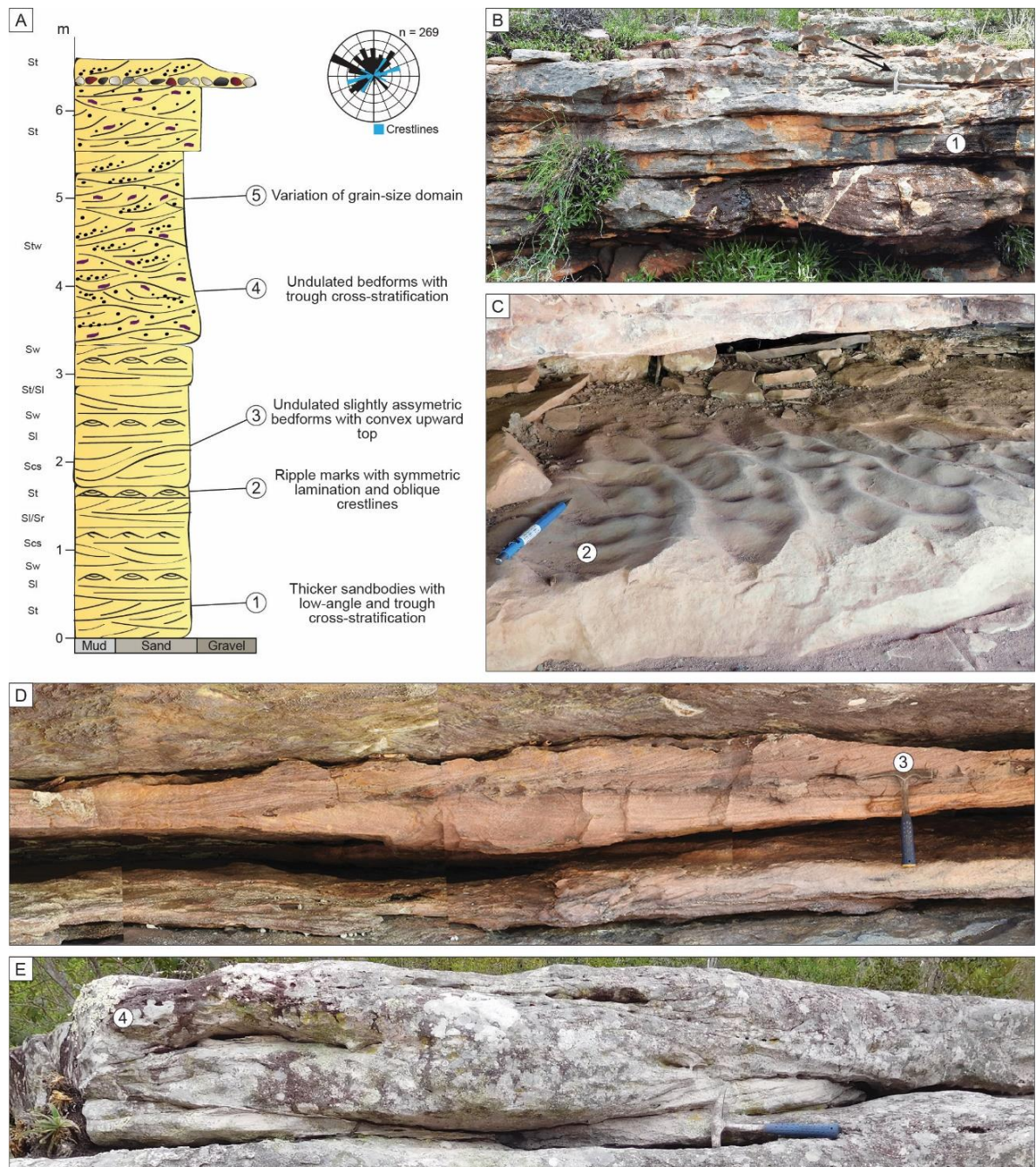
225 *Interpretation:* The local coarsening-upward succession, the upward increase in flow
226 strength indicated by the sedimentary structures, and the abundance of swaley cross-
227 stratification and wave ripples, allowed interpreting this facies succession to be shoreface
228 deposits. The trough and planar tabular crossbedded sandstones are interpreted as deposits of
229 the surf zone, possibly rip-current bars (paleocurrent to 325), and low angle cross-stratified
230 sandstones are interpreted as swash-zone deposits. The two directions of the ripple marks
231 represent the longshore currents. The presence of SCS and HCS bedding indicate storm-
232 generated wave structures typically found in nearshore marine settings (Dott and Bourgeois,
233 1982; Leckie and Walker, 1982). This facies association preserves a record of high-energy
234 and probably high frequency episodic deposition, which is reflected by the abundance of
235 swaley cross-stratified sandstone (Vakalerov et al., 2012). Preferential formation of swales
236 rather than hummocks has been attributed to the lower aggradation rates due to low
237 deposition-to-transport ratios that typically occur in shallower water during storms (Dumas
238 and Arnott, 2006). This characteristics suggests deposition dominated by combined
239 oscillatory and unidirectional flow conditions on the shelf during storms (Swift et al., 1993).

240



241 **Fig. 7.** A) Stratigraphic columnar section of subtidal deposits and main characteristics enumerated; B)
242 Trough cross-stratified sandstones with mud drapes marking the foresets intercalated with low-angle
243 lamination and current ripples; C) Surfaces inclined in the same direction of foresets; D) Current
244 ripples with opposite direction to the foresets (2). Note the lamination truncated by reactivation
245 surface (1); E) Reactivation surface with relief of 10 cm; F) Regularly spaced reactivation surfaces
246 with sigmoidal profile; G) Centimetric alternation of between Sl, Stm and Sr facies.

247

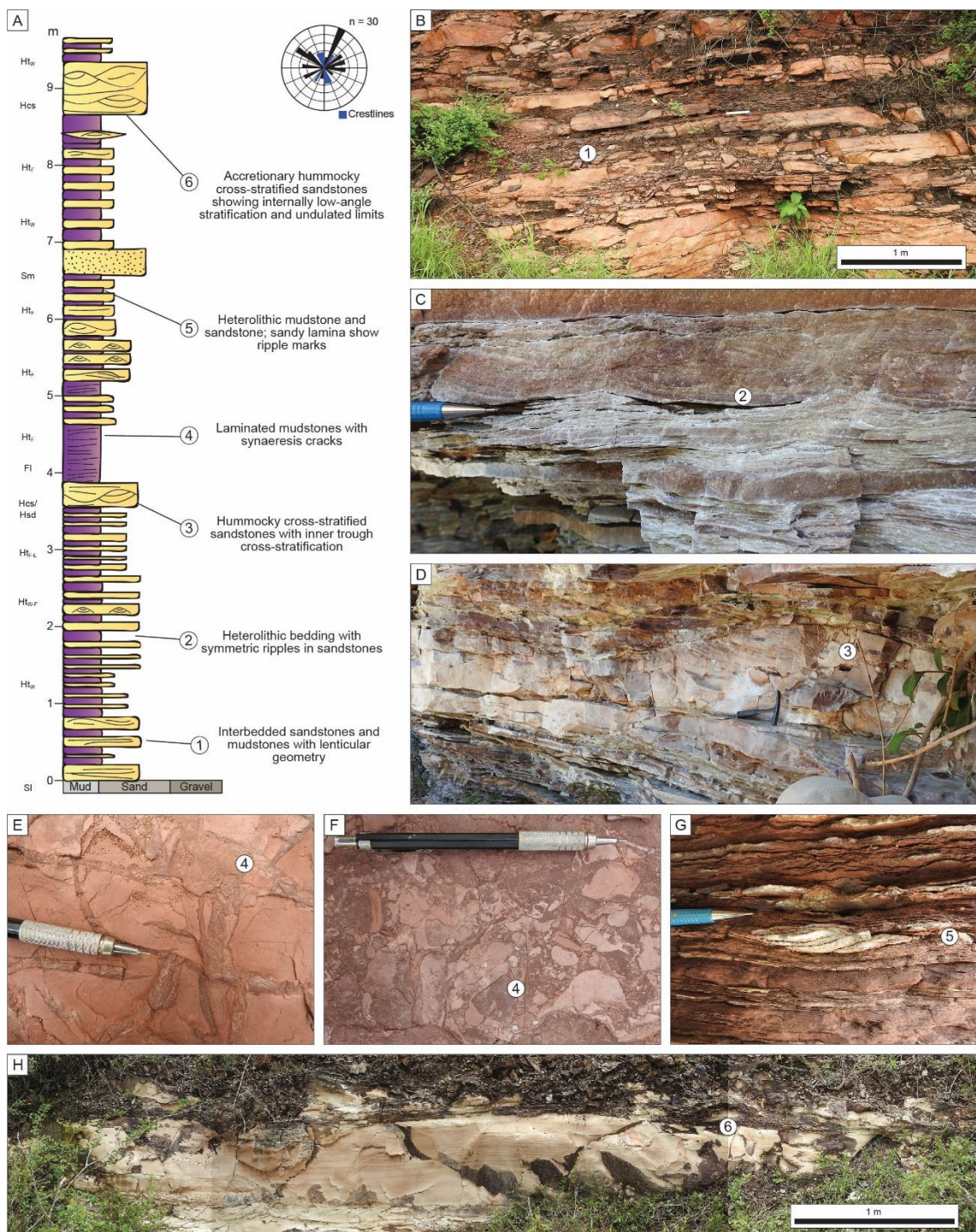


248 **Fig. 8.** A) Schematic stratigraphic section of shoreface deposits and main characteristics enumerated;
 249 B) Undulated sandy bodies with low-angle lamination and laterally trough cross-stratified; black circle
 250 indicates the scale; C) Ripple marks with oblique crestlines; D) Trough cross-stratified, coarse-grained
 251 sandstones with lenticular geometry and symmetric ripples at the top; E) Undulated bedforms with
 252 trough cross-stratification with lenticular geometry.

253 5.1.6 Lower shoreface deposits (FA6)

254 *Description:* Thick package (20 m) composed internally by metric intervals of
 255 laminated mudstones (Fl) and massive siltstones (Fm) with discontinuous sandy laminae and
 256 local syneresis cracks (Fig. 9). The sandy laminae show symmetric wave ripple cross-

257 lamination (Sw) and alternate with mudstones forming cyclical coarsening and thinning
 258 upward stacking patterns (Fig. 9A and B). Sometimes the alternation between sandstones and
 259 mudstones compose heterolithics (Ht) with mm- to cm-scale thicknesses (Fig. 9C and G).
 260 There are some local occurrences of hummocky cross-stratified sandstones (< 0.4 m) with
 261 irregular lower limits and sparse coarser sand grains (Fig. 9 D and H).



262 **Fig: 9.** A) Schematic stratigraphic section of lower shoreface deposits and main characteristics
 263 enumerated; the middle interval with thicker mudstone represents the offshore occurrence; B)

264 Interbedded lenticular sandstones and mudstones; C) Detail of symmetric ripple marks alternating with
 265 mudstones; D) Hummockys with inner trough cross-stratification; E) Syneresis cracks with irregular
 266 and discontinuous form in plain view on offshore deposits; F) Syneresis cracks with breccia aspect in
 267 plain view on offshore deposits; G) Ripple mark with symmetrical geometry and inner trough cross
 268 lamination; H) Accretionary hummocky with internally low-angle stratification.

269 *Interpretation:* These deposits were deposited under quiet water conditions with periods
 270 of wave interference. The occurrence of hummockys and oscillatory ripples suggest that this
 271 facies was deposited between the storm-weather wave-base (SWWB) and fair-weather wave-
 272 base (FWWB) in offshore transitions zone. Syneresis cracks result from contraction of the
 273 swelling clay lattices in response to the salinity changes (Plummer and Gostin, 1981; Pratt,
 274 1998).

275 5.1.7 Offshore deposits (FA7)

276 *Description:* This facies associations is characterized by thin beds of laminated
 277 mudstones (Fl), compounding thin package (< 4 m) without facies variation (Fig. 9 E and F).
 278 The lower and upper contacts are diffuse due to sandy laminae increase (Fig. 9 A).

279 *Interpretation:* These mudstones were deposited under quiet water conditions. The lack
 280 of unequivocal current or oscillation ripples suggest that this facies was deposited below of
 281 the storm-weather wave-base (SWWB) in offshore zone. Syneresis cracks result from
 282 contraction of the swelling clay lattices in response to the salinity changes (Plummer and
 283 Gostin, 1981; Pratt, 1998). The sandy laminae increase that mark the offshore limits probably
 284 result of material transported into the muddy area during higher energy events (e.g. Noe-
 285 Nygaard and Surlyk, 1988).

286 6. Discussion

287 The main characteristics of the Morro do Chapéu Fm. are: 1) the entire succession of
 288 deposits exhibit minor lateral changes in thickness with relatively tabular geometries and have
 289 a slight internal variation of facies composition; 2) dominant paleocurrents to NW; and 3) two
 290 transgressive trends separated by continental deposits.

291 6.1 Paleocurrents

292 Paleocurrent data from various stratigraphic intervals and their respective facies
293 successions provide extensive documentation of sediment transport directions. The data
294 analyze implies a southeast (proximal) to northwest (distal) axis for system progradation and a
295 south-west/north-east shoreline orientation. In the context of the northeast/southwest oriented
296 paleoshoreline, the dominant northwestward direction is attributed to fluvial and ebb-tidal
297 currents, and the subordinate southeastward direction to flood-tidal currents. Northeast-
298 directed paleocurrents may be attributed to local wave-driven longshore drift, which could
299 have deflected deltaic distributary channel. Overall, the MCF succession preserves this
300 paleocurrent pattern, from bottom to top, recording a homogeneous arrangement in which the
301 tidal occurrence is the main variation. The offshore-directed currents recorded the combined
302 dominance of deltaic and ebb-tidal currents.

303 6.2 Stratigraphic architecture

304 Two incomplete depositional sequences are bounded by two subaerial unconformities
305 showing an abrupt change in facies and grain size. In the figure 10, a sequence boundary has
306 been interpreted near the base of the succession. The lower subaerial unconformity (SU)
307 separates sharp-based alluvial deposits from siltstones of Caboclo Formation. The thin layers
308 of alluvial deposits begin in a very abrupt manner, without any gradual trend in three
309 outcrops. These layers are lost towards the west (i.e. further basinward) and the lower SU are
310 covered and not cropping out.

311 The lower proximal interval of MCF is a coarsening-upward succession of FA2
312 representing upward shallowing and progression of genetically linked facies on a wave-
313 dominated delta front. The lateral continuity of the sand-rich and dominating northwest flow
314 indicate that mud was removed from the proximal delta front, probably caused by a
315 combination of wave reworking (Legler et al., 2014; Cappelle et al., 2016) and strong seaward
316 currents. The wave reworking of the delta front is demonstrated by the occurrence of swaley,

317 hummockys and wave ripples and provides a mechanism for transporting sand and mud to
318 seaward.

319 The abrupt change in grain-size across the regular surface between FA2 and FA6, as well
320 as a conformable shift from a progradational to a retrogradational stacking pattern, record the
321 maximum regressive surface (MRS). A landward position from the shoreline can be inferred
322 by the surface preservation, since the seaward surface extent is typically reworked by the
323 transgressive ravinement surface (Zecchin and Catuneanu, 2013). The transgressive system
324 tract is characterized by a thin retrogradational interval (< 8 m) of lower shoreface deposits
325 that overlay the MRS. Such deposits derive from shoreface erosion given that southeastern
326 paleocurrent direction. The sediment probably trapped in the alluvial and coastal plain
327 environments reduce the sediment influx to the basin and occur the cannibalization and
328 ravinement of sediments previously deposited in early stages of transgression (Cattaneo and
329 Steel, 2003). The absence of ravinement evidences characteristics (e.g. erosion and associated
330 lag) and mud-dominated deposits suggest a low-energy setting, without significant waves or
331 tides in the shorezone.

332 The retrogradational stacking pattern keeps until the maximum flooding surface (MFS),
333 indicated by mudstone domain and few sandy bodies occurrence. The MFS marks a change to
334 progradational stacking pattern, which is characterized by coarsening and thickening upward
335 of sandy bodies. Wave evidences like wave ripple marks and hummocky cross-stratification
336 are the most common structures. However, as the increase in the sand domain the storm-wave
337 processes with combined-flow structures become predominant. Almost entirely of shoreface
338 deposits are composed by erosionally amalgamated tempestites, with the break between lower
339 and upper shoreface not recognizable. The upper shoreface deposits increase in thickness in
340 response to the increasing size of waves affecting the coastline, dominating low-angle and
341 trough-cross undulatory sandstones. The coarser-grained debris and low-angle scour surfaces
342 suggest storms action in sand-dominated foreshores (Dashtgard et al., 2012).

343 The second subaerial unconformity (SU') is a regular and continuous surface traceable at
344 five outcrops. This surface is marked by an increase in grain size (granules and pebbles) with
345 localized conglomeratic portions. The overlying deposits of FA3 are coarse-grained with
346 tabular geometry and wide lateral extent. The unidirectional paleocurrent, coarser grain size
347 without mudstone interbeds suggest high degree of amalgamation. It is widely recognized that
348 Precambrian fluvial systems were braided as consequence of lack of vegetation and poor soils
349 development, which promote rapid runoff of surface water and high rate of channel migration
350 compared to vegetated systems from the Phanerozoic (Miall, 1996; Bose et al., 2012;
351 Magalhães et al., 2014). The tabular amalgamated deposits could indicate limited
352 accommodation space, associated to lowstand systems tract.

353 Presence of subtidal deposits (FA4) with angular clay chips, double mud drapes and
354 sigmoidal lamination, lying at conglomeratic level with white granules and pebbles, indicate
355 the end of shoreline seaward migration and the MRS'. The abrupt change to FA 4 suggest a
356 progressive landward migration of a tidal inlet during transgression. In the middle interval of
357 Morro do Chapéu Formation the tidal succession form tabular and widely lateral continuous
358 deposits suggesting a coastal area connected to a wide and low gradient alluvial braidplain,
359 within distal deposits were reworked by tidal currents responsible for the cross-bedded
360 sandstones (FA4). The tides may operate also during deposition of wave-dominated delta and
361 shoreface occurrence, but in areas sheltered from waves. The disappearance of the wave-
362 generated deposits requires a relative increase in tidal energy or decrease in wave energy. This
363 evidence suggests that tidal range increased from lower to upper stratigraphic sequence. The
364 tidal range may increase with an increased width of a platform or just because tidal resonance
365 became active (Dalrymple, 1992).

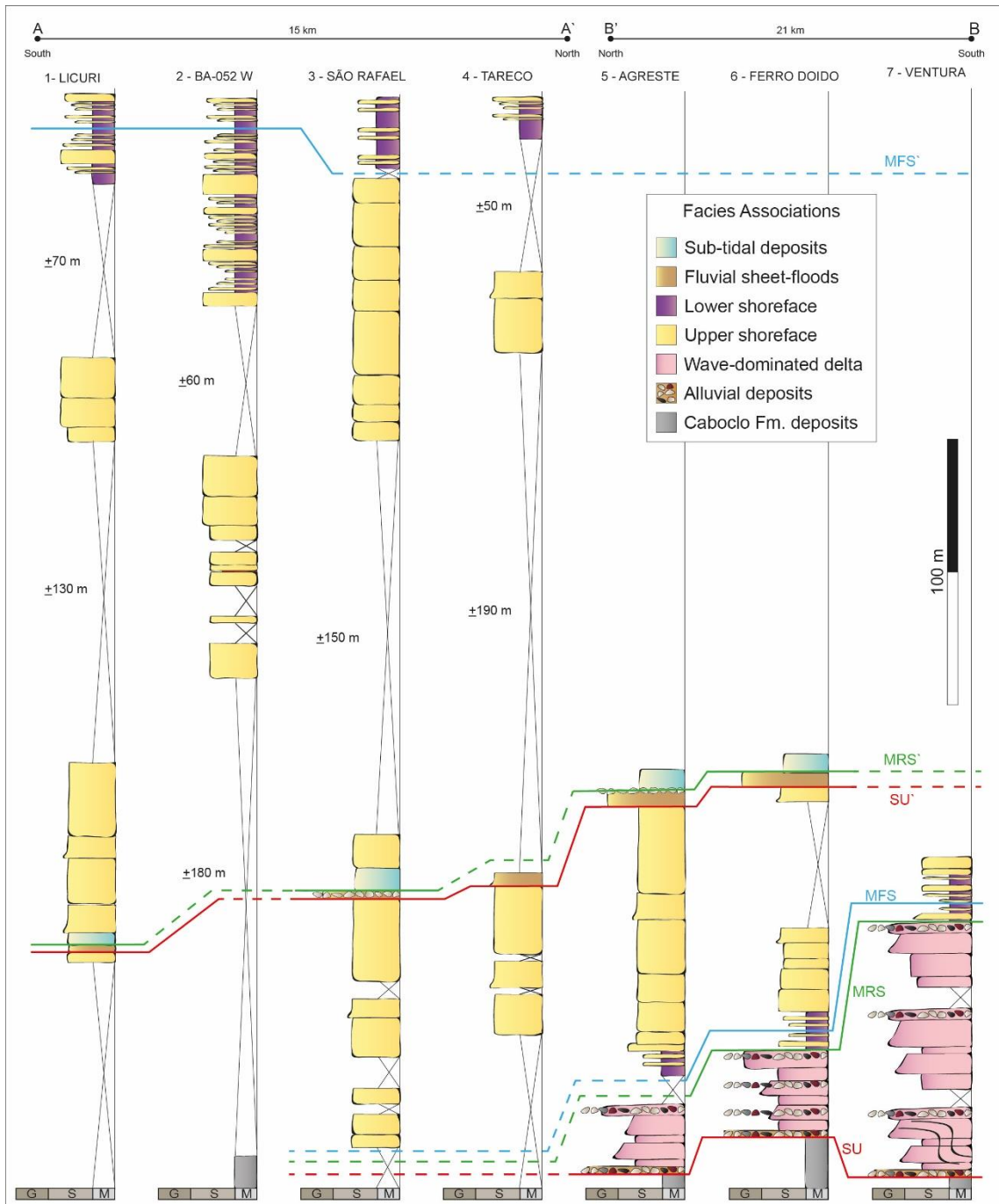
366 An abrupt change of FA3 to shoreface deposits of FA5, as well as a retrogrational stacking
367 pattern, is visible in two outcrops. The dominant preserved sedimentary structures on the
368 upper shoreface are current-generated structures, oriented seaward to the shoreline. Wave

369 ripples and low-angle beds are the dominant fair-weather wave-generated structures, whereas
370 swaley and hummocky cross-stratification comprise the dominant storm-wave-generated
371 structures. The bedforms generated by combined-flow can be explained by unidirectional ebb-
372 flow from tides acting with oscillatory flow from waves. Besides tidally generated
373 sedimentary structures are not present, rhythmic interbedding of combined-flow/current
374 ripples and/or low angle/trough-cross stratification occur. This rhythmic records sediment
375 deposition by shoaling waves, breaking waves and surf, which occurs as tides force the lateral
376 translation of wave zones across the intertidal zone (Dashtgard et al., 2012). The thick
377 shoreface deposits suggest a coastal aggradation, could be favored by high rates of base-level
378 rise, weak transgressive ravinement erosion and shallow topographic gradients (Catuneanu,
379 2006).

380 With progressive landward shoreline migration, FA5 and FA6 interfinger laterally and
381 vertically to form a complex association of combined flow structures pointing to fair- and
382 storm-weather waves, which domain on upper Morro do Chapéu Fm. The decreasing grains
383 size at the top of succession is attributed to a pronounced decrease in the sedimentation rate,
384 probably related to rising relative sea level. The MFS' is attributed at thick interval of
385 mudstones where the stacking pattern change to progradational again.

386 6.3 Depositional model

387 Exposures on eastern cliffs allowed the successions correlation of lower interval along a
388 wide lateral extent (< 300 m), within depositional sequence display changing of facies from
389 lowstand deltaic system to transgressive shoreface systems. In some sections, highstand
390 shoreface strata are the principal deposits preserved, changing facies to lowstand fluvial
391 system. The upper interval is better exposed in western area where a mountain ridge allowed
392 the correlation of upper transgression and the changing facies from upper to lower shoreface
393 deposits.



394 **Fig. 10.** Seven stratigraphic logs in study area with main surfaces that allow the correlation between
 395 them.

396 In all these exposures, coastal systems from Morro do Chapéu Fm. exhibits tabular
 397 successions and sheet-like geometry with broad lateral continuity, without any evidence of
 398 fluvial incised-valley. Nevertheless, the studied succession has the criteria related to subaerial
 399 unconformity and transgression of estuarine-systems, but those are not exclusive of incised-
 400 valley systems, being applied to unincised fluvial-shallow marine systems also. Furthermore,
 401 the Espinhaço Upper Megasequence was deposited in a shallow and low gradient rift-sag

402 basin margin (Chemale et al., 2012); within wave action is the main actuating process during
403 the entire Morro do Chapéu deposition. Only in the middle interval, when fluvial and tidal
404 deposits prevail, occurs the disappearance of wave-generated deposits.

405 All these conditions corroborate to interpret the Morro do Chapéu Fm. as a coastal area
406 connected to a wide and low gradient alluvial braidplain. Thus, the evolution of Formation
407 may be described by relative sea level variation. The wave-influenced deltaic systems were
408 formed during periods of lowered relative sea level, within rivers flowed on a gentle dipping
409 shelf surface. Lowstand deltaic aggraded followed by transgression in which shoreface
410 deposits accumulate until another fall in relative sea level. The fluvial sand sheet were
411 deposited and the new transgression marks the development of areas where tides extended
412 their effects upstream. The following transition to thick shoreface deposits suggest a coastal
413 aggradation favored by high rates of base-level rise, weak transgressive ravinement erosion
414 and shallow topographic gradients.

415 **7. Conclusions**

416 Sedimentary facies analysis of Morro do Chapéu Formation reveals deposition across two
417 incomplete stratigraphic sequences. A wide fall in relative sea level represented by irregular
418 surface between Caboclo Formation and alluvial deposits of Morro do Chapéu Formation
419 establishes the beginning of lower sequence. The progradational wave-dominated delta
420 constitutes the lowstand system tract and is followed by lower shoreface deposits. The thin
421 transgressive interval is overlapped by upper shoreface deposits, representing the highstand
422 system tract. The lower sequence is limited at the top by a subaerial unconformity laying
423 fluvial sheet floods above shoreface deposits. This new fall in relative sea level may have
424 modified the shoreline and tidal becomes main active processes and the major difference
425 between the sequences. The following upper shoreface deposits are mainly composed by
426 tempestites, and intercalate with lower shoreface deposits. The thick interval of mudstones
427 represents the maximum flood surface of upper sequence.

428 The domain of NW paleocurrents indicates the rip currents predominance, associated to
 429 minor long shore currents (SW-NE) parallel oriented to de paleoshoreline. The successions
 430 studied and the correlation of them corroborates to interpret the Morro do Chapéu Formation
 431 as a coastal area connected to a wide and low gradient alluvial braidplain. Thus, the evolution
 432 of Formation may be described by relative sea level variation, which our sedimentary facies
 433 analysis indicate development of at least two falling stage systems tracts. The described
 434 sequence of events contributes to a better understanding of coastal sedimentation in
 435 Precambrian basins placed in similar tectonic settings.

436 **8. Acknowledgments**

437 This research was completed as part of the doctoral Project carried out by the first author
 438 and fully sponsored by Petrobras. We thank Francisco Barbosa for the primordial assistance
 439 in the fieldworks, and Antônio José Dourado for the helpful and constructive comments that
 440 greatly improved this study.

441 **9. References**

- 442 Alkmim, F.F., Martins-Neto, M.A., 2012. Proterozoic first-order sedimentary sequences of the São Francisco
 443 craton, eastern Brazil. *Marine and Petroleum Geology* 33, 127-139.
- 444 Allen, J.R.L., 1980. Sand waves: a model of origin and internal structure. *Sedimentary Geology* 26, 281–328.
- 445 Babinski, M., Van Schmus, W.R., Chemale, F.Jr, Neves, B.B.B., Rocha, A.J.D., 1993. Idade isocrônica Pb-Pb
 446 em rochas carbonáticas da Formação Caboclo em Morro do Chapéu, BA. II Simpósio sobre o Cráton do
 447 São Francisco, Sociedade Brasileira de Geologia 2, Salvador (BA), Anais, 160–163.
- 448 Battilani, G.A, Gomes, N.S, Guerra, W.J., 1997. Evolução diagenética dos arenitos da Formação Morro do
 449 Chapéu, Grupo Chapada Diamantina, na região de Morro do Chapéu, Bahia. *Geonomos* 4, 81-89.
- 450 Bhattacharya, J.P., Giosan, L. (2003) Wave-influenced deltas: geomorphological implications for facies
 451 reconstruction. *Sedimentology* 50, 187–210.
- 452 Blair, T.C., 2000. Sedimentology and progressive tectonic unconformities of the sheetflood-dominated Hells
 453 Gate alluvial fan, Death Valley, California. *Sedimentary Geology* 132, 233-262.
- 454 Blair, T.C., McPherson, J.G., 1994. Alluvial fan processes and forms. In: Abrahams, A.D., Parsons, A. (Eds.),
 455 *Geomorphology of Desert Environments*. London: Chapman & Hall, 354-402.
- 456 Bose, P.K., Eriksson, P.G., Sarkar, S., Wright, D.T., Samanta, P., Mukhopadhyay, S., Mandal, S., Banerjee, S.,
 457 Altermann, W., 2012. Sedimentation patterns during the Precambrian: a unique record? *Marine Petroleum
 458 Geology*, 33, 34 – 68.

- 459 Bosence, D.W.J., 1998. Stratigraphic and sedimentological models of rift basins. In: Purser, B.H., Bosence,
 460 D.W.J. (Eds.), *Sedimentation and tectonics of rift basins: Red Sea – gulf of Aden*. Chapman and Hall,
 461 London, pp. 9–25.
- 462 Brito Neves, B.B., 1967. Geologia das folhas de Upamirim e Morro do Chapéu Bahia. Relatório 17 Companhia
 463 Nordestina de Sondagens e Perfurações CONESP – SUDENE.
- 464 Brito Neves, B.B., Kawashita, K., Delhal, J., 1979. A evolução geocronológica da Cordilheira do Espinhaço;
 465 dados novos e integração. *Revista Brasileira de Geociências* 9, 71–85.
- 466 Cappelle, M.V., Stukins, S., Hampson, G.J., Johnson, H.D., 2016. Fluvial to tidal transition in proximal, mixed
 467 tide-influenced and wave-influenced deltaic deposits: Cretaceous lower Sego Sandstone, Utah, USA.
 468 *Sedimentology* 63, 1333–1361.
- 469 Cattaneo, A., Steel, R.J., 2003. Transgressive deposits: a review of their variability. *Earth-Science Reviews* 62,
 470 187–228.
- 471 Catuneanu, O., 2006. Principles of sequence stratigraphy. Amsterda: Elsevier, 375 p.
- 472 Chemale Jr., F., Alkmim, F.F., Endo, I., 1993. Late Proterozoic tectonism in the interior of the São Francisco
 473 craton. In: Findlay, R.H., Unrug, R., Banks, M.R., Veevers, J.J. (Eds.), *Gondwana eight: assembly,*
 474 *evolution and dispersal*. Balkema, Rotterdam, 29–41.
- 475 Chemale Jr., F., Dussin, I.A., Alkmim, F.F., Martins, M.S., Queiroga, G., Armstrong, R., Santos, M.N., 2012.
 476 Unravelling a Proterozoic basin history through detrital zircon geochronology: The case of the Espinhaço
 477 Supergroup, Minas Gerais, Brazil. *Gondwana Research* 22, 200–206.
- 478 Clifton, H.E., 1983. Discrimination between subtidal and intertidal facies in Pleistocene deposits, Willapa Bay,
 479 Washington. *Journal of Sedimentary Petrology* 53 (2), 353–369.
- 480 Dalrymple, R.W., 1992. Tidal depositional systems. In: Walker, R.G., James, N.P., (Eds), *Facies Models;*
 481 *Response to sea level change*. Geological Association of Canada, 195–218.
- 482 Dalrymple, R.W., Choi, K., 2007. Morphologic and facies trends through the fluvial-marine transition in tide-
 483 dominated depositional systems: a schematic framework for environmental and sequence-stratigraphic
 484 interpretation. *Earth-Science Reviews* 81 (3-4), 135–174.
- 485 Dashtgard, S.E., MacEachern, J.A., Frey, S.E., Gingras, M.K., 2012. Tidal effects on the shoreface: Towards a
 486 conceptual framework. *Sedimentary Geology*, 279, 42 -61.
- 487 Dott R.H.Jr, Bourgeois, J., 1982. Hummocky stratification: Significance of its variable bedding sequences. *Geol.*
 488 *Soc. Am. Bull.* 93, 663–680.
- 489 Dumas, S., Arnott, R.C.W., 2006. Origin of hummocky and swaley cross-stratification. The controlling influence
 490 of unidirectional current strength and aggradation rate. *Geology* 34, 1073–1076.
- 491 Guadagnin, F., Chemale, F., Magalhães, J., Santana, A., Dussin, I., Takehara, L., 2015. Age constraints on
 492 crystal-tuff from the Espinhaço Supergroup – insight into the Paleoproterozoic to Mesoproterozoic
 493 intracratonic basin cycles of the Congo–São Francisco Craton. *Gondwana Research*, 27, 363–376.
- 494 Guimarães, J.T., Pedreira, A.J., 1990. Geologia da Chapada Diamantina Oriental, Bahia (Folha Utinga). In:
 495 Guimarães, J.T. & Pedreira, A.J. (Orgs.) - *Programa de Levantamentos Geológicos Básicos do Brasil.*
 496 Utinga (Folha SD.24-V-A-II) Estado da Bahia, Texto Explicativo. Brasília, DNPM/CPRM, 19-92.
- 497 Hampton, M.A., Horton, B.K., 2007. Sheetflow fluvial processes in rapidly subsiding basin, Altiplano plateau,
 498 Bolivia. *Sedimentology* 54, 1121–1147.
- 499 Leckie, D.A., Walker, R.G., 1982. Storm and tide-dominated shorelines in Cretaceous Moosebar-Lower Gates
 500 interval outcrops equivalents of Deep Basin gas trap in western Canada. *AAPG Bull.* 66, 138–157.

- 501 Legler, B., Hampson, G.J., Jackson, C.A., Johnson, H.D., Massart, B.Y.G., Sarginson, M. and Ravns, R. (2014)
 502 Facies Relationships and Stratigraphic Architecture of Distal, Mixed Tide- and Wave-Influenced Deltaic
 503 Deposits: Lower Sego Sandstone, Western Colorado, U.S.A. *Journal of Sedimentary Research* 84, 605–
 504 625.
- 505 Loureiro, H.S.C., Lima, E.S., Macedo, E.R., Silveira, F.V., Bahiense, I.C., Arcanjo, J.B.A., Moraes Filho, J.C.,
 506 Neves, J.P., Guimarães, J.T., Teixeira, L.R., Abram, M.B., Santos, R.A., Melo, R.C., 2008. Projeto Barra–
 507 Oliveira dos Brejinhos Geological map. Brazilian Geological Survey and Bahia Mineral Research
 508 Company, scale 1:200.000.
- 509 Lowe, D.R., 1979. Sediment gravity flows: their classification and some problems of application to natural flows
 510 and deposits. *SEPM Special Publication* 27, 75–82.
- 511 Lowe, D.R., 1982. Sediment gravity flows II: Depositional models with special reference to the deposits of high-
 512 density turbidity currents. *Journal of Sedimentary Geology* 52 (1), 279–297.
- 513 Magalhães, A.J.C., Scherer, C.M.S., Raja Gabaglia, G.P., Bállico, M.B., Catuneanu, O., 2014. Uninccised fluvial
 514 and tide-dominated estuarine systems from the Mesoproterozoic Lower Tombador Formation, Chapada
 515 Diamantina basin, Brazil. *Journal of South American Earth Sciences*, 56, 68–90.
- 516 Marshak, S., Alkmim, F.F., 1989. Proterozoic contraction/extension tectonics of the southern São Francisco
 517 region, Minas Gerais, Brazil. *Tectonics* 8, 555–571.
- 518 Martins-Neto, M.A., 2000. Tectonics and sedimentation in a paleo/Mesoproterozoic rift-sag basin (Espinhaço
 519 basin, southeastern Brazil). *Precambrian Research* 103, 147–173.
- 520 Massari, F., Parea G.C., 1990. Wave-dominated Gilbert-type gravel deltas in the hinterland of the Gulf of
 521 Taranto (Pleistocene, southern Italy). In: Colella, A., Prior D.B. (Eds.), *Coarse-grained Deltas*. Spec. Pub.
 522 of Int. Ass. Sediment. 10, 311–331. Oxford: Blackwell Scientific Publications.
- 523 Miall, A.D., 1996. *The Geology of Fluvial Deposits: Sedimentary Facies, Basin Analysis and Petroleum
 524 Geology*. Heidelberg: Springer, 582 p.
- 525 Nemec, W., Postma, G., 1993. Quaternary alluvial fans in the southwestern Crete: Sedimentation processes and
 526 geomorphic evolution. In: Marzo, M., Puigdefábregas, C. (Eds.), *Alluvial Sedimentation*. Spec. Pub. of Int.
 527 Ass. Sediment. 17, 235–276. Oxford: Blackwell Scientific Publications.
- 528 Nemec, W., Steel, R.J., 1984. Alluvial and coastal conglomerates: Their significant features and some comments
 529 on gravelly mass-flow deposits. In: Coster, E.H., Steel, R.J. (Eds.), *Sedimentology of gravels and
 530 conglomerates*. Canadian Society of Petroleum Geologists Memoir 10, 1–31.
- 531 Noe-Nygaard, N., Surlyk, F., 1988. Washover fan and backish bay sedimentation in the Berriasian-Valanginian
 532 of Bornholm, Denmark. *Sedimentology* 35, 197–217.
- 533 Pedreira, A.J., 1988. Sequências deposicionais no Precambriano: Exemplo da Chapada Diamantina Oriental. In:
 534 35º Congresso Brasileiro de Geologia, Belém, 1988. Anais. Sociedade Brasileira de Geologia, 648–659.
- 535 Pesonen, L.J., Elming, S.A., Mertanen, S., Pisarevsky, S., D'Agrella-Filho, M.S., Meert, J.G., Schmidt, P.W.,
 536 Abrahamsen, N., Bylund, G., 2003. Paleomagnetic configuration of continents during the Proterozoic.
 537 *Tectonophysics* 375, 289–324.
- 538 Plummer, R.S., Gostin, V.A., 1981. Shrinkage cracks: desiccation or syneresis. *Journal of Sediment. Petrol.* 51,
 539 1147–1156.
- 540 Postma, G., Nemec, W., Kleinspehn, K., 1988. Large floating clasts in turbidites: A mechanism for their
 541 emplacement. *Sedimentary Geology* 58, 47–61.

- 542 Pratt, B.R., 1998. Syneresis cracks: subaqueous shrinkage in argillaceous sediments caused by earthquake-
543 induced dewatering. *Sedimentary Geology* 117, 1-10.
- 544 Rocha, A.J.D., 2003. Geologia (Folha Morro do Chapéu). In: Rocha, A.J.D. (Org) - Programa Levantamentos
545 Geológicos Básico do Brasil. Morro do Chapéu (Folha SC.Y-C-V) Estado da Bahia.- scale 1:100.000.
546 Brasília: CPRM, 1997, 148 p.
- 547 Rossi, V.M., Steel, R.J., 2016. The role of tidal, wave and river currents in the evolution of mixed-energy deltas:
548 Example from the Lajas Formation (Argentina). *Sedimentology* 63, 824-864.
- 549 Santos, M.N., Chemale Jr., F., Dussin, I.A., Martins, M., Assis, T.A.R., Jelinek, A.R., Guadagnin, F.,
550 Armstrong, R., 2013. Sedimentological and paleoenvironmental constraints of the Statherian and Stenian
551 Espinhaço rift system, Brazil. *Sedimentary Geology* 290, 47-59.
- 552 Shanley, K.W., McCabe, P.J., Hettinger, R.D., 1992. Tidal influence in Cretaceous fluvial strata from Utah,
553 USA: a key to sequence stratigraphic interpretation. *Sedimentology* 39, 905-930.
- 554 Schobbenhaus, C.; 2012. Geoparques do Brasil: propostas. Org. por Carlos Schobbenhaus e Cássio Roberto da
555 Silva. Rio de Janeiro: CPRM.
- 556 Swift, D.J.P., Figueiredo, A.R., Freeland, G.L., Oertel, G.F., 1983. Hummocky cross stratification and
557 megaripples: a geologic double standard? *Journal of Sedimentary Petrology* 53, 1295-1317.
- 558 Todd, S.P., 1989. Stream-driven, high-density gravelly traction carpets: possible deposits in the Trabeg
559 Conglomerate Formation, SW Ireland and some theoretical considerations of their origin. *Sedimentology*
560 36, 513-530.
- 561 Todd, S.P., 1996. Process deduction from fluvial sedimentary structures. In: Carling, P.A., Dawson, M.R. (Eds.),
562 Advances in Fluvial Dynamics and Stratigraphy. Chichester: John Wiley & Sons Ltd., 299-350.
- 563 Tohver, E., D'Agrella-Filho, M.S., Trindade, R.I.F., 2006. Paleomagnetic record of Africa and South America
564 for the 1200–500 Ma interval, and evaluation of Rodinia and Gondwana assemblies. *Precambrian Research*
565 147, 193–222.
- 566 Tunbridge, I.P., 1981. Sandy high-energy flood sedimentation - some criteria for recognition, with an example
567 from the Devonian of S.W. England. *Sedimentary Geology* 28, 79–95.
- 568 Vakalerov, B.K., Ainsworth, R.B., MacEachern, J.A., 2012. Recognition of wave-dominated, tide-influenced
569 shoreline systems in the rock record: Variations from a microtidal shoreline model. *Sedimentary Geology*
570 279, 23-41.
- 571 Visser, M.J., 1980. Neap-spring cycles reflected in Holocene subtidal large-scale bedforms deposits: a
572 preliminary note. *Geology* 8, 543-546.
- 573 Weil, A.B., Van der Voo, R., Niocaill, C.M., Meert, J.G., 1998. The Proterozoic supercontinent Rodinia:
574 paleomagnetically derived reconstructions for 1100 to 800 Ma. *Earth and Planetary Science Letters* 154,
575 13–24.
- 576 Zecchin, M., Catuneanu, O., 2013. High-resolution sequence stratigraphy of clastic shelves I: Units and
577 bounding surfaces. *Marine and Petroleum Geology* 39, 1-25.

CAPÍTULO IV

[Pesq Geoc] Agradecimento pela Submissão ➔ Caixa de entrada x



Pesquisas em Geociências - Comissão Editorial <pesqgeoc@ufrgs.br>

✉ para eu ▾

Sr. Ezquiel Galvão,

Agradecemos a submissão do seu manuscrito "FLUXOS COMBINADOS E AS FORMAS DE LEITO HÍBRIDAS NO PROTEROZOICO: O EXEMPLO DA FORMAÇÃO MORRO DO CHAPÉU, SUPERGRUPO ESPINHAÇO/BA" para Pesquisas em Geociências. Através da interface de administração do sistema, utilizado para a submissão, será possível acompanhar o progresso do documento dentro do processo editorial, bastando logar no sistema localizado em:

URL do Manuscrito:

<http://seer.ufrgs.br/index.php/PesquisasemGeociencias/author/submission/84994>

Login: ezgs_ufrgs

Em caso de dúvidas, envie suas questões para este e-mail. Agradecemos mais uma vez considerar nossa revista como meio de transmitir ao público seu trabalho.

•••

Pesquisas em Geociências - Comissão Editorial

Pesquisas em Geociências

Pesquisas em Geociências

<http://www.seer.ufrgs.br/index.php/PesquisasemGeociencias>

◀ Responder

▶ Encaminhar

FLUXOS COMBINADOS E AS FORMAS DE LEITO HÍBRIDAS NO PROTEROZOICO: O EXEMPLO DA FORMAÇÃO MORRO DO CHAPÉU, SUPERGRUPO ESPINHAÇO/BA

Ezequiel GALVÃO de Souza¹, Claiton Marlon dos Santos SCHERER¹, Lucas Medeiros BOFILL¹, João Pedro Formolo FERRONATTO¹, Manoela Bettarel BÁLLICO², Adriano Domingos dos REIS¹ & Carrel KFUMBI¹

¹ Programa de Pós-graduação em Geociências, Instituto de Geociências, Universidade Federal do Rio Grande do Sul. Av. Bento Gonçalves, 9500, CEP 91.540-000, Porto Alegre, RS/Brasil (E-mail: ezequiel.geol@gmail.com).

² Departamento de Geociências – Universidade Federal de Santa Catarina (UFSC), Campus Universitário. Florianópolis/SC, CEP 88040-900, Brasil.

RESUMO

Sistemas deposicionais híbridos são criados pela interação de dois ou mais processos hidrodinâmicos que controlam a distribuição das fácies e suas características em termos de estruturas sedimentares e geometria deposicional. Ambientes costeiros híbridos são identificados pelas evidências da ação de ondas, marés e rios. Os depósitos de *shoreface* são bem estabelecidos conceitualmente e representados pelo domínio da ação de ondas. Entretanto, a sua ocorrência sob diversas condições resulta em uma ampla variabilidade de suas características sedimentológicas. Fatores como clima (tempestades), marés e enxurradas fluviais influenciam na formação destes depósitos, e suas interações têm sido pouco descritas na literatura, tanto no âmbito de registros geológicos quanto de ambientes deposicionais atuais. A análise faciológica de detalhe nos depósitos de *shoreface* da Formação Morro do Chapéu (Supergrupo Espinhaço/BA) permitiu a identificação de 6 litofácies que são produtos da combinação de fluxos oscilatórios e unidireccionais. Tais fácies são caracterizadas por variações na granulometria, intervalos agradacionais, formação de domos nas calhas, truncamento lateral e variação na espessura das laminationes. A variação na granulometria pode ser explicada por enxurradas fluviais que alcançaram a costa, já as outras características são geradas pela variação da maré. Em períodos de maré baixa a amplitude do movimento oscilatório que interage com o fundo é maior, predominando o truncamento de baixo ângulo e a agradação da forma. Já em períodos de maré alta, a amplitude do movimento oscilatório que interage com o fundo é menor, fazendo com que a corrente unidirecional atuante seja mais efetiva e gerando formas anisotrópicas.

PALAVRAS-CHAVES: Fluxos combinados, sistemas costeiros, Proterozóico.

1.INTRODUÇÃO

Os processos sedimentares relacionados a ondas, marés e rios são amplamente estudados e permitem a definição de modelos faciológicos e deposicionais para os sistemas onde atuam. Tais modelos, embora simplificados em relação aos depósitos encontrados na natureza, permitem um melhor entendimento das condições de formação dos depósitos. Entretanto, apesar de vários estudos sobre as características dos depósitos nas regiões costeiras, há diversas incertezas sobre quais são as fáceis geradas quando há a combinação de ondas, maré e rios, e a maneira como estes interagem na formação dos corpos sedimentares.

A interação entre as correntes geradas nas regiões costeiras e a consequente combinação de seus vetores formam fluxos combinados. As formas de leito geradas por fluxos puramente unidirecionais ou oscilatórios são amplamente encontradas e discutidas no registro geológico e, por consequência, possuem modelos característicos (Harms, 1979; Dott & Bourgeois, 1982; Davis & Hayes, 1984; Boyd *et al.*, 1992; Dumas & Arnott, 2006; Plint, 2010). Por sua vez os depósitos gerados pelos fluxos combinados são mais estudados e observados através de modelagem física em tanques de experimentos, focados principalmente na geometria das formas de leito. Entretanto, quando analisamos principalmente os depósitos das regiões costeiras, as fácies apresentam características mistas, das quais grande parte reflete mais de um processo sedimentar.

Dada à variabilidade na classificação dos ambientes costeiros em função da tríade rio/onda/maré, torna-se necessária a análise faciológica em detalhe dos depósitos para uma correta reconstituição e classificação dos sistemas. Para tanto, o reconhecimento das formas de leito geradas por fluxos combinados e a compreensão dos processos deposicionais envolvidos são de suma importância na caracterização destes sistemas.

Assim, este estudo objetiva a descrição das formas de leito geradas por fluxos combinados, visando identificar os processos deposicionais atuantes nos espessos pacotes arenosos da Formação Morro do Chapéu (FMC - Proterozóico/BA). Além disso, esta caracterização auxiliará em outros estudos na compreensão faciológica das formas de leito que não se assemelham com as formas puramente oscilatórias e nem com as puramente unidirecionais.

2.FLUXOS COMBINADOS

Fluxos combinados são formados pela interação de dois ou mais tipos de fluxo no espaço e tempo, sendo usado mais comumente para indicar a combinação de fluxos unidirecionais e oscilatórios. Tais fluxos originam-se a partir da interação de quatro componentes básicos: 1) unidirecional (U_u); 2) oscilatório periódico (U_o); 3) multidirecional

rotatório periódico (Ur); e 4) multidirecional aleatória (UR) (Allen, 1982; Clifton, 1976). Os componentes 1 e 2 são lineares, pois os fluxos movem-se em uma única direção, por exemplo, a oscilação que ocorre no plano vertical XY produz deslocamentos para trás e para frente, mas sempre na mesma direção. Os componentes 3 e 4 são multidireccionais por permitir as partículas do fluido e consequentemente os sedimentos moverem-se em todas direções, predominantemente em um plano horizontal XZ (Tinterri, 2011). Entretanto, o componente 4 é definido como aleatório porque quando comparado aos componentes oscilatório e rotatório, não apresenta um padrão temporal ou direcional.

Assim, conforme alguns autores, os fluxos combinados podem ser definidos como lineares, quando resultam da combinação de fluxos unidireccionais e oscilatórios, ou multidireccionais, quando os componentes 1 e 2 combinam-se com um componente multidirecional periódico. De maneira geral, apesar de uma existência contínua entre fluxos unidirectionais, oscilatórios e multidirectionais, os fluxos combinados podem ser divididos em duas categorias principais: 1) Fluxos assimétricos, nos quais as componentes oscilatória e rotatória são maiores que a unidirecional; e 2) Fluxos pulsantes, nos quais a componente unidirecional é maior ou igual que a oscilatória e a rotatória. Estas duas categorias compreendem tanto fluxos combinados lineares quanto multidirectionais.

3.LOCALIZAÇÃO DA AREA DE ESTUDO

A FMC aflora nos arredores da cidade homônima, no domínio geomorfológico Chapada Diamantina, região central do Cráton São Francisco (Bahia/BR – Fig. 1). Esta região é caracterizada por uma sequência de anticlinais e sinclinais alinhadas N-S, resultantes do evento orogênico Brasiliano (Brito Neves, 1967). A geomorfologia compõe um relevo acidentado, de serras tabulares e vales longos e estreitos onde afloram boas seções da FMC através de escarpas, cachoeiras e cortes de estrada. O estudo focou-se nos principais afloramentos ao longo da BA-052 e nos principais rios paralelos a esta (Fig. 1B).

O Supergrupo Espinhaço no domínio Chapada Diamantina é composto por três grupos: Rio dos Remédios, Paraguaçu e Chapada Diamantina (Pedreira, 1989; Dominguez, 1996). Chemale *et al.* (2012) e autores posteriores (Santos *et al.*, 2013; Guadagnin *et al.*, 2015) dividem o Supergrupo em três megasequências (Inferior, Médio e Superior) que se acumularam em numerosas bacias desenvolvidas em resposta a pelo menos duas fases de rifteamento.

O Grupo Rio dos Remédios compõe a Megasequência Inferior (1.8 – 1.68 Ga). Ocorre em um contexto *rifte*, sendo formada por depósitos fluviais e eólicos da Fm. Serra da Gameleira, vulcânicos ácidos alcalinos da Fm. Novo Horizonte, sistemas lacustres da Fm.

Lagoa de Dentro e aluviais da Fm. Ouricuri do Ouro. A Megasequência Média (1.6 – 1.4 Ga) corresponde a uma bacia *sag* preenchida na base por sistemas aluviais/fluviais e eólicos da Fm. Mangabeira que são sobrepostos por depósitos transgressivos, marinhos rasos e deltaicos da Fm. Açuá. Sobre estes, em discordância angular, deposita-se a Fm. Tombador como uma nova fase *sag* (Fig.1).

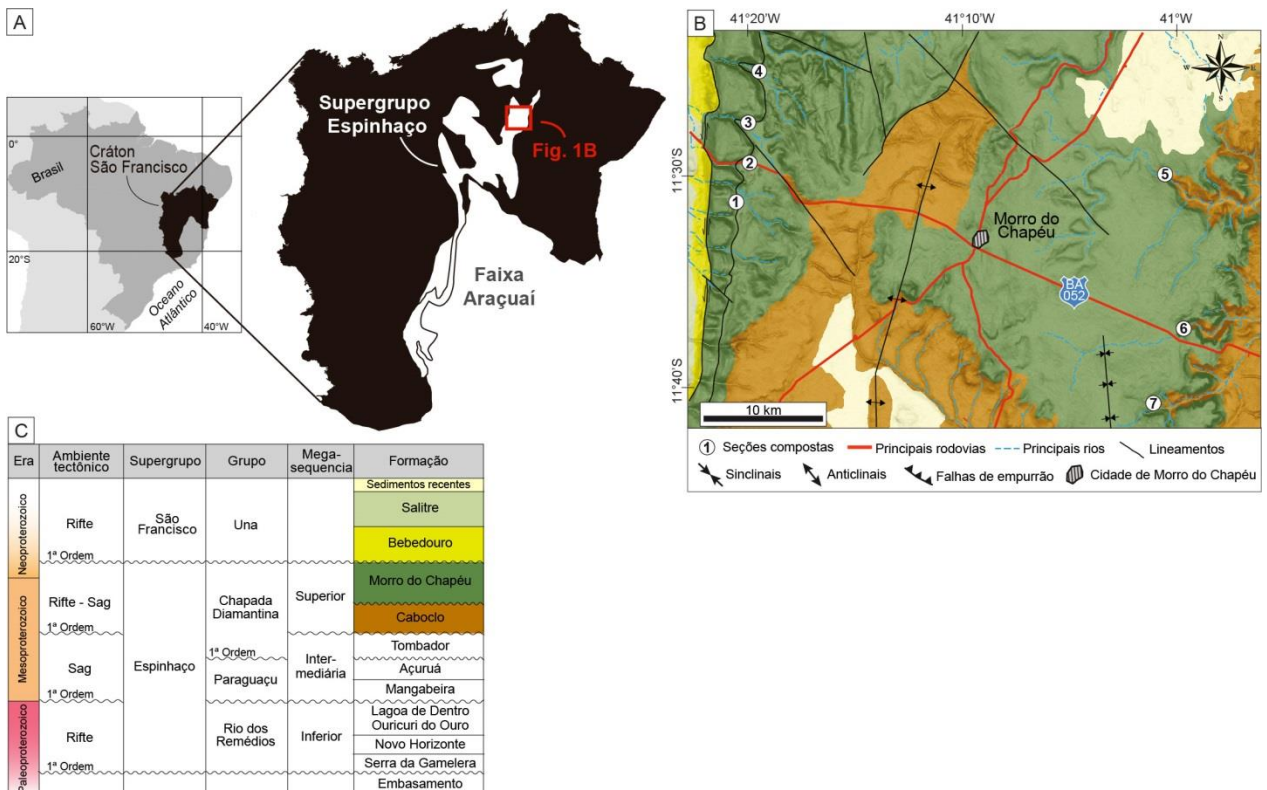


Figura 1: A) Localização do Cráton São Francisco e delimitação do Supergrupo Espinhaço; B) Área de estudo e localização das seções estratigráficas levantadas. Cores explicadas na figura C. C) Coluna estratigráfica do Supergrupo Espinhaço no domínio Chapada Diamantina.

A Megasequência Superior (1.19 – 0.9 Ga) se formou em um ambiente tectônico rifte-sag. Essa fase tectônica é representada pelos depósitos marinhos rasos da Fm. Caboclo e Morro do chapéu, objeto do presente trabalho. Essa sequência marinha é interpretada como transgressiva e em paraconformidade com a Fm. Tombador (Megasequência Média; Fig.1). Estudos recentes demonstram que a FMC compreende duas sequências deposicionais incompletas (Sequência I e II), limitadas por discordâncias subaéreas, onde a principal diferença entre elas é a atuação da maré nos depósitos da sequência superior (Galvão, submetido). Cada sequência é composta pelos tratos de sistema de nível baixo (TSNB), transgressivo (TST) e nível alto (TSNA), onde as formas de leito oriundas de fluxos combinados encontram-se no TST e TSNA (Fig 2).

O TST na Sequência I é constituído por depósitos de *shoreface* inferior pouco espessos que, após o maior afogamento, gradam para depósitos de *shoreface* superior com um padrão de empilhamento progradacional, indicativo do TSNA. Na Sequência II os processos

de fluxos combinados são mais preservados nos depósitos de *shoreface* superior do TST, que gradam para depósitos de *shoreface* inferior até o máximo afogamento.

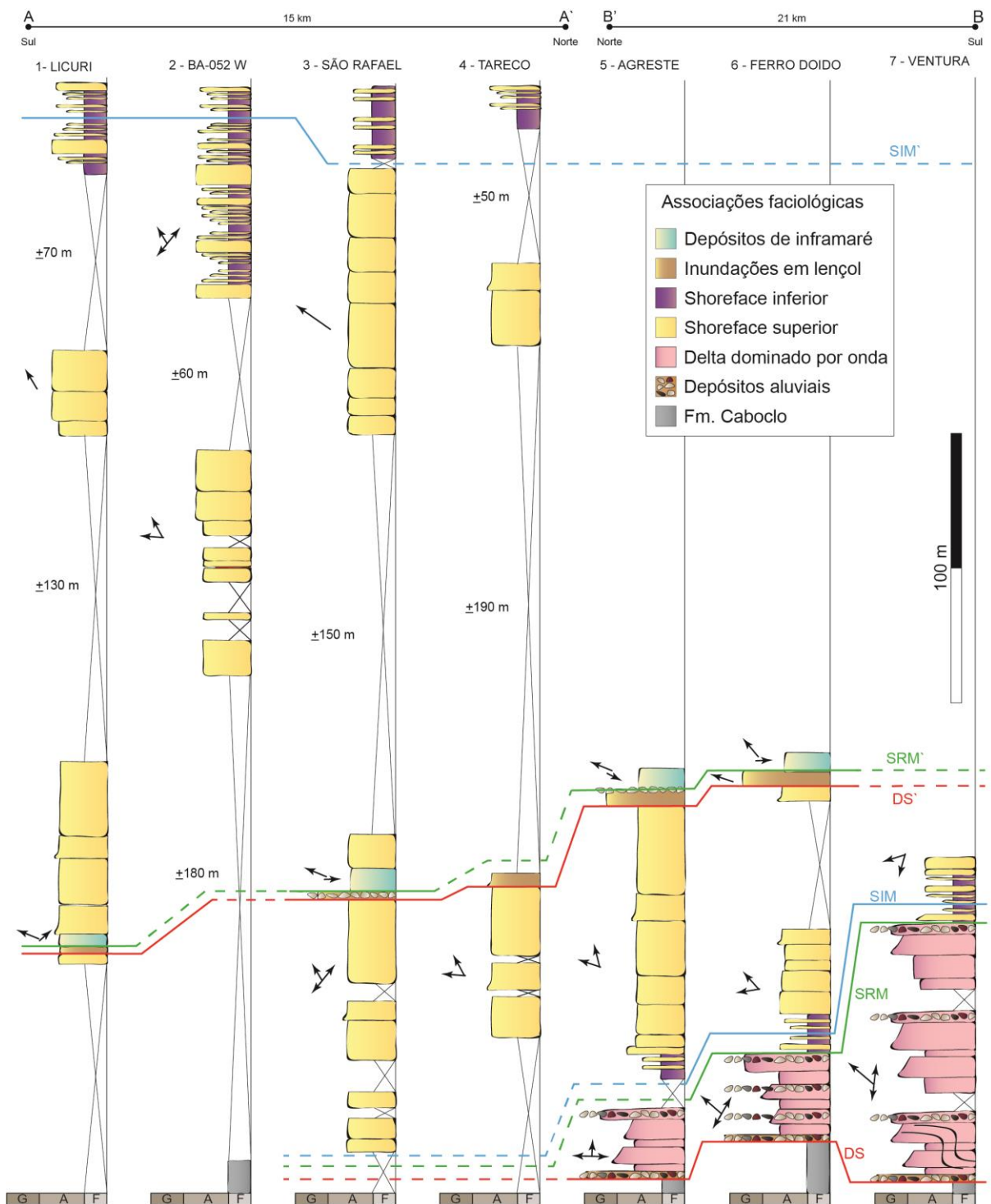


Figura 2: Correlação entre os perfis colonares da região de estudo. As setas indicam a direção das paleocorrentes predominantes. O presente estudo focou-se nos TST e TSNA de ambas as sequências. DS – Discordância subaérea, SRM – Superfície de máxima regressão, SIM – Superfície de inundação máxima.

4.METODOS

Para o desenvolvimento deste trabalho foram descritas as litofácies componentes dos TST e TSNA da Sequência I e do TST da Sequência II, utilizando os atributos: cor, geometria, composição, textura e estruturas sedimentares. Tais fácies foram comparadas com as formas clássicas descritas na literatura (Allen, 1982; Walker *et al.*, 1983; Mutti *et al.*, 1984; Walker & James, 1992; Yokokawa, 1995; Fielding, 2006; Dumas & Arnott, 2006; Collinson *et al.*, 2006) a fim de identificar quais são geradas por fluxos combinados. As paleocorrentes foram medidas a partir da direção de mergulho dos *foreset*s presentes nas laminationes cruzadas e posteriormente corrigidas para remover a inclinação estrutural da camada. Com base no contexto deposicional e associação faciológica em que se encontram as fácies podemos interpretar quais foram os processos responsáveis pela geração dos fluxos combinados.

5.RESULTADOS

A partir do levantamento faciológico de detalhe foram identificadas 6 estruturas sedimentares que não se enquadram nas formas de leito já conhecidas de fluxos puramente oscilatórios e unidireccionais. Tais formas de leito podem ser divididas a partir de seu porte em formas de pequena ou grande escala. As de grande escala são: (1) hummocky levemente anisotrópico; (2) hummocky anisotrópico; (3) estratificação cruzada sigmoidal; e (4) estratificação cruzada tangencial com topo ondulado. Por sua vez, as formas de leito de pequena escala são: (1) marcas onduladas simétricas anisotrópicas; e (2) marcas onduladas assimétricas anisotrópicas.

1.1. Hummocky levemente anisotrópico – Hcs:

Arenito muito fino a fino com laminatione interna de baixo ângulo ondulada truncada que lateralmente gradam para estratificação cruzada tangencial (Fig. 3). Em planta os corpos são dômicos, limitados por superfícies convexas e com cristas descontínuas e fora de fase sobrepostas por pelitos. A distância entre as calhas é de 0,8 a 1,8 m, com 0,5 m de espessura. Localmente ocorrem intraclastos argilosos alongados de até 10 cm ao longo da laminatione. Estas formas ocorrem principalmente nos depósitos de *shoreface* superior (TST e TSNA – Seq. II) e são geradas pela migração de formas de leito grandes e atenuadas, com alta razão comprimento de onda/amplitude. Resultam a partir de fluxos unidireccionais oscilatórios levemente assimétricos onde $U_o \gg U_u$ ($U_o/U_u > 1$), aliados a períodos com altas taxas de decantação.

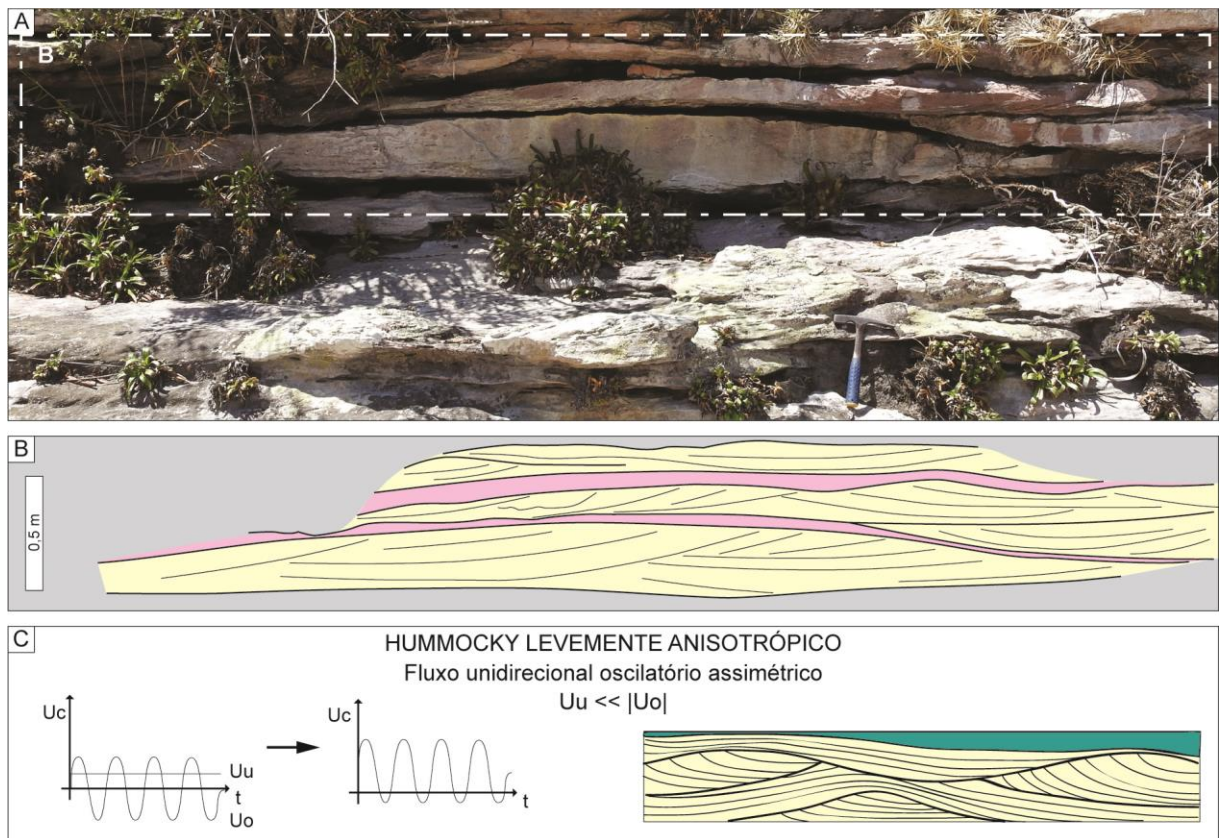


Figura 3: Hummockys levemente anisotrópicas. A) Forma de leito encontrada nos depósitos de *shoreface* inferior. B) Interpretação baseada nas estruturas visíveis em campo, os intervalos em cor rosa representam sedimentos finos (silte e argila laminados). C) Modelo de geração destas formas conforme Tinterri (2011).

1.2. Hummocky anisotrópico – Hct:

Arenito muito fino a fino com estratificação cruzada tangencial e intraclastos argilosos alongados dispersos e nas laminações (Fig. 4). Os corpos são limitados por superfícies planas e regulares na base e onduladas no topo. As cristas são tênues e arredondadas, com marcas onduladas assimétricas e pelitos sobre as mesmas, sendo a face de sotavento convexa e a de barlavento côncava. A distância entre as cristas é de 3,6 m, com 0,8 m de espessura e a ocorrência é limitada aos depósitos de *shoreface* inferior (TST – Seq. I). Estas formas também são geradas pela migração de formas de leito grandes e atenuadas, com alta razão comprimento de onda/amplitude, resultantes a partir de fluxos unidireccionais oscilatórios levemente pulsantes a fortemente assimétricos onde $U_o > U_u$ ($U_o/U_u > 1$). Nestes, os fluxos oscilatórios de alta frequência são superpostos aos fluxos pulsantes de baixa frequência, aliados a períodos de decantação. Os estratos cruzados tangenciais apresentam um sentido preferencial de mergulho, indicando uma maior competência da U_u do que na atuante em formas levemente anisotrópicas.

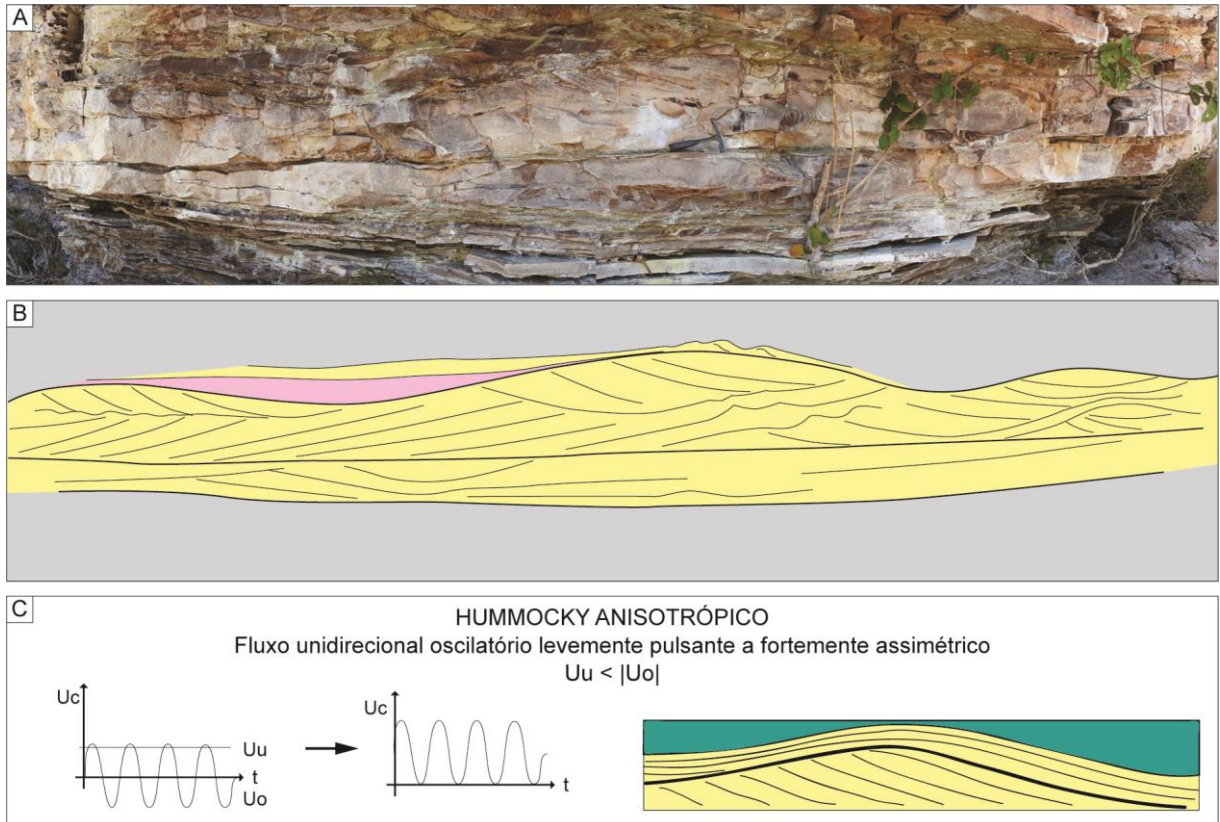


Figura 4: Hummockys anisotrópico. A) Forma de leito encontrada nos depósitos de *shoreface* inferior. B) Interpretação baseada nas estruturas visíveis em campo, os intervalos em cor rosa representam sedimentos finos (silte e argila laminados). Notar a variação no mergulho das laminações, bem como os intervalos agradacionais. C) Modelo de geração destas formas conforme Tinterri (2011).

1.3. Estratificação cruzada sigmoidal – Ss:

Arenito médio com estratificação cruzada sigmoidal de médio porte ($<0,5$ m), com ampla variação no ângulo de mergulho dos *foresets* (Fig 5). As faces são convexas e superfícies regularmente espaçadas sigmoidais truncam o topo das laminações. Ocorrem principalmente nos depósitos de *shoreface* superior (TST – Seq. II). São geradas pela migração de formas de leito com crista sinuosa sob fluxos pulsantes contínuos onde $U_u > U_o$ ($U_o/U_u < 1$), onde há a desaceleração da U_u devido a um incremento ou na U_o ou na taxa de sedimentação. As superfícies que erodem o topo dos *foresets* resultam ou da U_o com sentido oposto, ou de um momento de maior velocidade da U_u .

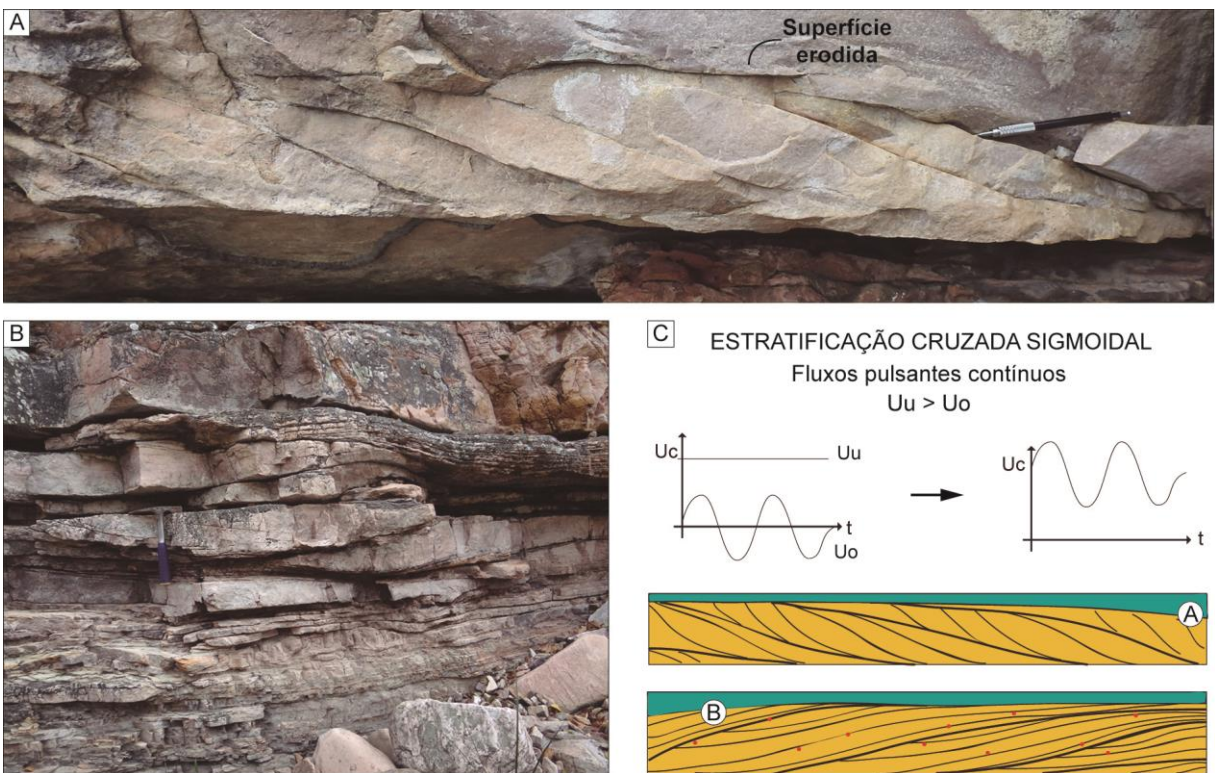


Figura 5: Arenitos com estratificação cruzada sigmoidal. A) Forma de leito encontrada nos depósitos de *shoreface* superior. Notar a superfície superior truncando as laminationes espaçadas regularmente. B) Estratificação cruzada sigmoidal de maior porte em depósitos de *shoreface* superior, onde as laminationes encontram-se menos inclinada do que em A. C) Modelo de geração destas formas conforme Tinterri (2011).

1.4. Estratificação cruzada tangencial com topo ondulado – Stw:

Arenito médio a grosso, mal selecionado, com estratificação cruzada tangencial e com grânulos e seixos dispersos ou concentrados na base dos *sets* (Fig. 6 e 7). Internamente é possível observar a estratificação gradando lateralmente para lamination de baixo ângulo. Os corpos são amalgamados com espessura média de 0,4 m e lateralmente extensos (> 2 m), limitados por superfícies retas e contínuas na base. A superfície superior das formas é ondulada e as faces tendem a ser convexas. Ocorrem nos depósitos de *shoreface* superior (TSNA – Seq. I e TST – Seq. II). São geradas pela migração de formas de leito com crista sinuosa, resultantes de fluxos unidireccionais oscilatórios pulsantes a levemente assimétricos onde $U_o < U_u$ ($U_o/U_u < 1$). Entretanto, o predomínio da estratificação cruzada tangencial, com nenhum intervalo agradacional e nem pelitos associados sugerem que: 1) baixas taxas de decantação e; 2) os fluxos pulsantes de alta frequência são sobrepostos por fluxos oscilatórios de mais baixa frequência.

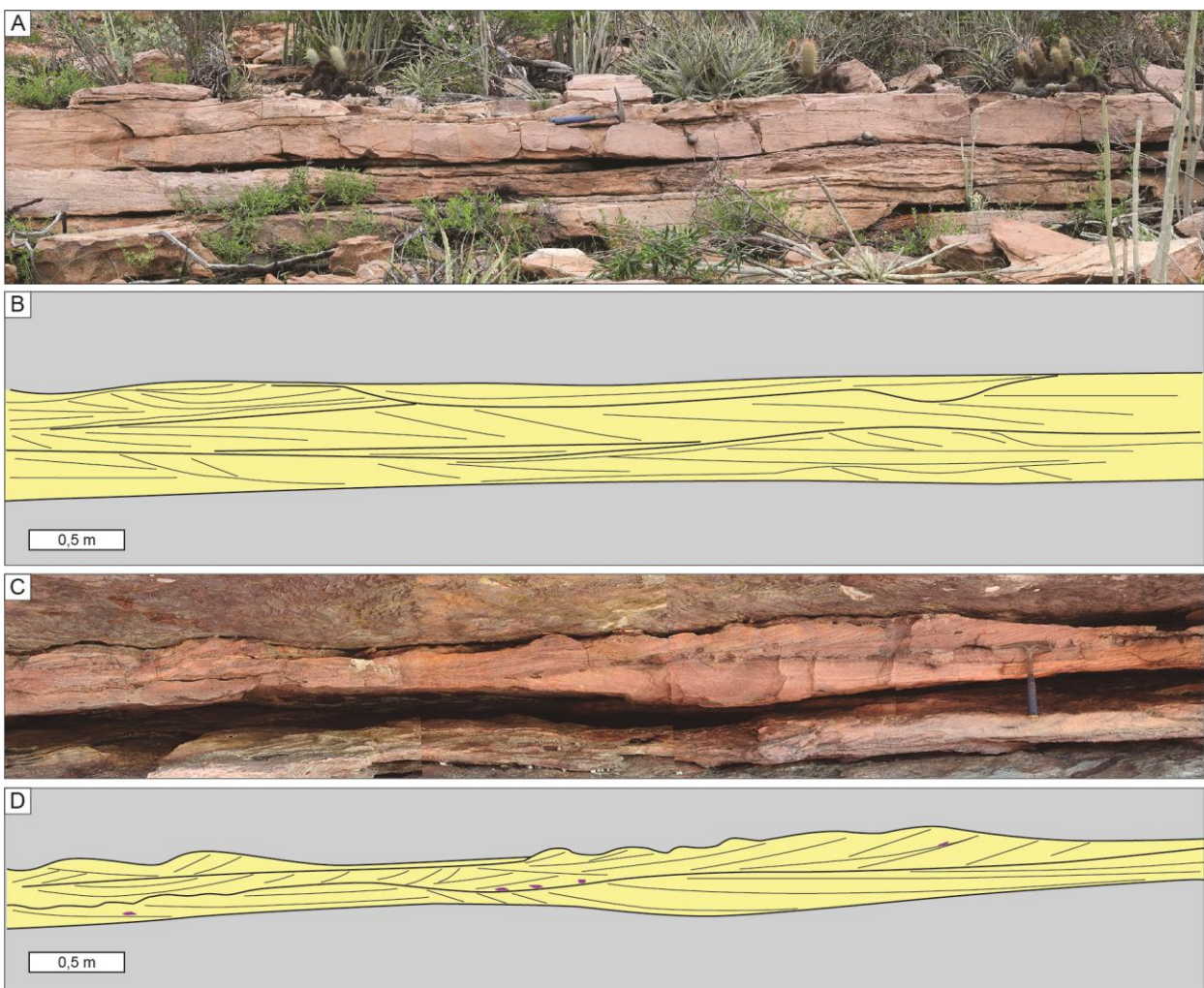


Figura 6: Arenitos com estratificação cruzada tangencial e topo ondulado. A) Forma de leito encontrada nos depósitos de *shoreface* superior. B) Interpretação de estruturas visíveis em campo, notar a variação lateral no ângulo de mergulho das laminationes e topo convexo das formas. C) Arenito mal selecionado, com intraclastos argilosos e marcas onduladas no topo. D) Interpretação das feições mais características da forma, notar o limite convexo dos *sets* e a variação na direção de mergulho.

1.5. Marcas onduladas simétricas anisotrópicas – Sw :

Arenito muito fino caracterizado por ter cristas retilíneas a levemente sinuosas, calhas suavemente arredondadas e faces convexas (Fig. 8 A, B, C, D e E). A lamination interna grada de isotrópicas e truncadas para anisotrópicas tangenciais, podendo haver intervalos agradacionais internos ou sob a forma de leito. O comprimento de onda varia de 3 a 6 cm com altura máxima de até 2,5 cm. Estas estruturas são geradas pela migração de formas de leito sinuosas, geradas por fluxos unidirecionais oscilatórios assimétricos com $U_o >> U_u$ ($U_o/U_u > 1$) e taxas de decantação elevedas. O desaparecimento das superfícies truncadas internas é relacionado a um incremento da U_u .

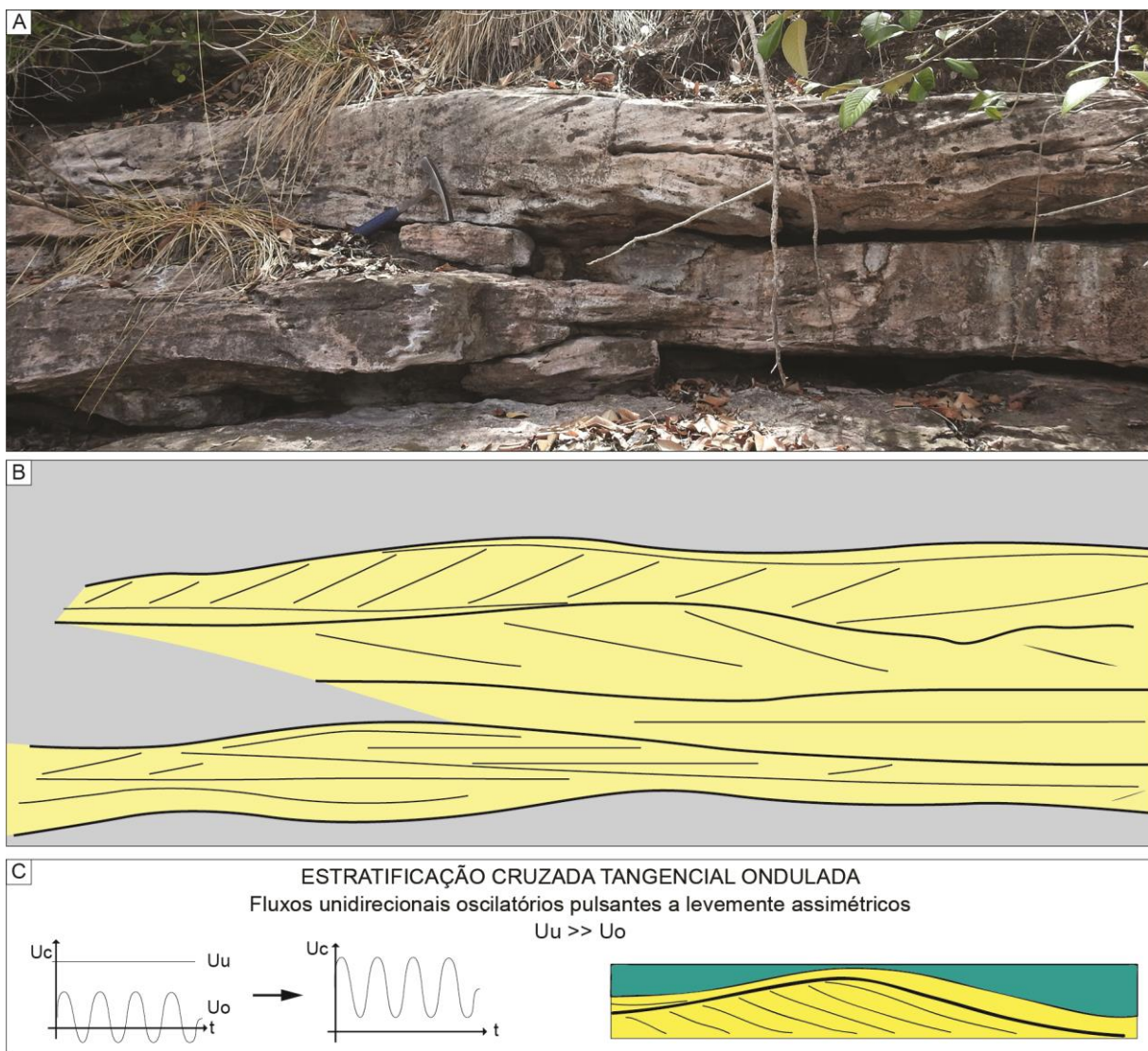


Figura 7: Arenitos com estratificação cruzada tangencial e topo ondulado. A) Forma de leito encontrada nos depósitos de *shoreface* superior. B) Interpretação de estruturas visíveis em campo, notar a variação lateral no ângulo de mergulho das laminações e topo convexo, por vezes com laminação agradacional. C) Modelo de geração das formas, notar a U_u mais elevada e a laminação agradacional pouco desenvolvida.

1.6. Marcas onduladas assimétricas anisotrópicas – Sr:

Arenito fino com laminação cruzada tangencial e cristas sinuosas e espessas A face de barlavento é convexa, enquanto a de sotavento é côncava (Fig. 8 F, G e H). O comprimento de onda médio é de 10 cm e altura máxima de 5 cm. São geradas pela migração de formas de leito sinuosas, geradas por fluxos pulsantes onde $U_o < U_u$ ($U_o/U_u < 1$), com baixas taxas de decantação. A geometria externa deriva do pouco deslocamento do vortex de suspensão, já que as resultantes da combinação dos fluxos apresentam mesma direção.

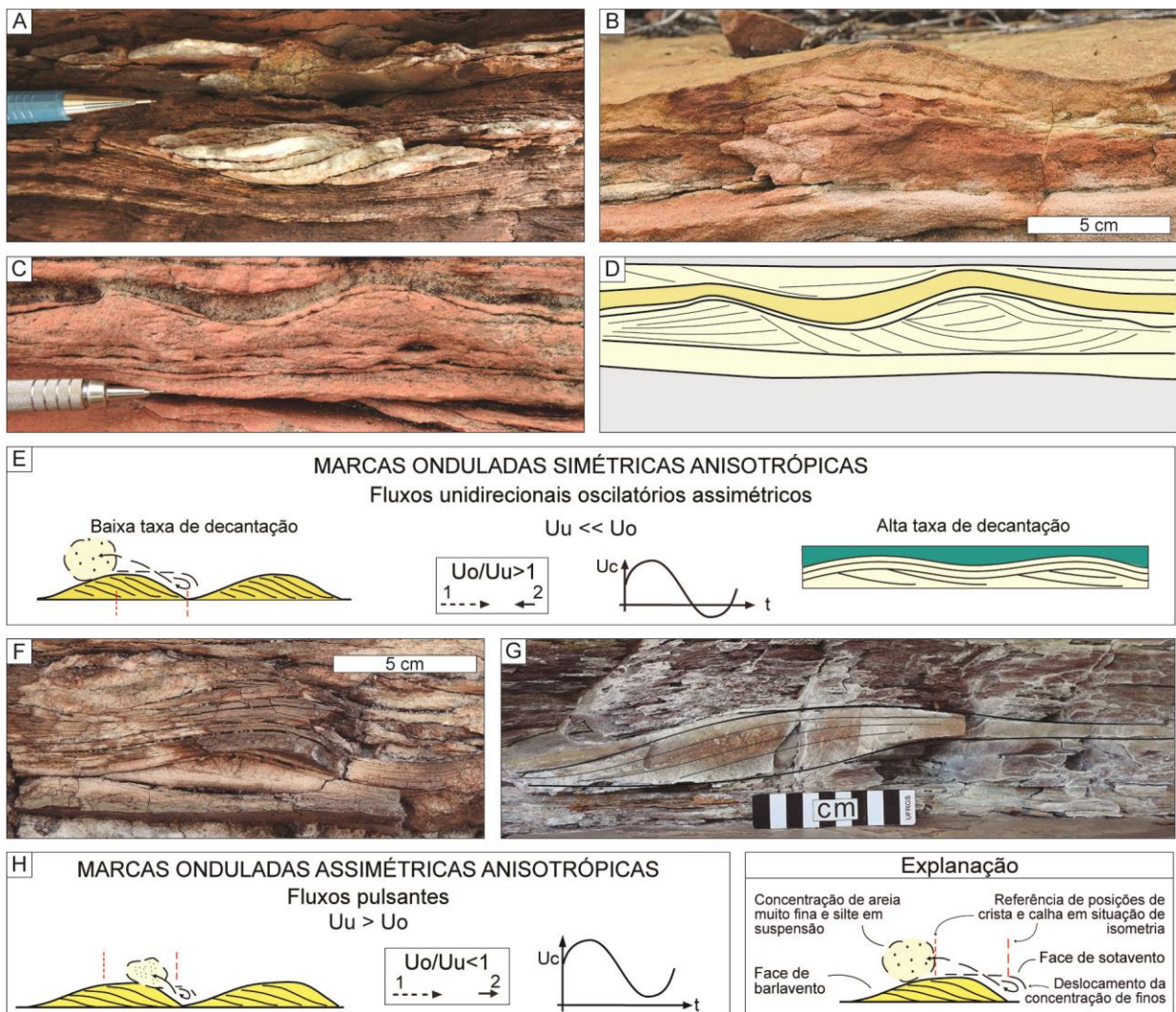


Figura 8: Formas de leito de pequena escala. A, B e C) Marcas onduladas simétricas anisotrópicas, com calhas arredondadas e faces levemente convexas. D) Interpretação das feições visíveis em campo da foto C, o amarelo escuro representa granulometria mais grossa (areia média). Notar a anisotropia interna e a simetria das formas com laminationes agradacionais no topo. E) Modelo de geração destas formas de Tinterri (2011), observar a assimetria entre os fluxos com sentidos opostos. F e G) Marcas onduladas assimétricas anisotrópicas, com faces côncavo-convexas e lamination interna sigmoidal. H) Modelo de geração destas formas, notar a assimetria entre os fluxos com mesmo sentido.

6.DISCUSSÕES

Conforme pode ser visualizado na figura 2, a sucessão da FMC expõe características sedimentares peculiares: 1) uma fonte fluvial próxima e retrabalhada por ondas; 2) frequente ação de ondas de tempo bom e tempestade; 3) depósitos de inframaré; e 4) estruturas geradas por fluxos combinados. Tais características, junto às associações faciológicas já descritas anteriormente (Galvão, submetido), permitem classificar os depósitos da Fm. Morro do Chapéu como um sistema costeiro misto, onde o processo sedimentar predominante é diretamente afetado por um dos outros dois existentes (rio/onda/maré) (Boyd *et al.*, 1992; Dalrymple, 1992).

Como regra geral para estes sistemas, a seleção dos sedimentos é um indicativo do grau de retrabalhamento: sedimentos bem selecionados são provavelmente produtos da ação de ondas e/ou maré, enquanto sedimentos mal selecionados tem sua origem ligada ao sistema fluvial (Plink-Björklund, 2012; Rossi & Steel, 2016). De forma geral os sedimentos de *shoreface* da FMC são bem selecionados, exceto algumas ocorrências das fácies Stw que apresentam grânulos e seixos dispersos ou concentrados nos *foreset*s, possibilitando assim uma inferência a respeito de alguma contribuição fluvial. O domínio de paleocorrentes para NW, tanto do sistema deltaico quanto do *shoreface* (Fig. 2), associados ao mal grau de seleção dos sedimentos sugere que as correntes de retorno, além de serem predominantes, podem ter sido influenciadas por enxurradas fluviais que atingiram a costa (e.g. Ichaso & Dalrymple, 2014).

As demais fácies (Hcs, Hct, Ss, Sw, e Sr) são bem selecionadas e apresentam algumas características que indicam a atuação de uma componente além da oscilatória, tais como: 1) intervalos agradacionais; 2) formação de domos nas calhas; 3) truncamento lateral; e 4) variação na espessura da laminação. Tais características sugerem que durante a geração destas formas de leito, períodos dominados pela oscilação (agradacion) alternaram-se a períodos dominados pelos fluxos combinados (migração lateral). Assim, podemos inferir que a atuação das ondas, de tempo bom ou de tempestades, nos depósitos de *shoreface* da FMC foi afetada por outros agentes que atuaram durante a sedimentação. Entretanto, o alto grau de seleção exclui a hipótese de contribuição fluvial, restando como possibilidade somente a maré.

Os depósitos de maré bem definidos ocorrem somente no intervalo intermediário e não ao longo de toda FMC, como interpretado por autores anteriores (Battilani, 1997; Rocha, 1997). Tal ocorrência isolada sugere que em determinado momento a atuação da maré foi mais efetiva que a atuação das ondas. Porém, cabe ressaltar que as assinaturas da maré no registro sedimentar tendem a ser discretas devido aos seguintes fatores: 1) as correntes de maré não são necessariamente retílineas, podendo ser descritas como elipsóides; 2) o pico de velocidade da corrente pode ocorrer paralelamente à costa e não perpendicular (e.g., Wright *et al.*, 1982); 3) os indícios de maré tendem a ter menor potencial de preservação devido ao retrabalhamento por ondas; e 4) as características de maré que são preservadas tendem a ser sutis (Vakarelov *et al.*, 2012). Além disso, a maré em costas extensas tende a ser afetada por padrões de correntes mais complexos, tornando os indicadores de maré menos desenvolvidos (e.g. Yang *et al.*, 2008; Dashtgard *et al.*, 2009).

Os depósitos de *shoreface* da FMC, além de apresentarem as estruturas geradas por fluxos combinados, não possuem suas quebras e limites zonais bem definidos. Uma

alternativa para explicar estes depósitos de *shoreface* é o reconhecimento do papel desempenhado pela maré, que predominou no intervalo intermediário, e no restante da seção correspondente às fácies descritas teve a sua influência marcada pela componente unidirecional combinada com o fluxo oscilatório dado pelas ondas. Tal reconhecimento é dificultado devido à homogeneização nos valores de paleocorrentes (NW), sem o registro de bimodalidade e à ausência de ciclicidades nos depósitos.

Porém, as mudanças no nível relativo do mar a partir dos ciclos de maré podem modificar tanto as estruturas formadas por ondas e tempestade quanto a arquitetura sedimentar do sistema deposicional (e.g. Dashtgard *et al.*, 2012). Outra mudança acarretada pela variação do nível do mar durante os ciclos de maré é a variação no tamanho da órbita das ondas que interagem com o fundo. Em amplitudes de maré significativas, a profundidade da lâmina de água é reduzida durante a maré baixa e as oscilações que atingem o leito tendem a apresentar amplitudes maiores do que nas marés altas (Vaucher *et al.*, 2016). Do mesmo modo, erosões podem ocorrer devido às velocidades de correntes geradas pelas tempestades serem maiores durante a maré baixa.

Estes processos podem explicar a combinação de fluxos e a geração das formas de leito apresentadas. Conforme observamos na figura 9, em períodos de maré baixa a amplitude do movimento oscilatório que interage com o fundo é maior, predominando o truncamento de baixo ângulo e a agradação da forma. Já em períodos de maré alta, a amplitude do movimento oscilatório que interage com o fundo é menor, fazendo com que a corrente unidirecional atuante seja mais efetiva e gerando formas anisotrópicas.

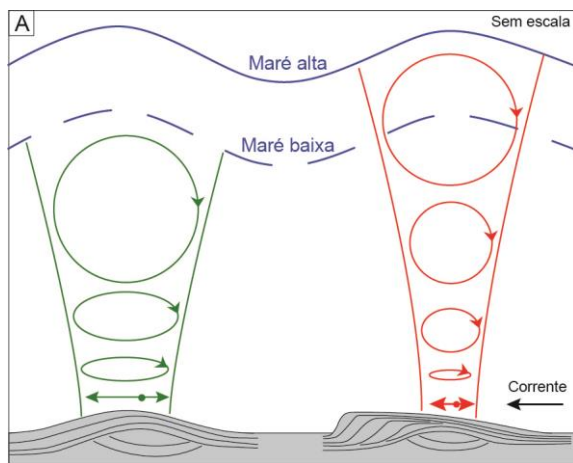


Figura 9: Representação da combinação de correntes oscilatórias e unidireccionais variando com a maré. Durante a maré baixa a amplitude do movimento oscilatório que chega ao leito é maior do que durante a maré alta.

7.CONCLUSÕES

As formas de leito encontradas nos depósitos de *shoreface* da Formação Morro do Chapéu são produtos da interação de dois tipos de fluxos (unidirecional e oscilatório). Tais fácies podem ser divididas a partir da sua escala e são caracterizadas por variações na granulometria, intervalos agradacionais, formação de domos nas calhas, truncamento lateral e variação na espessura das laminações. A variação na granulometria pode ser explicada por enxurradas fluviais que alcançaram a costa, já as outras características podem ser explicadas pela variação da maré. Mais estudos são necessários para avaliar variações cíclicas no tamanho das formas e da granulometria a fim de correlacionar a ciclicidade dos depósitos de *shoreface* à ciclicidade das marés.

8. REFERÊNCIAS BIBLIOGRÁFICAS

- ALLEN J.R.L., 1982. *Sedimentary structures: Their Character and Physical Basis*, Volume I. Elsevier Scientific Publishing Company: Amsterdam.
- BATTILANI, G.A, GOMES, N.S, GUERRA, W.J., 1997. Evolução diagenética dos arenitos da Formação Morro do Chapéu, Grupo Chapada Diamantina, na região de Morro do Chapéu, Bahia. *Geonomos* 4, 81-89.
- BOYD, R., DALRYMPLE, R. AND ZAITLIN, B.A., 1992. Classification of clastic coastal depositional environments. *Sed. Geol.*, 80, 139–150.
- BRITO NEVES, B.B., 1967. Geologia das folhas de Upamirim e Morro do Chapéu Bahia. Relatório 17 Companhia Nordestina de Sondagens e Perfurações CONESP – SUDENE.
- CHEMALE JR., F., DUSSIN, I.A., ALKMIM, F.F., MARTINS, M.S., QUEIROGA, G., ARMSTRONG, R., SANTOS, M.N., 2012. Unravelling a Proterozoic basin history through detrital zircon geochronology: The case of the Espinhaço Supergroup, Minas Gerais, Brazil. *Gondwana Research* 22, 200-206.
- CLIFTON H.E., 1976. Wave-formed sedimentary structures, a conceptual model. In: Davies R.A.J and Ethington, R.L. (eds.) *Beach and Nearshore Sedimentation*, SEPM special publication 24, 126-148.
- COLLINSON, J., MOUNTNEY, N., THOMPSON, D., 2006. *Sedimentary structures*. 3Rev Ed Edition.
- DALRYMPLE, R.W., 1992. Tidal depositional systems. In : *Facies Models: Response to Sea Level Change* (Eds R.G. Walker and P.J. Noel), pp. 195–218. *Geol. Assoc. Can.*, St. John's, Newfoundland, Canada.

- DASHTGARD, S.E., GINGRAS, M.K. AND MACEACHERN, J.A., 2009. Tidally modulated shorefaces. *J. Sed. Res.*, 79, 793–807.
- DASHTGARD, S.E., MACEACHERN, J.A., FREY, S.E. AND GINGRAS, M.K., 2012. Tidal effects on the shoreface: towards a conceptual framework. *Sed. Geol.*, 279, 42–61.
- DAVIS, R.A., JR AND HAYES, M.O., 1984. What is a wave-dominated coast? *Mar. Geol.*, 60, 313–329.
- DOMINGUEZ, J. M. L., 1996. As coberturas plataformais do Proterozoico Médio e Superior. In: BARBOSA, J. S.; DOMINGUEZ, J. M. L. (Coord.) *Geologia da Bahia*: texto explicativo para o mapa geológico ao milionésimo. Salvador: SICT/SGM, p. 105-125.
- DOTT R.H.JR. and BOURGEOIS J., 1982. Hummocky stratification: Significance of its variable bedding sequences. *Geol. Soc. Am. Bull.* 93, 663-680.
- DUMAS S. and ARNOTT R.C.W., 2006. Origin of hummocky and swaley cross-stratification. The controlling influence of unidirectional current strength and aggradation rate. *Geology* 34, 1073-1076.
- FIELDING C.R., 2006. Upper flow regime sheets, lenses and scour fills: extending the range of architectural elements for fluvial sediment bodies. *Sed. Geol.* 190, 227-240.
- GALVÃO, E.S, Submetido. A wave-dominated mesoproterozoic sedimentary sequence, Espinhaço Supergroup, Chapada Diamantina – NE/Brazil. Submetido em 18 de julho de 2018 para o periódico Precambrian Research.
- GUADAGNIN, F., CHEMALE, F., MAGALHÃES, J., SANTANA, A., DUSSIN, I., TAKEHARA, L., 2015. Age constraints on crystal-tuff from the Espinhaço Supergroup – insight into the Paleoproterozoic to Mesoproterozoic intracratonic basin cycles of the Congo–São Francisco Craton. *Gondwana Research*, 27, 363–376.
- HARMS, J., 1979. Primary sedimentary structures. *Annu. Rev. Earth Planet. Sci.*, 7, 227.
- ICHASO, A.A. AND DALRYMPLE, R.W., 2014. Eustatic, tectonic and climatic controls on an early synrift mixed-energy delta, Tilje Formation (early Jurassic, Smørbukk Field, offshore mid-Norway). In: *Depositional Systems to Sedimentary Successions on the Norwegian Continental Shelf* (Eds A.W. Martinus, R. Ravn_as, J.A. Howell, R.J. Steel and J. P. Wonham), *Int. Assoc. Sedimentol. Spec. Publ.*, 46, 339–388.
- MUTTI, E., ALLEN, G.P. and ROSELL, J., 1984. Sigmoidal-cross stratification and sigmoidal bars: depositional features diagnostic of tidal sandstones. 5th IAS European Regional Meeting, Marsiglia, Abstract volume, 312-313.

- PEDREIRA, A. J.; DOSSIN, I. A.; UHLEIN, A.; DOSSIN, T. M.; GARCIA, A. J. V., 1989. Kibaran (Mid-Proterozoic) evolution and mineralizations in Eastern Brazil. *Newsletter*, v. 2, p. 57-63.
- PLINK-BJORKLUND, P., 2012. Effects of tides on deltaic deposition: causes and responses. *Sed. Geol.*, 279, 107–133.
- PLINT, A.G., 2010. Wave-and storm-dominated shoreline and shallow-marine systems. In: *Facies Models* (Eds R.W. Dalrymple and N.P. James), 4th edn, pp. 167–200. Geol. Assoc. Canada, St John's.
- ROCHA, A.J.D., 1997. Programa de Levantamentos Geológicos Básicos do Brasil. Morro do Chapéu (Folha SC.24-Y-C-V) Estado da Bahia. Brasília, CPRM, 157pp.
- ROSSI, V.M. AND STEEL, R.J., 2016. The role of tidal, wave and river currents in the evolution of mixed-energy deltas: example from the Lajas Formation (Argentina). *Sedimentology*, 63, 824–864.
- SANTOS, M.N., CHEMALE JR., F., DUSSIN, I.A., MARTINS, M., ASSIS, T.A.R., JELINEK, A.R., GUADAGNIN, F., ARMSTRONG, R., 2013. Sedimentological and paleoenvironmental constraints of the Statherian and Stenian Espinhaço rift system, Brazil. *Sedimentary Geology* 290, 47–59.
- TINTERRRI, R., 2011. Combined Flow Sedimentary Structures and the Genetic Link Between Sigmoidal- and Hummocky-Cross Stratification. *GeoActa*, v.10, p. 43-85.
- VAUCHER, R.; PITET, B., HORMIÈRE, H., MARTIN, E.L.O., LEFEBVRE, B., 2017. Wave-dominated, tide-modulated model for the Lower Ordovician of the Anti-Atlas, Morocco. *Sedimentology*, 64, 777-807.
- WALKER R.G. and JAMES N.P., 1992. Facies Models: Response to Sea-Level Change. Geological Association of Canada. p. 409.
- WALKER R.G., DUKE W.L. and LECKIE D.A., 1983. Hummocky stratification: Significance of its variable bedding sequences: Discussion. *Geol. Soc. Am. Bull.* 94, 1245-1249.
- WRIGHT, L.D., NIELSEN, P., SHORT, A.D., GREEN, M.O., 1982. Morphodynamics of a macrotidal beach. *Marine Geology* 50, 97–128.
- YANG, B.C., DALRYMPLE, R.W., CHUN, S.S., JOHNSON, M.F., LEE, H.J., 2008. Tidally modulated storm sedimentation on open-coast tidal flats, southwestern coast of Korea: distinguishing tidal-flat from shoreface storm deposits. *Recent Advances in Models of*

Siliciclastic Shallow-Marine Stratigraphy. : In: Hampson, G.J., Steel, R.J., Burgess, P.B., Dalrymple, R.W. (Eds.), Special Publication, 90. SEPM (Society for Sedimentary Geology), Tulsa, pp. 161–176.

YOKOKAWA M., 1995. Combined flow ripples: genetic experiments and application for geologic records. Kyushu University, Faculty of Science, Memoirs, Series D, Earth and Planetary Sciences, 29, 1-38.

APÊNDICE

ANEXO I

Título da Dissertação/Tese:

" ESTRATIGRAFIA DE SEQUÊNCIAS E ARQUITETURA FACIOLÓGICA DA FORMAÇÃO MORRO DO CHAPÉU, CHAPADA DIAMANTINA-BA "

Área de Concentração: Estratigrafia

Autor: Ezequiel Galvão De Souza

Orientador: Prof. Dr. Clayton Marlon dos Santos Scherer

Examinador: Prof. Dr. Juliano Kuchle

Data: 27/07/18

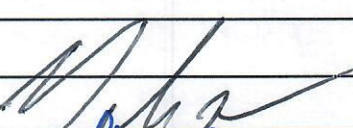
Conceito: A

PARECER:

O candidato apresenta uma tese de doutoramento relevante, em um tema importante, com impacto científico e bem completa. O volume de dados é compatível, e as metodologias são bem definidas e funcionais dada a aplicabilidade. A redação do volume da tese carece de profundidade, principalmente nas hipóteses e proposta de tese, e de uma síntese integradora final. Entretanto, tal ausência foi usada na apresentação oral completa, clara e no tempo previsto. O estado da arte é excessivamente simplista na análise dos sistemas costeiros. Deveria ter mais conteúdo.

Os artigos são relevantes, bem escritos e bem organizados. A metodologia e a relação descrição do dado e interpretação são bem definidos. Os resultados são coerentes e ~~corretos~~ as conclusões são bem limitadas pelos dados.

Desta maneira, o candidato Ezequiel apresenta plena capacitação para o título, e PARABÉNS pela qualidade do trabalho apresentado.

Assinatura: 
Ciente do Orientador: 
Ciente do Aluno: 

Data: 27/07/18

ANEXO I

Título da Dissertação/Tese:

"ESTRATIGRAFIA DE SEQUÊNCIAS E ARQUITETURA FACIOLÓGICA DA FORMAÇÃO MORRO DO CHAPÉU, CHAPADA DIAMANTINA-BA"

Área de Concentração: Estratigrafia

Autor: Ezequiel Galvão De Souza

Orientador: Prof. Dr. Claiton Marlon dos Santos Scherer

Examinador: Dra. Renata dos Santos Alvarenga Kuchle

Data:
27/10/2018

Conceito:
A

PARECER:

O trabalho apresenta grandes contribuições para a área e o intervalo analisado. O autor apresentou grande domínio, conteúdo sobre o tema principalmente na apresentação.

Na apresentação representou os artigos de forma organizada e clara com a determinação das hipóteses, objetivos, dados, resultados e conclusões.

Na cópia escrita faltou algum desses itens, inclusive um capítulo final para a integração dos artigos submetidos.

Os artigos I e II apresentam uma boa redação, ampla contextualização e referenciamento do tema necessitando de algumas menores correções. Já o artigo III necessita de algumas maiores correções mas nada que influencie no trabalho como um todo.

Assinatura:		Data:
Ciente do Orientador:		
Ciente do Aluno:		

ANEXO I

Título da Dissertação/Tese:

"ESTRATIGRAFIA DE SEQUÊNCIAS E ARQUITETURA FACIOLÓGICA DA FORMAÇÃO MORRO DO CHAPÉU, CHAPADA DIAMANTINA-BA"

Área de Concentração: Estratigrafia

Autor: Ezequiel Galvão De Souza

Orientador: Prof. Dr. Claiton Marlon dos Santos Scherer

Examinadora: Profa. Dra. Joice Cagliari

Data: 27/07/2018

Conceito:

B

PARECER:

A tese apresentada pelo autoranda é composta por um capítulo introdutório, com introdução e estado da arte, e por outros três capítulos, cada um com um manuscrito submetido. Os três manuscritos juntos compõem a tese de autoranda. Sua relação ao capítulo 1, sugere rever os objetivos específicos. O primeiro manuscrito está bem redigido, estruturado e organizado. As contribuições que presta são pontuais e servirão para melhorar ainda mais o artigo. Sua relação ao segundo manuscrito, pensa que é necessário reponcionar o tópico "stratigraphic architecture", por se tratar de resultados e não de discussão. É preciso deixar claro qual o modelo stratigráfico foi utilizado. Além disso, no caso dos três artigos é necessário inserir a metodologia utilizada. O terceiro manuscrito precisa de um trabalho maior na complementação das revisões técnicas e na interpretação dos resultados. O texto do terceiro manuscrito tem uma abordagem bem interessante, sugere que a publicação seja realizada em periódico internacional. Na apresentação, o autoranda apresentou domínio do tema e respondeu adequadamente a todos questionamentos.

